A Novel Digital Twin Framework for Monitoring Inventory and In-Bin Drying in Grain Storage

by

George Dyck III

A Thesis Submitted to
The Faculty of Graduate and Postdoctoral Studies of
The University of Manitoba
in partial fulfillment of the requirements
for the degree of

DOCTOR OF PHILOSOPHY

Department of Biosystems Engineering
University of Manitoba
Winnipeg, Manitoba

Abstract

This research addressed the absence of proactive grain storage management methods through the development of a Digital Twin (DT) for grain bins, a previously undocumented approach in academic literature or industry practice. The investigation was guided by, "How can one develop a high-fidelity virtual model with minimal input data that accurately represents real-world conditions and statuses of grain storage bins?" This work established the "sensorless monitoring" approach, which required minimal farmer-accessible data to present an inventory status and run simulations capable of predicting future states of grain bin inventory. This approach to inventory management differed from existing technology by providing predictive data for proactive storage. In contrast, modern inventory systems provide reactive data, only alerting users to problems after they occur.

The work began with a theoretical exploration of computer control systems in agriculture, followed by analytical pressure distribution models. Rogers et al. (2024) was developed to describe radial stress variation. Experimental validation of this mathematical model employed a novel tri-axial in-situ pressure sensor, designed and calibrated for this research. Measurements revealed radially variable vertical-to-lateral pressure ratios throughout the silo radius (0.22 near walls, 0.19 in the middle, and 0.37 at the center).

A functional DT platform was successfully implemented as a web application using Streamlit for the front-end interface and Google's Firebase NoSQL server for database architecture. The system featured comprehensive inventory tracking capabilities, including layer-by-layer monitoring of grain properties (commodity type, date of addition, height, mass, moisture content, and bulk density), visual representation of bin contents with colour-coded moisture distribution, and grain addition/removal functionality. The DT integrated pressure calculations based on Rogers et al.'s model, compaction equations, and a prototype drying simulation demonstrating how grain compaction significantly affects drying performance, with simulated differences in moisture content of 3.8% between compacted and uncompacted simulations.

This DT framework represents a significant change from conventional grain management by emphasizing predictive, proactive solutions rather than reactive monitoring with extensive instrumentation. While acknowledging current limitations in sensor design, mathematical modelling, and implementation architecture, this research establishes a foundational framework for future innovations in grain storage management.

Acknowledgments

Dr. Jitendra Paliwal, for providing a candid and approachable environment that made feedback very effective, along with humour and reassurance. I am especially grateful for the trust and freedom you gave me to pursue a left-field idea. This work truly would not have been possible without your support and guidance.

Dr. Qiang Zhang, for introducing me to the world of bulk solids and Janssen's work. Your feedback, always delivered with friendliness and humour, consistently revealed areas of research I was entirely unaware of, which greatly enriched my perspective.

Dr. Kurt Hildebrand for introducing me to the idea of Digital Twins; this was the beginning of my work. As well as taking my work seriously and providing very rigorous and robust feedback, which I always needed to take laying down.

Dr. Adam Rogers, for teaching me how to do real-world math, and encouraging me to turn over every stone on the math-path because there might be something interesting under it. You taught me how to be an academic. I really value the friendship we developed while working on new and interesting topics.

Eric Hawley, for being a loyal and close friend, encouraging me to enter grad school, and consistently dreaming on a scale magnitudes larger than I thought was possible. Your insanity is sublime.

The friends I made in the US whose collaboration was instrumental to my experiments: Michael D. Montross, Aaron P. Turner, Carlos S. Jarro, and Barry Farmer. Your collective humour, approachability, and generosity made our work together an absolute delight.

My mom and dad, George and Teresa Dyck, always encouraged me to pursue higher education. You are the fundamental reason I am here... but I might never leave!

Hannah Muhajarine, for understanding when I needed to discuss my research (and when I did not), remarkable grace in accommodating my often-late arrivals, and her unwavering support as a partner have been essential.

Also, the University of Manitoba for the UMGF, Steward Pugh External Study Scholarship, The Lord Selkirk Association of Rupert's Land Agriculture Scholarship, mitacs, and AGCO.

Publications

Portions of this text have been published previously in

- Dyck, G., Hawley, E., Hildebrand, K., & Paliwal, J. (2023). Digital Twins: A novel traceability concept for post-harvest handling. Smart Agricultural Technology, 3, 100079.
- Dyck, G., Rogers, A., & Paliwal, J. (2024). A review of analytical methods for calculating static pressures in bulk solids storage structures. KONA Powder and Particle Journal, 41, 108-122.
- Dyck, G., Rogers, A., Montross, M., Hildebrand, K., Turner, A., Paliwal, J., Farmer B., Jarro, C. (2025). Novel in-situ pressure sensors for bulk solids in silos: design, calibration, data acquisition, and analysis. *Computers and Electronics in Agriculture*
- Rogers, A., Dyck, G., Zhang, Q., Hildebrand, K., & Paliwal, J. (2024). A general continuum modelling approach for variable shear stress as a separable function in stored bulk solids. Powder Technology, 434, 119331.
- Rogers, A., Dyck, G., Paliwal, J., Hildebrand, K., Montross, M. D., & Turner, A. P. (2024). The Janssen effect and the Chini ordinary differential equation. Powder Technology, 436, 119493.

Contents

List of Figures

List of Tables

Chapter 1

Introduction

1.1 Overview

In post-harvest grain handling, efficient management is crucial to preserve grain quality, reduce losses, and improve logistical operations. As global grain demand increases and with Canada's reputation as a leading quality grain provider, there is a pressing need for innovative and proactive management tools. This document outlines the application of Digital Twins (DTs) for grain storage management. DTs are virtual replicas (twins) of physical entities that enable real-time monitoring and simulations to optimize operations. Although they have been implemented in many factory settings as part of "Industry 4.0," offering real-time monitoring and simulations to optimize operations, they have not yet been meaningfully applied to grain storage. Agriculture presents unique challenges for these systems compared to engineered factory settings. One fundamental difficulty lies in agriculture's inherently variable nature.

Throughout this document, the concept of "sensorless monitoring" is introduced, with the aim of providing a virtual representation of grain storage without requiring extensive sensor systems. The goal is to develop a virtual grain bin that can simulate real-world grain inventory statuses with minimal input, serving as a foundation for data-driven proactive decisions in grain storage management. This technology has important implications for farmers and global supply chains, where oil seeds and

grains are processed into food, feed, fuel, and fibre. This is because grain storage management presents challenges that affect food quality, safety, and economic efficiency. This work focuses on how DTs can help farmers, but will discuss the larger impacts on the supply chain, an important topic to consider within the greater literature.

The primary research question is, "how can we develop a high-fidelity virtual model with minimal input data that accurately represents real-world conditions and inventory statuses of grain storage bins?" This question will first be approached by a systematic review of the literature on computer-controlled systems in agriculture. This will be followed by the study of pressure distribution mathematical models, which can be found in the various publications on the experimental work conducted in the realm of this thesis research. Pressure is an important factor and a low-level phenomenon in grain systems that could affect higher-order simulations, such as drying, which is why it is the focus of much of this research. Experimental studies were conducted to validate the mathematical models developed. The experimental studies used a novel triaxial sensor developed and calibrated for this work. These findings were then used to develop a DT of a grain bin.

This DT served as a dynamic virtual representation, mirroring the real-world condition of grain within storage infrastructures. Monitoring and simulating grain moisture content, temperature, pressure distribution, and compaction in bulk solid storage structures, which would provide a real-time, comprehensive snapshot of the storage environment. Farmers would have access to an accurate inventory summary that serves as a foundation for advanced simulations used to make decisions.

The primary objective of this research is to precisely reproduce the conditions within a grain bin, capturing the moisture content, the pressure field, and grain compaction. Moreover, it will serve as the basis for conducting complex simulations such as temperature movement and drying processes. As a proof of concept for this approach, a drying algorithm was developed and tested, demonstrating the system's practical potential.

1.2 Rational and Current Challenges

The world's grains and oilseeds occupy approximately 12% of Earth's ice-free land and are processed into food, feed, fuel, and fibre for global supply chains [6]. Despite their importance, grain storage management remains a critical challenge, with approximately 9% of global cereals and pulses spoiled yearly [7]. Developing nations experience even greater losses, up to 50-60% due to inefficient storage systems [8]. In developed countries, farmers often store grain at high moisture levels while waiting for favourable market prices, risking spoilage and financial losses. This highlights the need for innovative technological solutions like DTs to mitigate losses, improve efficiency, and ensure global food security, which this work will investigate.

Traditional grain quality monitoring in large storage structures typically relies on cable systems. These systems, though useful, face challenges due to their limited spatial coverage (around 0.3 m diameter), since the grain acts as an insulator. They use temperature and humidity sensors to gather data from the intergranular air, which is then converted into grain equilibrium moisture content using empirical models. Consequently, due to the material properties of grain, many potential hot spots could be overlooked, with accurate monitoring confined to a small section of the bin. It has been demonstrated that fifteen cables, positioned 0.3 to 1 m from an artificial hot spot, failed to detect temperature changes in the surrounding grain [9, 10]. This challenges the industry's claim of achieving up to 100% coverage with seven temperature cables in a 53,000-bushel bin, which assumed an unrealistic sensing diameter of 4.46 m. Cables can thus provide a false sense of security, preventing informed grain aeration and management choices [10]. Despite these systems' availability, their adoption is hindered by concerns over cost-effectiveness, bin compatibility, reluctance towards technology, and the accuracy in detecting hot spots. In practice, these systems only inform a farmer of a problem once it is too late, and are fundamentally reactive.

Another popular technology found in academia and industry is CO_2 monitors, which identify spoilage through microbiological activity resulting in CO_2 production

at high moisture levels (above 18%). However, it does not provide early detection or moisture content information, essential for effective grain management [11]. This is because large amounts of grain are needed to spoil to produce a high concentration of gas to become detectable. This limitation prevents such sensors from offering predictive feedback, and they are another reactive technology.

In addition to moisture information, farmers also require capacity information for proper inventory management. Many volume measurement technologies, from basic cable and weight systems to advanced electromagnetic imaging, struggle to account for test weight, moisture variation, and compaction effects. Moreover, more advanced methods are still in the experimental phase, overlooking the dependence of the agricultural industry on weight for financial transactions [12, 13, 11].

Current grain monitoring technologies have significant limitations, highlighting the need for more robust predictive modelling in storage management. The DT proposed in this document offers a potential new approach, providing farmers with actionable information to help their decision-making processes and optimize grain storage operations.

1.3 Sensorless Monitoring

Standard sensor systems in grain monitoring provide snapshots of the status of a bin, which makes them fundamentally reactive. This approach means that the farmer is only informed of a problem after it occurs. This work suggests an alternative called “Sensorless Monitoring”. The first fundamental principle is predictive monitoring, which uses models and simulations to guess when a problem (such as grain spoilage) will occur rather than simply reacting to it once it is detected. The second fundamental principle is that it should not require advanced sensor systems. Each system needs to determine the fundamental infrastructure needed to visualize and predict/simulate the inventory status at a site (past, present, and future). The final principle of “sensorless monitoring” is that it includes much more than a grain bin in isolation. It represents grain handling as an interconnected system of processes

over time and can be expanded far beyond the bin. This can include intra-farm operations or global supply chain factors. Traditional systems cannot represent these three principles because they are exclusively reactive, designed solely to host sensor data without simulation capability, and operate in technological isolation without intra/inter-farm communication. The Sensorless Monitoring approach is absent from both the existing literature and industry, which is the research gap this work aims to address using DTs.

1.4 Objective

The main objective of this research is to begin the application of DTs in post-harvest crop inventory management systems, with a specific focus on pressure systems and compaction within a grain bin. In the last four years, there has been a growing interest in applying DTs to the agricultural field, and there is a small but growing number of works published on this topic [14, 13, 15]. Notably, the work done in this thesis remains the sole published paper on the application of DTs to post-harvest grain handling [13].

This research proposes the application of DTs to post-harvest crop inventory management systems through the concept of "sensorless monitoring," which would manifest as a virtual bin powered by bulk solid models and farming principles. This would require few (or potentially any) sensors to simulate a grain bin, enabling low-input requirements for high-output predictive capabilities. The work aims to accurately represent post-harvest inventory management of grain (including packing, drying, etc.) using the most basic data available to most farmers (volume, test weight, moisture content, weather data, fan status, etc.). The accuracy of the DT's representation will depend on the quality of these inputs and models.

The dynamic representation is purely synthetic, using models and data to predict future states, which can inform or control decisions on fan states and incorporate real-time volume or moisture measurement sensors if available. The term "sensorless" is used because one can build the most basic framework for a dynamic and

virtual site representation while still encapsulating much of the system's function for a range of users, planning for "the lowest common denominator." It should be stressed that this dynamic representation includes historical states, perhaps including predicted changes alongside data input "checkups" or "synchs" that could be very basic (manual inputs from workers) or more advanced (automated data acquisition from advanced sensors). It is a reality that some users have not adopted sensors or that sensors cannot represent a complete picture of a grain management system due to their inherent limitations. Consequently, the DT does not require sensors, but could be incorporated into the framework to increase input accuracy and predictive capabilities.

The future potential of sensorless monitoring's representation would be a virtual bin that includes many functional virtual representations of assets such as bins, fans, agricultural commodities, farming land, events such as weather, connections between combines and bins, as well as "ideas" or "expert experience" represented as drying models, packing models, historical records, future predictions, financial information, and relationships to supply chains. Using terms more familiar to DTs, sensorless monitoring is the virtual representation of the physical handling facility along with approximations of expert knowledge or an operator's mental representation of the system (perhaps even new insights or perspectives). As the virtual bin's representation becomes more comprehensive, its ability to simulate reality increases in accuracy. The above idea can impact more than just farmers' concerns with inventory management. The application of DTs to the management of farm inventory will provide a dynamic picture of commodities, an essential step in the future global issue of food traceability, a topic gaining importance among many governing bodies. Dyck et al. (2023a) offer an overview of this subject in their literature review on the theoretical application of DTs to post-harvest handling[13].

This research's goal focused on a crucial aspect of sensorless monitoring's virtual bin: grain mass management. The specific goal was to create accurate models of pressure systems within grain bins. This involves understanding how the bulk of

grains in silos exerts pressure on the grain itself and compacts. Understanding pressure in silos is critical because it impacts several properties and processes that impact grain quality, usability, and profitability. Inefficiencies or inaccuracies can lead to increased operational costs and potential grain damage. A comprehensive understanding of grain mass and the associated pressure systems within storage bins is fundamental for developing a DT. This knowledge is the cornerstone for predictive, DT-powered grain storage management.

1.4.1 Objective List

The objectives are organized into four themes.

Introduction and Literature Review:

1. Investigate the relevance and applicability of DTs to post-harvest crop inventory management systems.

2. Review and analyse historical and contemporary pressure theories, including the work of H.A. Janssen, lateral-to-vertical pressure ratio, and the relationship between pressure and density changes in grain storage.

Mathematical Modelling and Experimental Studies:

3. Investigate an analytic model of pressure systems that can account for variation in pressure fields within grain bins.

4. Design and conduct experiments to collect data on the pressure field within a grain bin, which will be used to refine the analytic model in 4.

DT Development:

5. Develop a DT to virtually represent a grain storage bin.

    a. The DT should have a web interface with a front end for displaying historical, current, and potential future states of bin inventory management, and a back end incorporating the developed mathematical models and data.

b. The input data for the bin's DT should represent post-harvest inventory management using basic farmer data. For example, input data such as volume, test weight, moisture content, etc.

Discussion and Conclusions:

6. Explore the theoretical ability to integrate the DT approach with other virtual representations, such as weather, expert knowledge, fan status, models, records, predictions, and supply chains.

7. Explore the potential social impact of applying DT technology to farmer inventory management, contributing to the global food traceability issue.

Each of the above objectives provides valuable information used to answer the question of how to develop a virtual model of a grain storage bin, both conceptually and practically. Together, they integrate high-level conceptual development, sensor development, experimental data collection, and mathematical modelling, ultimately resulting in a practical DT solution that addresses the research gap identified.

Chapter 2

Literature Review

Computer-assisted practices for post-harvest grain handling have experienced challenges, shown progress, and are currently at a critical and potentially influential time. In the 1980s, the research community began focusing on conceptualizing and implementing 'Expert systems'. These systems had the goal of capturing the expertise of grain handlers to convert into algorithmic decision-making frameworks. The goal was to better manage grain, ensuring that the best decisions were always made for inter- and intra-facility handling. However, these systems ran into their inherent limitations. Researchers struggled with the absence of real-time sensor integration, a consequence of the early state of sensor technology and computational capabilities, as well as the ability to translate knowledge into these systems. This made these systems largely prescriptive and rigid.

With recent technological advancements in computing and sensor technologies, DTs have emerged as a promising approach where previous expert systems failed. This framework has attracted substantial academic and industrial interest as a part of "Industry 4.0," the fourth industrial revolution, as theorized by Lasi et al. (2014), particularly within the manufacturing sector [16]. This revolution is part of a larger trend of combining digital technologies, automation, artificial intelligence (AI), and the Internet of Things (IoT). Unlike expert systems, this technology can potentially offer a comprehensive real-time digital duplicate that bridges virtual and physical spaces.

What follows consists of a literature review on a brief history and the future of computer-assisted practices for post-harvest grain handling and a historical review of analytical models to describe pressure within a grain bin. Before discussing expert systems and DTs, it would be appropriate to consider the original scientific approach to studying systems, feedback, control, and communication, which is the theoretical foundation for computer-assisted control: cybernetics.

2.1 Cybernetics

Computer-assisted control has its basis in cybernetics, traditionally understood as the science of control and communication. The term was first introduced by a Massachusetts Institute of Technology (MIT) mathematician named Norbert Wiener and was taken from the Greek word *kubernēétēs*, meaning "steersman" or "governor." Before organising his thoughts, Wiener applied his initial insights on control and communication to World War II (WWII). He was tasked to predict the future state of enemy aircraft based on its current trajectory and possible movements, which was hoped to increase the accuracy of anti-aircraft missiles. Notably, WWII provided many of the earliest applications of computer technology to human decision-making. After the war, Wiener formalized his thoughts in the influential and paradigm-creating book, "Cybernetics or Control and Communication in the Animal and the Machine" in 1948. Cybernetics was meant to serve as the science of communication and control in systems, studying components' interactions and the resulting behaviour in animal and machine. Moreover, a system was understood to be a combination of components and produced synthetic results [17, 18]. Feedback played an essential role in system control, providing the foundational principles of computer-assisted control. Using computers to monitor, adjust, and optimize systems is an application of cybernetic concepts. This makes cybernetics worth investigating to incorporate some of its insights into this work or to understand the origins of computer control.

In their book "Cybernetics for Agriculture Production Systems" Huan and Zhang

(2021) point out that agricultural production systems are uniquely complex. They suggested that this is caused by the relationship between agricultural production systems and natural and ecological systems, which brings significant uncertainty to operations. Cybernetics provides a framework for understanding how these complex systems work, as well as how they can be designed and optimized. In the context of agriculture, it provides a methodology for describing, characterizing and representing agricultural systems. This approach reveals essential features and interactions of control and communication in agricultural production and management [18]. Huan and Zhang (2021) provide a significant mathematical basis and concrete application to control, communicate, and model agricultural production systems. For example, they discuss the specific control theory of drying harvested grains.

Two critical central principles of cybernetics are self-organization and feedback. The self-organization and correction mechanism is evident in both mechanical and biological systems. Feedback involves a closed "signalling loop" where system actions generate environmental changes, influencing subsequent system actions. This feedback can be positive, amplifying changes and potentially leading to instability, or negative, reducing changes and promoting stability [18]. These principles of cybernetics suggest that the grain bin functions are an intricate system characterized by the interplay of its many components and emergent behaviours of the entire system. Collectively, these interactions come together in a synthetic self-organizing outcome driven by self-regulating feedback loops.

These principles of cybernetics are not vague claims, but directly relate to an approach to grain storage management called "The Ecosystem Approach to Grain Storage" [19]. The ecosystem approach views a grain bin as a collection of complex interacting systems. These include factors such as grain properties, structure, biological systems (insects and microflora), management systems (technologies and practices), information and feedback systems, and the surrounding environment. Moreover, this system does not operate in isolation. It interacts with broader systems that include elements such as tractors, farm personnel, economics, policy,

transportation, and commerce.

In other words, this perspective not only views the grain bin's interior complexity but also how it fits into an exterior world of the agronomic and political landscape and how these interior and exterior worlds interact. Using the parlance of cybernetics, these systems will interact with each other via "negative feedback" that promotes stability (moisture and temperature control, grain quality control, supply chain, policy development) and "positive feedback" that amplifies changes (insect propagation, hot spot development, agronomic decisions). This understanding of feedback and the various scientific/mathematical/engineering approaches to studying and controlling systems will be investigated further in this research. This could provide insights into future automation potential and additional research topics outside the scope of this work.

Cybernetics offers a multidisciplinary approach that can help examine a system's structure, considering its inherent limitations and possibilities. One of its most relevant tools is the feedback mechanisms to maintain and achieve different system states. DTs are a direct application of this idea. When creating a digital representation of a system, in this case, a grain bin, that will influence or give feedback into the real world, cybernetics can provide valuable concepts and tools briefly mentioned above. With this in mind, let us consider two applications of cybernetics to grain storage, one old and one new: expert systems and DTs.

2.2 Expert Systems

Expert systems were developed from the research of Edward Feigenbaum through his Heuristic Programming Project and were an early application of AI. The peak of research interest occurred in the 1980s, with billions of dollars invested in the field [20]. Expert systems were an attempt to digitize domain-specific expertise. A well-designed expert system replaces the dependence on human experts to apply knowledge to solve problems [21]. As an early AI technology, expert systems operated using symbolic logic, developed from knowledge extracted from experts to

create facts and rules. The system took in data and output suggestions, decisions, and relevant knowledge, which could be used for many purposes: interpretation, prediction, diagnosis, design, planning, monitoring, debugging, repair, instruction, and control [22]. The potential of exporting domain-specific knowledge to increasingly affordable and user-focused computer systems in the 70s and 80s gained much attention. The ability to have an electronic expert who provided high-quality advice on situations in the field to supplement or replace existing personnel, with no downtime, was highly attractive. Although this was a very difficult task to complete within this framework.

By the middle of the 1980s, there were suspicions about whether general expert systems could replace the expert. Some difficulties in these early attempts at expert systems were from a purely technical perspective, citing issues with knowledge acquisition and translation [23], their "brittle nature," or lack of adaptiveness [24, 25], problems with the coupling of complex software and dedicated hardware [21]. Whereas others were from a philosophical perspective concerning the actual ability to capture human expertise on a subject, in other words, the general epistemological assumptions of expert systems [26]. By the mid-2000s, AI technologies had experienced the boom and bust and reemergence of research, with varying degrees of success in building an expert system [20]. The literature reflects this, with as many as eleven distinct approaches to creating expert systems [27].

The term expert system was never completely removed from the lexicon and evolved over time. AI shifted away from rules-based approaches towards fuzzy logic and statistical methods. New tools like machine learning algorithms and big data have enhanced the capacity of expert systems to digitize and process large amounts of data [25, 28, 29, 30]. Expert systems became helpful for deep and specific applications with these new approaches and tools, but not for general intelligence [31]. Early expert systems were described as "brittle," with abstraction being problematic because they operated on strict rules programmed into a series of "IF... THEN..." statements and subroutines. Unlike modern AI tools that can learn from data and

adapt to new situations, these early systems could not learn from experience or generalize beyond their explicitly coded rules.

With this being said, the new machine learning algorithms, specifically artificial neural networks (ANN), have their difficulties. For example, training and data acquisition were time-consuming and produced results that were difficult to interpret and came without thorough explanation or justification [32]. By incorporating machine learning into expert systems, the individual weaknesses of both could be overcome [33]. The two main approaches were a hybrid model, achieved by merging old and new approaches, or a standalone machine learning algorithm that infers its own rules from data, also called a connectionist expert system [32, 30, 28]. When the popularity of AI was relatively low in the 1990s, research on these hybrid and connectionist expert systems dominated, which laid important groundwork for later AI developments.

The synthesis of ANN and traditional expert systems created an excellent application for specific (narrow) environments with the ability to have significant and accurate (deep) data sets. Early attempts of these new expert systems were diverse: fault analysis [34, 35], medical diagnosis [36, 37], financial market analysis [38, 33, 39], electronic control [29], and agriculture [40, 41, 42, 43]. Liao's (2005) survey of expert systems from 1995-2004 devotes a section to ANN approaches [27]. Finally, in recent years, this same approach has been applied to predictive maintenance [44], material properties analysis [45], and agriculture [46, 47]. Today, there is an unprecedented ability to apply these expert systems due to the increase in machine learning techniques, data acquisition, and computing power.

Agriculture, specifically oil and cereal crops, was one of the many industries that attempted to apply expert systems to various subjects of research and field operations. At the height of expert systems research in the 1980s, there were considerable publications in the area, including pre-harvest crop and farm management [48, 49], natural resource management [50], agronomy [51], as well as several literature reviews of the topic and viable applications [52, 53, 54]. More specifically, there was

an interest in expert systems in grain storage and what they could offer to different facilities.

White (1992) wrote on the application of expert systems to stored-grain research and reminds the reader that expert systems must be an interdisciplinary subject. They bring together many models, knowledge, and approaches to problem solving from various perspectives that can describe the complex ecosystem of stored grain. He suggests three main applications of expert systems, "... (1) diagnostic systems, (2) simulation delivery systems, and (3) large-scale systems that integrate different types of knowledge such as simulation models, expert opinions, and objective information"[55]. Some existing applications of these systems relate to human hazards [56], grain management in facilities [57], but the majority are for the control of pests and fungi [58, 59, 60, 61, 62, 63, 64, 65]. These works point to the grain industry's interest in knowledge systems to help organize and systematically improve operational efficiencies centred on handling and preserving grain quality.

This overview of expert systems shows that some of the expertise of grain handlers can be incorporated into a digital infrastructure. However, facility optimization, fault handling (spoilage events, plugs, etc.), and some routine tasks (bin entry, cleaning, equipment inspection, etc.) can involve decisions that a designed expert system cannot solve without extensive modifications. In those situations, the grain handler's ability to resolve issues will be constrained by their awareness of the site and possible solutions. By providing cyber-physical twinning through DTs, operators can achieve the high levels of situational awareness required to identify issues and utilize powerful simulation tools to provide solutions.

2.3 Digital Twins

The emerging research field of DTs attempts this cyber-physical fusion to enable monitoring of assets and optimization of processes across their lifecycle. Currently, there is no clear definition of what it is or should be [66, 67, 68, 69]. The original white paper, developed over 15 years ago, outlines three elements that are still

present in most state-of-the-art descriptions: i) a physical product in real space, ii) a virtual product in virtual space, and iii) connections of data and information that tie the virtual and the physical products together. There is a bidirectional flow of information between the first two elements, mediated by the third. These elements create an up-to-date digital representation of a physical asset capable of informing processes that interact with the material object, creating a two-way relationship between the physical and the virtual [70]. Some sources recognized an extended definition of the physical asset as a potential or a past object [67]. It is generally agreed that there is a fourth essential element for constructing most forms capable of intelligent feedback: data.

It should be noted that a lack of clear standards could impact the field of DT research. Without a clear expectation of their qualities and functionality, research could become scattered without a cohesive element. This is a problem because it could lead to inconsistent expectations and a mistrust in the field, having the potential to turn it into a "buzz word." To address this, more precise definitions and levels of cyber-physical bridging are defined and discussed in this document.

The first occurrence of a DT could be traced back approximately half a century ago, during the National Aeronautics and Space Administration's (NASA) Apollo missions. The organization built two identical space vehicles: one would be sent into space carrying the crew, while the second would safely sit on Earth, mirroring the space-bound twin unit. Having two identical units allowed the Earth team to support the space crew and equipment with more detail and assurance, referencing what was made, and this was most notably used on the nearly devastating Apollo 13 mission [71]. This was long before the advent of computers with drafting and 3D rendering abilities. In 2004, Dr. Michael Greives, while working with NASA, published a white paper that would take this original physical twin to the digital realm, which he named DTs [72]. This idea would remain unused for a decade due to computing limitations. However, interest was stirred again, predominantly in Chinese factories in the mid-2010s, after computing power had sufficiently advanced

to overcome those limitations [71]. His original application was directed toward the production quality for factory-made products, focusing on managing the product throughout its life cycle. Modern implementations have been extended to many other applications by large companies such as General Electric, International Business Machines Corporation (IBM), Siemens, and Microsoft [71]. Both industry and academia have begun studying and developing this technology to understand and refine complex systems' control [69].

2.3.1 DTs in Agriculture

Some examples of DTs in agriculture include arable farming, dairy farming, greenhouse horticulture, organic vegetable farming, plant pathology, livestock farming, food supply chain, farm machinery/building and fleet management, and apiaries [73, 67, 14, 15]. Two comprehensive literature reviews exist on this topic. Pylianidis et al. (2021) produced a review of this framework in agriculture, documenting 28 cases [14]. They observed that most other disciplines' applications of them are to non-living assets, and a living organism is a complex and dynamic system that will interact directly or indirectly with its physical twin asset. Currently, existing DT solutions in agriculture are limited to providing hardware and software that monitor mechanical operations, enable optimization, support preventive maintenance, and offer access to both historical and current system data. These systems are concerned with the mechanical aspects of agriculture and fleet management.

The second was by Purcell et al. (2023), which had a slightly different perspective but a similar conclusion [15]. They reviewed 31 papers on DTs in agriculture, categorizing the research by integration level (digital model, digital shadow, and DT) across crop monitoring, livestock management, and controlled environments. Their analysis concluded that there were promising benefits, but challenges with data integration and modelling biological systems required attention before regular adaptation of them could occur. Their term "digital shadow" is a useful idea that will come up later in this research. It is a virtual representation that updates to

reflect changes in its physical asset, but lacks the bi-directional capability to influence the physical asset. This is the state of many so-called DTs currently implemented in agriculture.

There are no documented discussions of grain inventory management twinning outside of this research work. In the context of grain elevators, some partial internal traceability management systems for grain have been studied, most thoroughly in the Ph.D. work by Laux (2007) and Thakur et al. (2011) [74, 75]. This being said, their practices still do not adequately "twin" the grain inventory as a DT would. However, impressive early work has been done on the traceability of highly valued horticultural products. During transport, an artificial mango was used to model thermal changes using mechanistic models, leading to more transparent supply chains and fewer storage and transport losses [76]. There also exists more general work discussing sensors, statistical techniques, computational statistics, physics-based models, and machine learning, which focuses on estimating commodity changes at different stages of the supply chain using DTs [77].

The recent rise of DTs in agriculture is in part due to modern precision agriculture and automation, which uses distributed data to optimize agricultural outputs [67]. This integration is part of the broader transition to what is commonly called "smart farming," a phenomenon whose social implications have been thoroughly analyzed by Klerkx et al. (2019) [78]. They identified five current thematic clusters (adoption of technologies, effects on farmer identity, power and ethics, knowledge systems, and economics) and four emerging areas of research (socio-cyber-physical-ecological systems conceptualizations, policy processes, transition pathways, global geography of digital agriculture development). The authors further articulate that as digital agriculture moves beyond prototypes, interdisciplinary approaches are needed to guide technological development in ways that consider social dynamics and maximize benefits while reducing potential negative consequences.

Wolfert et al. (2017) theorized that Big Data and AI have the ability to completely transform the entire food supply chain through predictive insights, real-time

decisions, and new business models, while creating a power struggle between tech companies, big agriculture, startups, and public institutions [79]. Furthermore, Smith (2019) explores how agriculture will change from improved precision information and alerts to a deeper understanding of farm systems, better predictions, and ultimately automated decision making through robotics and DT. Smith acknowledges the possible negative impacts, particularly the breakdown of the roles and skills of farm workers, highlighting the importance of considering social and ethical implications when implementing these types of systems [80]. Novek (1990) documented similar transformational impacts when automation was introduced to Canadian grain elevators decades ago [81]. This work continues this discussion in the context of grain storage and is presented in Section 5.2.7. This topic is further discussed in Section 5.2.7.

For a DT to accurately represent stored grain, it is essential to incorporate precise mathematical models. Grain is classified as a bulk solid and exhibits a distinct pressure distribution system. The origins of understanding this unique pressure distribution can be traced back to the work of Charles-Augustin de Coulomb, who investigated how soil collapsed to design better retaining walls for the French military in the 18^{th} century. When grain is ensiled, its pressure distributions exhibit some counterintuitive aspects. The first robust mathematical expression to describe this phenomenon was by H.A. Janssen in 1895. A comprehensive theory of bulk solid pressure is essential to ensure that the DT effectively mirrors grain within storage.

2.4 Pressure Theory and Sensors

Bulk solids are composite materials of many solid particles that can display characteristics of liquids and solids. They can adapt their shape to fit containers like liquids, yet they react to internal stresses similarly to solids. A critical property of these materials is the "Janssen effect," which describes the unique pressure distribution of ensiled bulk solids. Based on H.A. Janssen's work, this effect shows that the base of a storage bin does not carry the entire weight of the material stored,

especially beyond a certain height. This phenomenon is due to friction between the sidewalls of the bin and the stored material, with the walls holding some of the weight of the material. The mathematical description of this behaviour is related to Coulomb's studies on friction and Rankine's analysis of material failure.

This section will first trace the historical progression of pressure models, delve into Janssen's pivotal contributions, and explore the subsequent refinements and critiques over the decades. It will conclude with a discussion on the application of pressure theory in density packing, all of which will be the mathematical models that will generate the DT's packing simulations. The second half will cover the state-of-the-art in situ bulk solid pressure sensors. These sensors are essential to advance grain storage management through the development of more accurate models and their experimental validation. Understanding the development of stress in silos is a necessary component for modelling other processes, such as how pressure affects compaction and air movement during aeration and drying [82, 83, 84, 85]. Such models are crucial for implementing advanced system control in bulk solid management [13].

The following literature review is essential to establishing the assumptions of Janssen's work, where it fails, and how this research will build on or challenge Janssen's assumptions. Specifically, this research incorporated models that allowed for pressure to vary across the diameter of the bin. Furthermore, the research experimentally investigated the radial variability in pressure, predicted by the model, by implementing novel pressure sensors to map pressure changes throughout wheat. This approach enabled the development of more accurate DT simulations that can predict variable compaction and eventually optimize aeration/drying strategies based on pressure data rather than idealized theoretical distributions.

2.4.1 Historical Pressure Theories

The phenomenon, later termed the "Janssen Effect," was observed prior to Janssen's mathematical description of it. Although Janssen's work did not properly cite this,

it was originally articulated by Gotthilf Heinrich Ludwig Hagen. Hagen's account is the oldest published theory of pressure in bulk materials, 40 years before Janssen in 1852 [86]. Hagen attempted to predict saturation pressure with respect to height in sand. Tighe et al. (2007) translated the article into English, providing a detailed view of this seminal work [87]. Hagen suggested that friction on the side of the wall acted in the upward direction as opposed to the gravitational force. The pressure felt by a disk that is "easily movable but seals tightly" was given by the expression,

$$\sigma_{disc} = r^2\pi\rho g y - 2r\rho g\mu y^2 \tag{2.1}$$

Here, r is the radius of the disc (bin), ρ the bulk density, y is the height of the bulk material, and μ the friction coefficient. This equation reaches a maximum at a characteristic height (related to the diameter of the bin, the height of grain, and the friction coefficient) and begins to decrease afterwards, a mathematically valid prediction, but physically incorrect. Hagen stated that the pressure followed this curve until this maximum was reached. Afterward, the bin pressure remained constant at this maximum, similar to the "Janssen Effect."

Hagen's formulation differed from Janssen's because it used a quadratic equation to explain the change in pressure. In contrast, Janssen's approach solved a differential equation whose solution was an exponential function, allowing for an asymptotic approach to the maximum pressure.

An interesting historical reference can be found in both Hagen's and Janssen's publications referencing an observation published by Huber-Bernand in 1829, which was likely the first published research on the so-called "Janssen Effect". Huber-Bernand noticed that when he filled a container with eggs, added sand in the voids between the eggs extending several inches above the eggs, as well as a 25 kg weight on top, the eggs placed at the bottom of the container remained unbroken, even though the weight should easily crush them. He concluded that only a portion of the pressure was transmitted to the bottom of the container, indicating some kind of saturation depth [88, 87]. Although it remains a historically significant fact

that informed Hagen and Janssen's scientific theory, Huber-Bernand's reason for the eggs' safety was likely wrong. It has been long established in rock mechanics that the failure stress of a cylindrical specimen can be increased by applying lateral compressive loads.

Another important pre-Janssen study was published in 1884 by the Welsh engineer Isaac Roberts, who observed an asymptotic trend in bulk solid bin pressures. He claimed that the pressures at the bottom of bins stopped increasing at the height of two diameters, which was an empirical demonstration of the Janssen effect [89]. He conducted two experiments on the topic. The first was prone to measurement errors due to the mechanical nature of the scales used, an issue other researchers (Prante) would struggle with and overcome; the second experiment produced reliable results that were widely referenced [90].

Ten years later, H.A. Janssen analytically formulated his seminal equation, improving on Roberts's work, although the work was not cited.

2.4.2 H.A. Janssen

H.A. Janssen would be the first to formulate a simple and accurate way to calculate pressures in deep bins, the standard reference for well over a century on the topic. The influence of this equation was enormous and has been used in many design codes and standards worldwide, such as the European bulk storage building codes (European Standard EN 1991-4, 2006)[91]. The American Society of Agricultural and Biological Engineers (ASABE) also used the expression to calculate the apparent weight of the bin capacities [92]. Janssen's work has been used by a vast community of researchers and industry professionals because it explains the complicated phenomenon of bin pressures via a straightforward expression (Eqn. 2.3 and 2.4).

Janssen was an engineer from Germany, and not much is known about the individual and his work outside of this one publication, a seminal paper for the science of bulk solids. Some researchers postulated that his work and records were likely destroyed during WWII [93]. The life and work of Janssen are accessed through his

1895 paper, "Experiments on Corn Pressure in Silo Cells." One year after its publication, an English translation of Janssen's abstract was published in the Proceedings of the Institution of Civil Engineers, the work often cited as Janssen (1895). Soon, the equation was added to the building practices outline in the "Des Ingenieurs Taschenbuch or The Hütte - Das Ingenieurwissen," a book of references for practicing engineers, initially written in German and later translated into many languages [90]. Many aspects of the work were validated, critiqued, and modified during this time, discussed later in this review.

It is an interesting historical point that Janssen referenced two other works incorrectly, which Sperl addressed in the translation of Janssen's original document [88]. The first was a fellow German researcher, C. Arndt, and was used to discuss the then-new developments in grain storage in North America. The paper's title is "The Silos of Galati and Braila," which are Romanian cities that hold the oldest concrete grain bins. These were built in the late 1880s, designed by an engineer, Anghel Saligny, and were two of the earliest examples of reinforced concrete bins. Janssen described these bins as "...iron-strengthened brickwork, and in six-fold profiles like honeycombs. The grain was introduced through a hatch through the upper end of the cell. For discharge, stock transfer, or embarkation, the bottoms of the cells provided closeable openings" [88]. This sounds like a description of modern grain storage bin design; Janssen saw these as the future of bin design and wanted to provide mathematical models for predicting pressures. The second citation was Hagen, discussed thoroughly above. Ketchum reviewed the design of concrete bins in Chapter XVIII of his text "The Design of Bins, Walls and Grain Elevators." Unfortunately, he did not mention Saligny and only discussed the concrete bins of North America.

Regarding his mathematics, Janssen began with a force-balance equation of a thin horizontal layer of bulk material in a deep bin. Two things should be commented on. First, Janssen investigated deep bins, but the theory can be applied to shallow bins [94]. Second, the following is not Janssen's formulation directly, but a

modernisation of the derivation (for clarity) that was made popular by Ketchum, but is essentially the same [90]. The first difference lies in incorporating a hydraulic radius R_H, which generalised the container geometry from Cartesian (rectangles) to arbitrary shapes. Secondly, in Janssen's work, he expressed $K = \mu k$ and solved for K experimentally. The lateral pressure ratio, k, is the ratio between horizontal stress and vertical effective stress, and μ is the coefficient of friction between grain and silo material. Within a filled container (bin), the force balance on an infinitesimal thin disk element of granular material in the vertical direction is given as:

$$A\sigma_y + g\rho A dy \;=\; A\left(\sigma_y + d\sigma_y\right) + \tau_w C dy \tag{2.2}$$

Where A is the cross-sectional area, C is the circumference of the bin, ρ the bulk density of the material, g is the gravitational acceleration, σ_x and σ_y the horizontal and vertical stresses, respectively, and τ_w the shear stress acting on the material at the wall, which opposes the gravitational force. x and y are the horizontal and vertical coordinates, respectively. It should be noted that the depth of the stored material is given by y, increasing in the downward direction. The following differential equation is produced (Eqn. 2.3) and solved for vertical pressure (Eqn. 2.4), which can be reviewed in more depth in Dyck et al. 2023 [95],

$$\frac{d\sigma_y}{dy} + \frac{\mu k}{R_H}\sigma_y = g\rho \tag{2.3}$$

$$\sigma_y = \frac{\rho g R_H}{\mu k}\left(1 - e^{-\frac{\mu y k}{R_H}}\right) \tag{2.4}$$

It should also be noted that M. Koenen worked on a similar pressure theory but published it a year after Janssen. Koenen's work is challenging to find because it was never translated from German to English, and the conclusions were passed down by secondary literature. His most significant contribution suggested that the lateral to vertical pressure ratio could be calculated using established equations, such as Rankine's active pressure state, $k = 1.10 \times (1 - \sin\phi)$, while Janssen experimentally

determined its value [96, 97, 98]. ϕ is the internal angle of friction. Koenen explicitly connected Janssen's work to the Mohr-Coulomb failure criterion by relating k to the principal stresses acting on a mass, whereas Janssen left this as an empirical value.

Janssen's work is mathematically connected to the Mohr-Coulomb failure criterion by assuming two points: a constant k, and that vertical and horizontal stresses are principal stresses [99]. This creates a fundamental contradiction in Janssen's work because principal stresses do not have shear stress acting on them. Yet shear stress existing at the wall is fundamental to the Janssen effect as it supports the grain, creating the characteristic asymptotic behaviour. This inconsistency undermines core assumptions in Janssen's formulation of grain pressure distribution. These two conditions cannot coexist in a consistent mechanical framework. Nevertheless, the fact that Janssen's model works reasonably well in practice for many applications, despite this theoretical inconsistency. Moreover, these assumptions lead to Koenen's contribution connecting k to

$$k = \frac{1 - \sin(\phi)}{1 + \sin(\phi)} \tag{2.5}$$

This relationship is particularly significant for Janssen's model because it provides a method of determining k based on an easily measurable material property. This is one reason Janssen's model, despite its theoretical problems, remains widely used in many granular storage applications.

2.4.3 After Janssen

The response of the community of engineers and researchers to Janssen's work was fast. Rigorous validation of Janssen's model occurred within the first decade of its publication [90, 93]. Wilfrid Airy (1898) acknowledged the works of Roberts and Janssen in his paper, but lacked access to specific friction coefficients because he only had access to Janssen's English-translated abstract [100, 101]. Airy discussed the geometry of the bins, focusing mainly on the limitations of small bins and their

impact on the coefficient of friction. Although Airy's approach to modelling pressure in bins was based on the Mohr-Coulomb failure criterion, it considered both shallow and deep bins.

Milo Ketchum (1911) published a classic book, "The Design of Bins, Walls, and Grain Elevators," which provided comprehensive guidance on the construction of modern elevators during the early 20th century, offering insights into bin design practices and equations of that era [90]. In his book, Ketchum discussed the mathematical models that both Janssen and Airy proposed regarding grain bin pressure, ultimately favouring Janssen's theory while deeming Airy's equations too intricate for practical application. Subsequent research by experts, including Prante, Toltz, and Jamieson, further explored and validated Janssen's model, highlighting the differences between static and dynamic pressures in grain bins and the importance of symmetrical grain removal to prevent bin failure.

Andrew W. Jenike (1961) published a groundbreaking work, "Gravity Flow of Bulk Solids," which provided a comprehensive mathematical description of bulk material flow, drawing on previous research and introducing new analytical theories. His work was pivotal in understanding the flow of bulk solids, categorising different flow types, and emphasising the influence of bin/hopper geometry on these flows. In addition to his seminal book, Jenike, together with collaborators such as Johanson and Carson, produced influential publications that became foundational in both research and engineering practices due to their practical design formulas and calculation examples [102, 103, 104, 105].

Marcel and André Reimbert's book "Silos-Theory and Practice" was a spiritual continuation of Milo Ketchum's project updated for the modern silo [96]. It introduced a new model for bin pressures along with building practices for elevators. The Reimberts critiqued the conventional Koenen-Janssen approach, emphasising the assumption that they used a constant k in their model while suggesting variations based on the geometry of the bin and the depth of the material. Their model produced results similar to Janssen's but employed an empirical equation to describe

pressure changes based on depth.

Figure 2.1 compares many of the historical bin pressure models mentioned above using identical variables, which can be found in Table 2.1. In this table grain height is h or y, bin diameter is d, mass density ρ, lateral-to-vertical stress ratio k, coefficient of friction μ, and ϕ is the internal angle of friction.

Analysis of these models in different depth/diameter ratios revealed that differences in pressure predictions between models can be divided into three main regions: low (0-1.5), intermediate (1.5-3), and high (3-5). In the low h/d ratio region, the equations showed the most variation between each other. The following percent differences were observed: Hagen vs Reimbert, 16.0%; Hagen vs Janssen, 31.3%; Hagen vs Airy, 64.6%; Reimbert vs Janssen, 15.6%; Reimbert vs Airy, 50.0%; and Janssen vs Airy, 35.1%. In the intermediate region, Reimbert and Janssen closely approached the Hagen asymptote, with Airy's equation being 10.0% lower during this intersection. At the extreme end of the high h/d ratio region, Reimbert and Janssen were very close, within 2.0% of each other, while Airy and Hagen's asymptotes were 5.1% above and 7.6% below them, respectively. It is important to note a 9.9% difference between the Hagen and Janssen asymptotes, with Janssen predicting a greater pressure.

Parameter	Value	Unit
d	4	m
h or y	30	m
ρ	770	kg/m^3
k	0.4	N/A
μ	0.7	N/A
ϕ	30	deg

Table 2.1: Parameter values and units

2.4.4 New Developments of Pressure Theories

With appropriate values, the Janssen equation can yield useful pressure results under static conditions to understand bin stresses. However, it does not fully capture

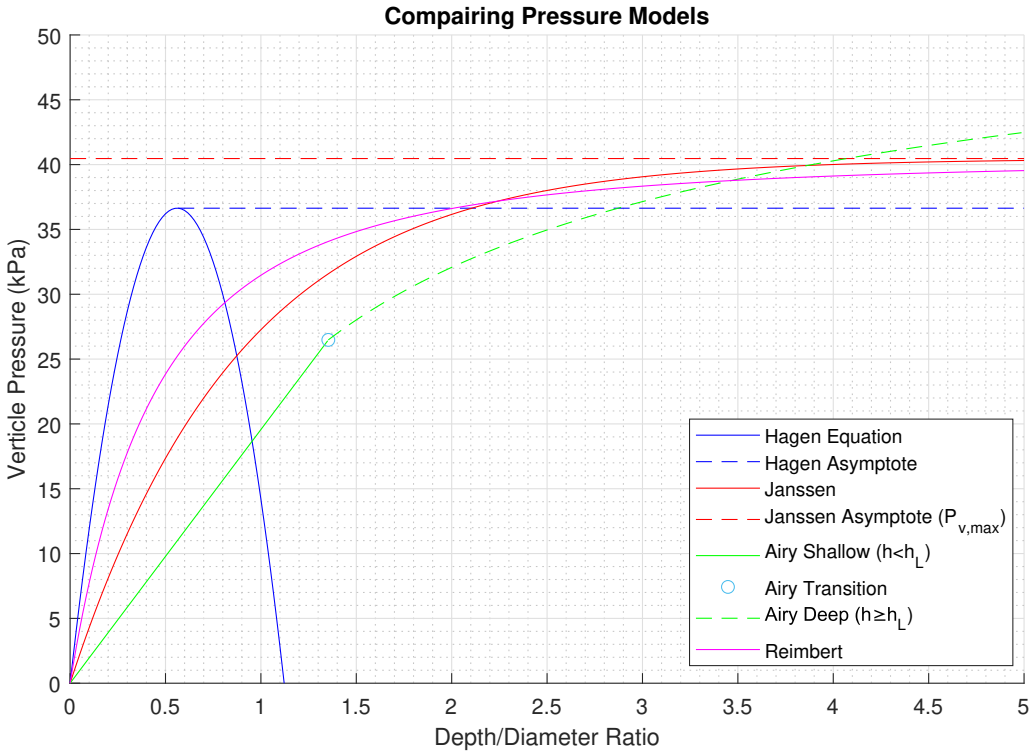

Figure 2.1: Comparison of historical bin pressure models showing vertical pressure (kPa) as a function of depth/diameter ratio. The graph presents four historical approaches to predicting pressure distribution in grain bins: the Janssen Equation (red curve) with its asymptotic limit (red dashed line), the Hagen Equation (blue curve) with its asymptotic behaviour (blue dashed line), and the Reimbert model (purple curve). Also shown are the Airy model's three pressure zones: shallow region (solid green) where $h < h_L$, transition zone (green circle), and deep region (green dashed line) where $h \geq h_L$. These models show how pressure approaches different asymptotic limits as depth increases, with variations in predicted pressures across the zones. The differences between these approaches, especially at lower depth/diameter ratios, show the uncertainties that differing assumptions in historical pressure modelling create. The values used to generate this figure are found in Table 2.1.

the pressure dynamics within a storage bin, specifically the bulk of the grain, and various models and theories have made advances. In particular, the elastic theory, as discussed by Bräuer et al. (2006) [106], Ovarlez and Clément (2005) [107], and Schillinger and Malla (2008) [108], as well as the ordinary stress linearity (OSL) and incipient failure everywhere (IFE) models highlighted by Vanel et al. (2000) [109]. Furthermore, microscopic theories presented by Xu et al. (1996) [110], the principal stress cap method introduced by Matchett (2006) [111], and a range of numerical techniques such as DEM, as described by Chen et al. (1999) [112], have added depth to understanding pressure fields within bins.

Many modern studies have attempted to validate or modify Janssen's model, instead of creating an entirely new theory. Di Felice et al. (2010) highlighted several works in the past decade and identified a literature gap that questioned important parameters in the Janssen model: μ and k [113]. Their work showed that, while many studies determined the numerical values of these parameters, their physical interpretation was not as clear. Moreover, empirically, their study showed some discrepancies when measuring these parameters. While De Felice et al. highlighted the need to investigate Janssen's assumptions, others have taken up this task. Janssen assumed bins to be a static and closed environment, where no forces are transferred from outside the system besides the weight of stored materials. This is not the case for most bins, which experience external forces from their environments, such as vibrations caused by machinery [114], earthquakes [115], intentional flow-inducing inertia forces [116], and bin honking (loud, resonant noise due to the slip-stick behaviour of the bulk material) [117]. Bertho et al. looked at the applicability of Janssen's model in dynamic environments, provided an overview of the current research, and considered the effect of wall movement on packing [118]. They found that the classical Janssen model was valid for bin walls that experienced several cm per second movement. Moreover, Windows-Yule et al. (2019) investigated horizontal wall movement and found that the Janssen model was also valid for a wide range of dynamic movements [119]. Notably, numerical methods have often investigated

this topic, an essential tool for understanding bulk solids, and this topic will be briefly introduced later.

Janssen's model is a macroscopic model, which treats the material as a continuum instead of a collection of particles. Bratberg et al. (2005) examined the threshold where microscopic behaviours turn into macroscopic behaviours through narrow granular columns [120]. They found that Janssen's model could not account for small container diameters. Similarly, for shallow granular pile heights, an interesting result discovered by Mahajan et al. (2020) was a "reverse Janssen effect." Specifically, the wall frictional forces could become compressive, effectively reversing the usual Janssen effect. Under this condition, the walls increase the effective mass of the bulk material at the bottom, which requires modification to Janssen's equation to predict the changes in effective mass as a function of height. This reverse effect was only observed when the height of a bulk solid pile was relatively small, that is, $h \leq 30d$ with d the diameter of a single particle. Thus, one generally do not expect to see this effect on large scales, such as within bins [121]. The continuum approach is typically used in analytical models, whereas numerical models can be applied to continuum and particulate material [112, 97].

Many works focused on addressing the inadequacies of Janssen's assumptions. Some examples include variable bulk density due to particle packing [122, 123, 124], variable angle of repose [125], horizontal bins [126], pressures in the hopper section [127], obstacles in bins [128], elastic deformation of bin walls [94], moisture content [129, 130], temperature [131], shallow bins [132, 94], as well as loading and unloading stresses [133], among others [134]. These modifications are relevant because they point toward higher-fidelity models that can better describe physical systems. Such modifications are potentially significant for future industrial applications and for advancing the literature.

Given the impracticality of addressing all the factors mentioned above, this research focuses on one key aspect: the variable stress field of a bin and its relation to k. The most fundamental and controversial assumption in Janssen's theory is the

constant lateral-to-vertical pressure ratio, k. The stress field fundamentally dictates this ratio in the bulk solid's mass. Many experiments have shown that this ratio is a function of material properties and location in a bin [130, 135].

The variation in radial stress in static pressure models can be traced back to 1948 [136] and was applied to a dynamic grain environment [137, 138]. Notably, Lvin (1971) and Cowin (1977) each developed models in which the vertical pressure across a bin's horizontal cross section was variable because k was not assumed to be constant, but these pressure theories are rarely referenced in the literature [139, 140]. More recent work has developed a theory of the behaviour of radial stress in the *2D* Cartesian coordinate system [129, 141, 1, 142], which was expanded to *3D* cylindrical coordinates [143, 1].

A unique and counterintuitive pressure distribution exists in a conical pile of bulk solids. Instead of the highest pressure occurring underneath the pile's peak, it forms a ring around this point. This phenomenon is well documented, but remains an open question in the literature today [144]. There is no comprehensive explanation for the phenomenon because it results from many complex properties of the pile that can be micro-, meso-, and macro-dependent, as well as time-dependent. Studies showed that it was a product of many factors such as the filling method [145], grain properties [146], and construction history [122], which have been further investigated with numerical methods [147, 148, 149, 150] and analytical models [151].

Most of the following covered the analytical approach to studying the stress within stored grain in a bin. However, the most widely applied tools have been modern numerical approaches. The origins of these methods can be traced back over half a century. On the first page of his foundational "Gravity Flow of Bulk Solids," A.W. Jenike, a leading figure in the mathematical study of grain flow, observed that the advent of computers could solve previously 'insoluble' mathematical problems related to the behaviour of bulk solids under gravity [152]. A decade after Jenike's statement, P.A. Cundall developed a computational method for solving problems in rock mechanics, initially named the Distinct Element Method, first presented

in 1971 at the International Symposium on Rock Mechanics. This computational method was later generalised to granular systems with the help of O.D.L. Strack [153].

At present, both Discrete Element Method (DEM) and Finite Element Method (FEM) are used in the study of bulk solids. DEM is a computational technique that is used to simulate the behaviour and interaction of many small particles, which makes it very effective for studying bulk solids [97]. FEM, on the other hand, is a numerical method for solving complex structural, fluid, and heat conduction problems by dividing a larger system, or continuum, into smaller, simpler parts called 'finite elements', enabling an approximate but detailed analysis of relevant system properties [154]. DEM is a more appropriate approach to studying bulk solids because it uses discrete particles that reflect the nature of bulk solids. Ramrez-Gómez (2020) created an in-depth review of the literature that discussed the main applications of DEM to bulk solids in silo research analysis of flow [155, 156, 157, 158], wall pressure, discharge rate, segregation, drying, rarefaction, particle packing, self-heating, and dust concentration [159]. In DEM research, parameters require calibration or tuning, so the simulation matches the physical behaviour of the system [160]. Additionally, DEM simulations need to limit the number of particles for computational purposes, and particle shape sometimes needs to be crudely approximated. However, strategies have been developed to mitigate these limitations [159].

Numerical approaches based on DEM have been utilised to investigate various properties of granular systems. The vertical stress variation in bins influenced by different filling methods was studied using DEM, which provided a valuable discussion on the use and limitations of the Janssen equation, the presence of a radial pressure distribution, and the ability of DEM to investigate these phenomena [161]. A combination of numerical DEM models and experimental observations showed that the radial distributions of normal pressure and shear stress at the bottom of a shallow silo demonstrated variable patterns (constant, increasing, decreasing, linear, convex, or concave) and were influenced by factors such as particle shape and filling

method, as was the lateral-to-vertical pressure ratio k [162]. Numerical approaches have also demonstrated the Janssen effect and suggest that k decreases asymptotically with packing depth [163]. The bulk density is affected by the height of the grain drop and the distribution of the kernel size [164]. Additionally, DEM was used to simulate the pore structures of a grain bulk within a silo. This structure was used to develop a pore-scale model to predict airflow resistance compared to experimental results [165].

2.4.5 Relating Pressure to Density Changes

The Janssen formula is widely used to understand the pressure systems experienced by the structure containing the grain and to account for the robustness of the grain bin's design. This emphasises structural safety and does not express accurate internal pressure systems. This research attempts to represent the complex internal system more accurately, whose importance will become more evident in this section. The compression of grains is caused by the pressure experienced by the weight of the grain, which is usually and perhaps problematically explained by the Janssen equation. The pressure experienced by the grain bulk produces a change in bulk density, packing the bulk tightly and causing an increase in bulk density.

Studies have been conducted to understand and predict grain packing factors, as they significantly impact storage management and inventory management accuracy. Research focused on error analysis of stored grain inventory has been investigated by Turner et al. (2016a) and showed that packing can be influenced by many factors, highlighting its difficulty. Such factors include initial bulk density, grain depth, moisture content, grain friction properties, shape of the storage structure, grain type, filling method, kernel dimensions, density, machine-induced vibrations, and biological activity from insects and moulds [12].

With this complexity in mind, many researchers focus on the role of the overburden pressures on the packing capacity of various commodities [166, 167]. Models have also been developed specifically for packing in hard red wheat [4], soybeans,

sorghum, oats, barley, and wheat [168]. Rogers et al. (2024) extended the Janssen effect model by incorporating parametric density models developed by Turner that transform the Janssen ODE into a Chini ODE, allowing the density to vary with depth along with other parameters [142]. Additionally, Thompson et al. (1991) created an Excel tool, WPACKING, which calculates the packing of various types of grain in different bin geometries. This tool is a direct application of the differential form of Janssen's equation and its intention was to be used by grain managers [169]. Finally, ASABE has created guidelines to predict the packing of several grains [92].

2.4.6 Lateral-to-Vertical Pressure Ratio

The Janssen equation remains the predominant theory used in industry despite its reliance on a critical simplifying assumption: a constant vertical-to-horizontal stress ratio (k). This assumption, which has been questioned since the introduction of the theory [90], forms the basis for the experimental work presented in this study.

In addition to producing the equation that bears his name, Janssen also gathered experimental data to validate his model. With novel instruments and techniques, Janssen measured the grain-wall friction coefficient (μ) and the pressure exerted at the bottom of the bin (σ_y). Although he intended to measure horizontal wall forces (σ_x), he encountered limitations due to material arching effects and apparatus constraints, leading to experimental improvements later implemented by Jamieson in 1906. To solve Eqn. 2.3 Janssen assumed that k was a constant, which many would immediately question: Bovey, Lufft, and Ketchum [90].

Rankine's formulation of k was one of the first theories of pressure for shallow bins because the pressure distributions within these structures behave analogously to retaining walls. It defines the stress ratio in terms of the internal angle of friction (ϕ). This assumption fails when the bin height increases; the pressure exerted on the bottom and sides of the bin no longer fits the observations because the bin walls were assumed to be frictionless [94]. This phenomenon is a property of bulk solids but was not considered until Janssen, barring the names mentioned earlier. Many different

numerical methods have adopted simplified versions of the Rankine formulation, along with many building codes for grain silos, for example, the Eurocode [91].

Even with the assumption of constant k, a wide variety of values is reported throughout the literature. This lack of consensus exists because k is not a fundamental innate physical property of bulk solids; it is an emerging result of the equilibrium arising from bulk materials' "fluid" nature [97]. The value of k is not realistically expected to be constant within a storage structure. The simplifying assumption is made because Janssen's equation works well within a contained column of material.

Ten years after Janssen's work was published J. Pleissner experientially showed that k varied throughout the depth of the matieral, and the result was widely accepted but mathematically ignored [90]. The variation of k through a large volume of bulk material has not been well studied experimentally. The research in this document conducts an experiment to observe the change in k by observing the radial variation in pressure, which will be discussed later.

It is difficult to include a varying k analytically, and Coulomb, Rankine, and Janssen all made the simplifying assumption of a constant $0 < k < 1$. Coulomb's approach produced a stress ratio that related the lateral and vertical pressure of the soil and was determined using the Mohr-Coulomb failure criterion [170]. Rankine simplified Coulomb's equations by assuming a frictionless and non-adhesive interface between the vertical wall and the bulk solid [171].

A mathematical model that took into account vertical and radial changes in stresses and k is discussed in the work of Zhang et al. [129]. They provided a literature review on the topic in the context of agricultural commodities up to the publication date. They reported that there was no consistent agreement on how pressure and the resulting k varied radially. Rusinek investigated the variation in the pressure of rape seeds using a hydraulic pressure transducer to determine the mean normal stress and mean shear stress on the wall, as well as the vertical pressure distribution, and found that k was significantly lower in the middle of the bin than

in the wall, and when the wall friction increased, so did k [172]. Horabik et al. discussed the behaviour of k within bins [173]. They reported that the pressure ratio was mainly dependent on the internal friction angle but also the shape of the seed (particles) and inversely related to the moisture content; the experimental uniaxial compression test produced values similar to the theoretical predictions given by the Rankine formulation of k. Qadir et al. (2010) showed experimentally that k increased with the ratio of the individual grain and diameter of the bin [174]. Sun et al. (2018) presented four independent approaches to k and applied them to deep and shallow bins. The results were compared with experimental data and three national standards [175]. They also compared different failure criteria to the typical Mohr-Coulomb criterion and recommended the Lade-Duncan (L-D) criterion to calculate wall pressure. Uniaxial compression tests showed that for cereal grains k decreased with an increase in moisture content [173]. In contrast, for calcareous sand, using a similar procedure, the increase in the water content initially increased k, which reached a maximum and eventually declined again [176].

Numerical studies that used discrete element methods suggested that k did not change with polydispersity [177]. Zhang et al. applied a two-parameter failure criterion typically used for soils to determine failure points [178]. When both parameters were non-zero, the lateral-to-vertical stress ratio increased with the vertical stress. At the same time, in other configurations, it was roughly equal to that determined by the Mohr-Coulomb failure criterion. Xu and Liang (2022) considered the elastic deformation of the bin walls in both static and dynamic states and demonstrated that the Rankine formulation of k would underestimate lateral forces [94]. Back et al. (2011) studied the effect of friction on the pressure ratio k [179]. Specifically, they focused on particle-particle friction, where the lateral pressure ratio was associated through analytical arguments. They established that k increased with particle-particle friction and packing.

The properties of a bulk solid environment have been shown to significantly influence the k patterns, which can drastically impact the accuracy of both analytical

and numerical models. Some factors that affect k are compression [180, 122, 181, 97, 182, 4, 167, 166] and fill conditions [182, 147, 183]. Handling procedures, commodity history, and wall-particle friction coefficients also contribute to the variable stress distribution [184]. Recent systematic measurements have provided robust evidence for k variation, with horizontal variations in vertical pressure documented in multiple studies [185, 186].

The complex nature of k variation in bulk solids highlights several key research needs. First, more comprehensive measurement systems are needed that can simultaneously monitor multiple parameters that affect k variation. Current understanding is limited by measurement technique discrepancies [187, 113], suggesting that improved instrumentation is needed to better characterize these relationships [13]. The development of more sophisticated models that can account for the complex interplay of factors affecting k distribution would advance our understanding of the behaviour of bulk solids. However, advancing these models requires better experimental validation through improved pressure measurement techniques. Despite these known limitations, the Janssen equation with its simplifying assumption of constant k remains the predominant industry standard.

This research attempted to address this gap through experimental work designed to systematically quantify variation in k. The following section will examine the development and current state of pressure sensor technology for bulk solids, which is crucial to implementing advanced control systems like DTs in grain storage management.

2.5 Bulk Solid Pressure Sensors

Understanding the pressure distribution in bulk solids is crucial for validating theoretical models and improving storage management systems. However, measuring these pressures presents unique challenges due to the complex nature of granular materials and their interaction with measurement devices. This section examines the evolution of pressure measurement techniques in bulk solids, from traditional

wall and floor sensors to specialized in-mass measurement systems, highlighting their contributions to our understanding of pressure dynamics in grain storage.

2.5.1 Uni-Directional Sensors

Experimental evidence has shown that pressures and the estimated k within a grain silo vary internally, but these studies are limited. This is because there is no standard approach to in-mass sensors used to capture the internal pressure data within bulk solids. Typically, only the wall or floor pressures are measured, with a few exceptions, which will be discussed below. With this being said, several studies have used various methods to measure vertical pressures at different locations within the grain mass.

A variety of sensors have been used to measure pressures in silos. Some have used a ring transducer method, which used five concentric rings that made up the bottom of the storage structure [188, 185, 181, 147, 172]. The weight of the bulk solid would bend the rings, causing deformations that would be translated into pressure readings. Studies have also used diaphragm-style sensors to measure vertical and horizontal pressure on floors and walls, which measure the deformation of a fixed plate [134, 181, 189, 190, 191, 192, 193, 194]. A membrane-style device is also used that transfers the load to a fluid behind it, which is then measured [172, 195, 196, 197]. Other pressure sensors functioned as a displaced rigid piston [187, 130, 94, 191, 192, 198]. Unique methods have also been used for specific applications outside of these more common approaches. A pressure "mat" was placed under a small pilot silo in a laboratory setting, providing a 2D map of vertical pressures at the bottom of the silo [199]. Another was a custom strain-type pressure sensor that functioned like deforming cantilever beams [184].

2.5.2 Triaxial Sensors

There is another set of novel pressure sensors that are all similar in approach. They are tensor-like triaxial devices that are placed in a bulk solid silo. The oldest example

is from Atewologun et al. (1991), who used three diaphragm sensors (strain-gauge) about 50 mm in diameter to capture normal stresses in three planes [188]. These sensors were held in place by a rigid wire frame. Each sensor was a circular thin plate with fixed support. The grains were glued to a cloth attached to each diaphragm, theoretically reducing the variation of the data due to grain orientation [188, 181]. Chen et al. used mass pressure sensors to investigate radially distributed horizontal and vertical pressures in a silo, but information on the sensor style was not included [130]. A significant limitation of this test was the small size of the test chamber, with a height of 500 mm and a diameter of 390 mm, and the sensors, with a diameter of 25 mm. Finally, Rusinek used six-faced sensors to measure the stress state from pressure measurements in six different directions [172].

Notable among triaxial sensors are two devices that attempted more comprehensive pressure measurements. The first used four flexible aluminum faces on a cube to measure stresses exerted on these faces via strain gauges [200]. The stress information was then converted to pressure information, and the device was used to analyse the pressure exerted during grain movement. The second, described in 1993, used three pressure sensors, each 18 mm in diameter, adhered to the acrylic sheets forming its housing [187]. This particular pressure sensor is no longer manufactured and no documentation is available, so the exact mechanism for data collection is unclear. The device was designed to sit at the bottom of a grain silo to measure stresses and was used to validate the pressure ratios for the Canadian Farm Building Code. To the knowledge of these authors, no publications were reported on the experimental data collected by these devices; only their design and calibration have been documented.

Chapter 3

Materials and Methods

3.1 In Situ Pressure Sensor

This section presents the development, calibration, and experimental setup of the novel triaxial pressure sensor for data acquisition. This experimental investigation aimed to characterize the radial pressure distribution within grain storage bins using triaxial pressure sensors. The primary objective was to collect comprehensive pressure data during both filling and emptying cycles to validate existing pressure distribution models and to understand the dynamic behaviour of granular materials in storage conditions.

3.1.1 Sensor Design

The triaxial pressure sensor was a 130 mm diameter 3D-printed sphere that contained three orthogonal sensors and electronic components, as shown in Figures 3.1a and 3.1b. Polylactic acid (PLA) was used to print the housing, which provided sufficient strength to withstand the pressure of the bulk solids during filling and unloading.

The size was minimized to prevent the disruption of the grain medium, which needed to be balanced with the sensor's electronics and mechanical requirements. More specifically, the diameter of the grain bin was 1.8 m, so the smaller the sensors

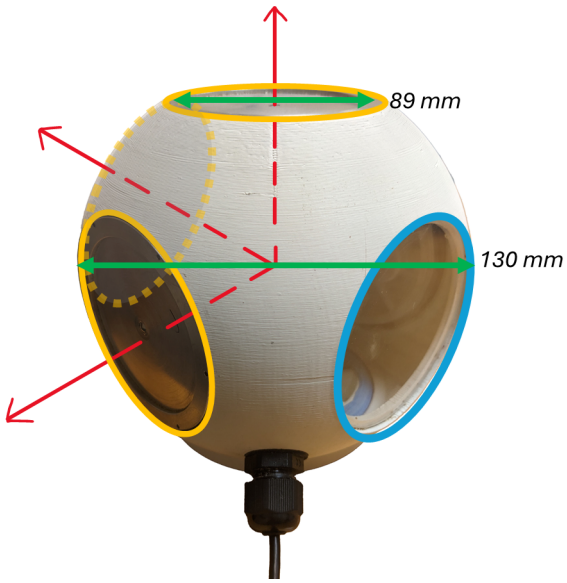

(a) External view of the 3D-printed spherical sensor shell (130 mm diameter) showing its key openings. The gray regions indicate the pressure sensor system locations, blue circles show the transparent viewing glass, and the bottom opening serves as an access porthole. There is also a black cable bushing to collect and feed the wires through of the shell. Red arrows indicate the axes of measurement.

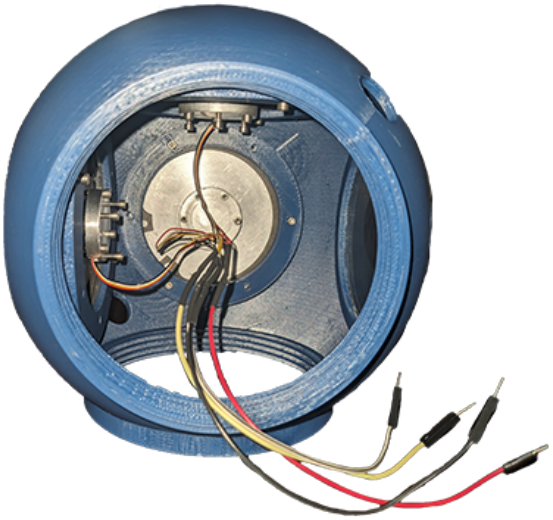

(b) Internal view of the sensor shell shows the three pistons mounted with their wiring harness within the spherical housing, which were connected to a microcontroller.

Figure 3.1: Two views of the Sensor Shell.

were, the less grain they displaced. This was important because it allowed pressure to normally transmit through the bulk. On the other hand, the sensors required hand assembly, which involved manipulating small components within the shell. The smaller the sensor chamber is, the more difficult it is to properly manipulate the mechanical and electronic parts without disrupting them.

This housing contains five 89 mm openings; three held the pressure sensor system (yellow circle), one was a transparent viewing glass (blue circle), and the final was used as an access porthole. The pressure sensor system was a piston-style design with a diameter of 89 mm, and the pressure plate was made of 3 mm-thick aluminum. The size of the pressure plate was strategically chosen to allow sufficient precision to monitor changes and prevent errors caused by deflection. The mathematical validation can be found in Appendix A.1

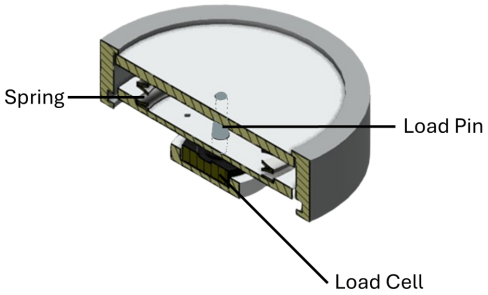

(a) Cross-section of the piston assembly showing the spring and load pin mechanism. The spring maintains stability while the load pin transfers force from the pressure plate to the load cell, ensuring accurate measurement of grain pressure.

(b) TE Connectivity's (TE) FX29 strain gauge.

Figure 3.2: Piston and Sensor

The pistons used a spring and load pin system that translated the force exerted on the face of the pressure plate to a load cell. As shown in Figure 3.2a, the load pin was connected to the top plate and pushed onto the sensor, while the spring was placed between two secure end points. The spring provided support and stability to the assembly to ensure that the load bin was always perpendicular to the load cell. A wave-style spring was used, as shown in Figures 3.2a and 3.4.

3.1.1.1 Piston System

The load cell was a button-style microscale strain gauge: the TE Connectivity's FX29K0-100A-0025-L (Figure 3.2b). It was glued to a separate cradle that was fastened to the back of the piston with six screws, three that drive the cradle towards the back of the piston and three set screws that limit the range of motion to prevent damage and provide structural stability: see Figure 3.3b. These screws were also used to align the cradle and piston surfaces, a process that is detailed later.

The accuracy of the load cell is ±1% of its full scale, which is 110 N. Given the cross-sectional area of the pressure plate of 0.0032 m^2, the highest pressure experienced by the system was 35000 Pa = 35 kPa. The sensor accuracy is ±1.1 N or ±0.35 kPa. The pressure plate area was partially limited by the size of the shell.

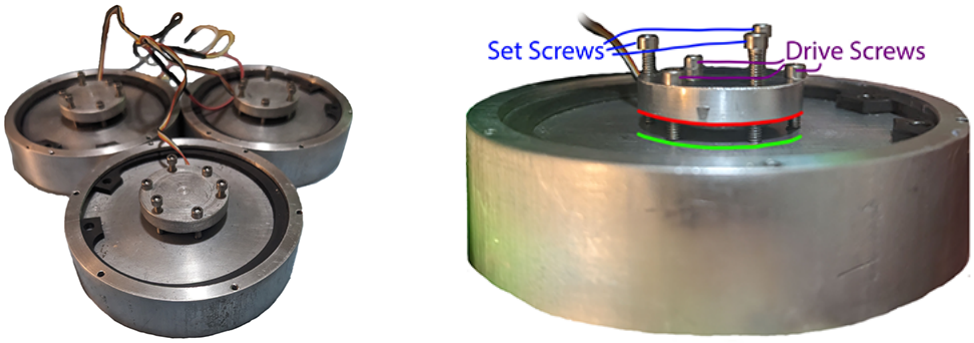

(a) Arrangement of three pressure cells (shown face down) used to collect pressure measurements at one location in different directions within the grain mass

(b) Detail of the sensor cradle and adjustment mechanism showing the critical set screws (blue) and drive screws (red). Set screws limited movement to protect the sensor, while drive screws allowed precise positioning of the sensor cradle against the piston body. The red and green alignment markers must be properly aligned to ensure accurate force transfer and measurement.

Figure 3.3: Piston-Style Pressure Cells

Figure 3.4: Wave Spring with End Shims

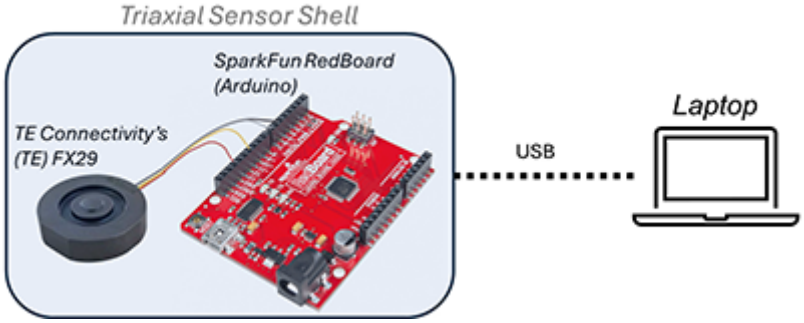

Figure 3.5: Microcontroller Setup

3.1.1.2 Integrated System

Piston systems were placed in three of the five shell portholes. They were positioned orthogonal to each other, allowing measurements to be taken along the x, y, and z axes. The portholes had a terminal ridge that allowed the pistons to be screwed into place, ensuring proper orientation. The three sensor systems communicated with the digital I/O pins on a SparkFun RedBoard (Arduino) using the Inter-Integrated Circuit protocol (I^2C). The setup is illustrated in Figure 3.5.

The final two portholes served as internal access and a camera viewport. The internal access hole was threaded to receive a PVC plug with a layer of Teflon tape, which ensured a secure fit; the shell included a threaded hole that can be seen in Figure 3.1b. Finally, the design included a camera to provide visual information on particle rearrangement, grain properties, or the presence of dockage/insects. This final porthole was covered with transparent glass to create the viewport. The camera also had a low-power LED light to provide sufficient light to capture images.

3.1.2 Calibration

To obtain accurate readings, the load sensor mount (red) and the back of the piston (green) had to remain parallel, as indicated in Figure 3.3b. The reason for this is that the load pin needed to be orthogonal to the pressure sensor's plane, or else it would be slightly distributed across this x-y-plane instead of directed at a singular point. This was achieved by making slight adjustments to the set and drive screws. This process used a caliper to measure the height at three points on the sensor mount plate. Then, the orientation of the sensor mount and the output count were fine-tuned by altering the set and drive screws. This was repeated until the mounting plate aligned parallel to the piston's face with 0.1 mm accuracy, while the sensor output was zeroed at approximately 4000 counts. This process is shown in Figure 3.6.

After the piston system was set up, the sensor output signal required calibration. The calibration process involved correlating the sensor output, measured in

(a) Measuring the height of the sensor mount at three points to ensure planar alignment.

(b) Using a digital caliper to verify the 0.1 mm alignment tolerance.

(c) Adjusting the set and drive screws to achieve planar alignment.

Figure 3.6: Piston calibration process

"counts", with the pressure exerted by a set of precision calibration test weights.

During calibration, known weights of 1 and 2 kg were placed on the pressure plate of the load cell, and their readings were recorded. The set of weights provided calibration points of 0, 1, 2, 3, 4, and 5 kg, which corresponded to pressures of 0, 3.097, 6.195, 9.292, 12.39, and 15.49 kPa, respectively. The data collected from the calibration tests were then analyzed using a MATLAB script to generate linear equations that directly related the sensor's output to the corresponding pressure for each of the nine pistons.

3.1.3 Experimental Setup and Data Acquisition

The experiment was designed to use the sensors in a real-world grain storage environment. Our goal was to capture a comprehensive pressure distribution of the grain silo, focusing on how it changed radially. This information would be used to tune the mathematical models used in this research, and discussed in Section 3.3.

3.1.3.1 Silo Characteristics and Grain Properties

A grain silo with a height-to-diameter ratio greater than two was selected to achieve the Janssen effect. The silo diameter was 1.8 m and was equipped with load cells to measure the grain's actual mass. The silo was built from corrugated steel with a

Figure 3.7: Experimental silo setup for pressure measurements. a) Material flow path showing grain transfer from main storage silo through elevator system to the instrumented test silo; b) Interior view looking upward at the silo inlet where grain enters from the elevator; c) Empty silo floor showing multiple radial discharge points (holes) that can be individually opened and closed to control the grain flow pattern during emptying; d) Exterior view of the test silo with sensor location marked (blue circle) where triaxial pressure measurements were taken.

peak-to-peak distance was 68 mm, and a peak-to-valley depth of 12 mm. Soft red winter wheat was used that had a moisture content of 13.5%, and a bulk density of 780 kg/m^3. The system is shown in Figure 3.7a), and the specific silo depicted in Figure 3.7d).

3.1.3.2 Sensor Placement and Filling Method

The filling process is shown in Figure 3.7a). Wheat was transferred from the main storage silo through an elevator system to our test silo at about 10 lb/s. From Figure 3.7b) the centre inlet of the grains is shown, which has a diameter of 0.1 m.

(a) First Setup

(b) Second Setup

Figure 3.8: Experimental setup used for Trials 1 and 2. This is a bird's eye view of the setup, where the sensors are all at the same height in the silo: the bottom. All angular sensors point counter-clockwise, and radial sensors inward. The coloured lines represent measurement distances, with the light green line showing the centre-to-wall distance, while all other coloured lines indicate centre-to-centre distances between sensors. The sensors' colour corresponds to the lines found in the figures that graph their data, such as Figure 4.2.

A small amount of grain was first added to the silo (about 0.2 m depth). Then we placed the triaxial sensors at specific radii on the silo floor, making sure they were oriented correctly as shown in Figures 3.8a and 3.8b. A small port hole in the side of the silo allowed personnel to enter and leave while the grain was less than 1 m deep, which can be viewed in 3.7b). The sensors were manually covered with grain to prevent them from shifting during the experiment, as seen in Figure 3.9 a). The depth of the sensors was determined by grain height, which ensured both their orientation and depth were correct (Figure 3.7). The sensor cables were fed through small openings in the silo wall and connected to laptops for data recording.

Both the triaxial devices and the bin's weight sensors logged data continuously. We resumed filling and periodically measured the grain height using a laser system. These height measurements were synchronized with the weight measurements from the silo's sensors. This allowed us to correlate time, mass, and grain height with the pressure data. We filled the silo to a final grain height of 6 m.

Figures 3.8a and 3.8b show a "bird's eye" view of the silo looking down, with

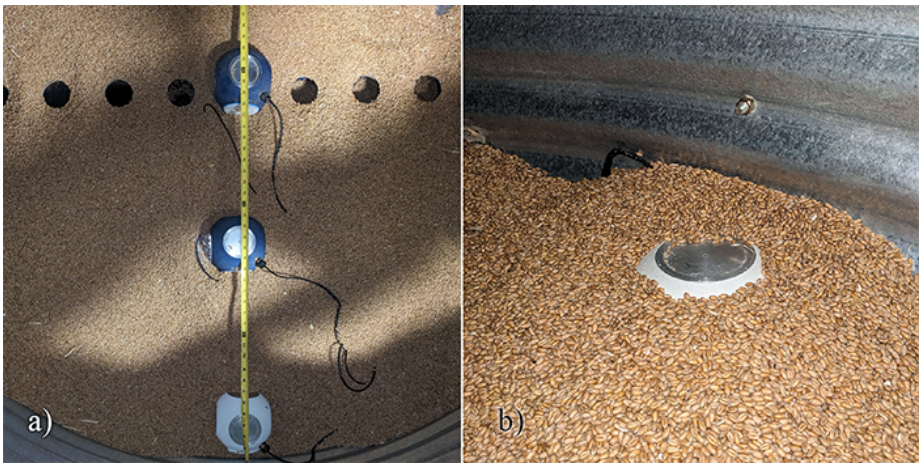

Figure 3.9: a) The three sensors are aligned along the silo radius at measured distances (marked by measuring tape) and surrounded by discharge openings (black holes) visible in the silo floor. This configuration corresponds to the straight-line arrangement used in Trial 2, and the sensors are semi-buried to promote stability while filling. b) After emptying, the sensors remained in their correct position and alignment, for example the wall.

the positioning of the sensors. All sensors are on the same plane, both in height and orientation, and are placed at the bottom of the silo in the 0.2 m of grain, as shown in Figure 3.7d. We used two sensor arrangements: a spiralling arrangement (Figure 3.8a) for the first data set and a straight-line arrangement (Figure 3.8b) for the second experiment. The radial sensor direction points to the centre of the bin, the angular direction is counterclockwise, and the vertical direction points upward.

3.1.3.3 Discharge Process

After filling was complete, the grain was emptied from the silo by opening the central outlet shown in Figure 3.7c. The multiple discharge points visible in the figure allowed us to control the speed and flow pattern if needed. We monitored pressures continuously throughout the emptying process until the silo was completely empty. After emptying the silo, it was confirmed that the sensors remained in their position and an example of the orientations is shown in Figure 3.9 b). Once all wheat was removed from the silo the data acquisition was terminated.

3.2 Digital Twin

A single-page application was generated to serve as the DT. The front end was powered by Python and Streamlit, and the back end was handled by Google's Firebase. The user is capable of inputting data corresponding to the bin's physical attributes, as well as grain entering the bin. The grain bin that was "twinned" was 1.8 m in diameter, 6.0 m high, made of corrugated steel, filled with wheat, and was located at the University of Kentucky. Novel mathematical models were included that have been informed by the data from the in situ pressure sensors described here [1, 201]. These mathematical models and sensors were specifically developed to create this DT, as there are few models and tools to investigate the static pressure distribution of the grain interior [88]. The functionality of the DT and the specific actions that it performed will be documented in the results Section 4.2.

3.2.1 System Overview

This DT application followed a three-tier architecture comprising data, application, and user interface layers. The backend handled data management and is built on Firebase. The application used Python to perform mathematical calculations of grain behaviour. The front end, developed using Streamlit, provided an interactive dashboard for users to manage grain inventory, visualize bin conditions, and run simulations. This architecture enabled the integration of physical models with operational data. Furthermore, Streamlit allowed the application to run Python code server-side instead of on a user's device.

The system provided simulations through background calculations that update when inventory changes occur. These simulations included pressure distribution, grain compaction, storage conditions, and drying, which provided real-time insight into bin conditions and possible future conditions. The modular design of the interface and calculations allowed for independent updating of simulation parameters and models, ensuring the DT could evolve with improved models of grain behaviour or specific storage requirements. This architecture supports scalability to handle in-

creased numbers of grain bins and larger farm operations through Firebase's cloud database, while enabling integration with other farm systems through standardized data formats like JSON. Python's scientific libraries provide flexibility for implementing additional grain behaviour models as research in this area progresses.

The Python code used several external libraries: SciPy for computational mathematics, numerical integration, special functions and optimization; Matplotlib for plotting; Streamlit for the user interface; NumPy for mathematical operations; Pandas to handle data; Requests for HTTP client functions; Plotly for 3D visualization; and Meteostat for weather data retrieval. It also uses built-in Python modules such as JSON to structure data.

3.2.2 Database

The backend used a Google Firebase set up as a NoSQL hierarchical structure, as shown in Figure 3.10. The advantages of using a NoSQL database were that it provided freedom and flexibility with structure while developing; the JSON tree format was used, a straightforward framework from which to work, requiring no SQL commands. The code was read and written to the database using HTTP requests. A fetching function used `GET` requests to retrieve inventory data and converted it to a pandas DataFrame for easy data manipulation. The updated function converted pandas DataFrame data back to JSON format before using `PUT` requests to update records.

The database path `users/{user_id}/{bin_id}` represented the hierarchy, which was then populated with multiple inventory records. These records were populated with information provided by the user or automatically: the date of their addition, the type of commodity, mass, test weight, and the moisture content. The record also included a calculation of the height of this grain slice, which did not include compaction. This is because global compactions and height changes were calculated separately, which will be discussed later. By reading and editing these entries, we were able to provide real-time data updates to inventory management, with auto-

```
DATABASE/
└── users/
    └── {user_id}/
        └── {bin_id}/
            └── inventory/
                ├── record1: {
                │   "Date": "2024-11-15 10:00",
                │   "Commodity": "Hard Wheat",
                │   "Mass_tonnes": 100.0,
                │   "Test_Weight_kg_m3": 780.0,
                │   "Moisture_Content_percent": 14.0,
                │   "Height_m": 5.2
                │ }
                └── record2: {...}
```

Figure 3.10: Firebase Realtime Database Structure for Grain Storage DT, showing one record.

mated calculations for more complex features such as pressure analysis, compaction, drying, and the effects of compaction on drying simulation.

Google's Firebase allowed for instant synchronisation across multiple clients or "users." Although the current implementation used public access, Firebase included strong security features through customisable rules and authentication protocols.

3.2.3 Data Inputs and User Interface

The front end provided a forum to allow users to input data into the bin, which populates the back-end database. The design goal of this was to track the minimal data input that most farmers have access to that would be needed for simulations of more complex bin processes, such as drying/aeration. The inputs required are commodity type, mass added, average bulk density, and moisture content. All these properties of a grain addition are reasonable to expect a farmer to have access to, except the latter. Moisture content data could be read off a bench-top device, harvester, or bin cables. This form provided a list of all potential commodities and properties on which the application layer had modelling data. Furthermore, each bin could be customized to reflect the geometry and material of the real-world bin, which will affect the simulations.

3.3 Mathematical Modelling

The core functionality of the DT relied on mathematical models that describe the pressure distribution and the resultant compression experienced by stored grain. The pressure model implements the separable function approach developed by Rogers et al. (2024), which was investigated using empirical data from the novel pressure sensor system in a 1.8-m-diameter grain bin with wheat heights 0 to 6 m [1, 201]. In addition to these main features, a drying simulation software was created as an early proof-of-concept prototype. It was based on the popular equilibrium air drying model theorized by Thompson [202]. Furthermore, the effects of variable density, as described in Section 3.3.1, on the drying model are investigated later in Section 4.2.4.

3.3.1 Pressure Distribution Model

Rogers' model was able to consider a radial variation in pressure because it treated the shear stress within the bin as a separable function. This allowed shear stress to be factored as the product of two independent, separable functions containing the radial (r) and vertical (y) dependencies. Therefore, shear stress would change across the diameter of the bin, resulting in variable pressure across the radius of the bin. Traditionally, shear stress (τ_{xy}) is known at the edge of the bin (the friction between the wall and the grains) and is the cause of the Janssen effect. In Rogers' work, this definition is nuanced and extended to the interior of the bin. At any point in the bin, the shear stress is described by,

$$\tau_{xy}(x, y) = S_f(y) \left(\frac{x}{b}\right)^h \tag{3.1}$$

However, the exact nature of how the shear stress changes across the radius of the bin is unknown. The advantage of the Rogers model is that it is completely general and any form of $f(x)$ can be used to describe this variation,

$$\tau_{xy} = f(x)S(y) \tag{3.2}$$

where b is the radius of the bin and h is the power-law exponent that controls the radial variation of the shear stress. The function $S_f(y)$ describes the vertical variation of the stress field and is given by,

$$S_f(y) = \rho g b \left[1 - \left(\cosh(\delta_1 y) + \frac{\sinh(\delta_1 y)}{\sqrt{1 - A/B^2}}\right) e^{-yB/A}\right] \tag{3.3}$$

The derivative of this function, which is crucial for determining the complete stress field, is,

$$\begin{aligned} S'_f(y) = \rho g b \Big[&- \delta_1 \left(\sinh(\delta_1 y) + \frac{\cosh(\delta_1 y)}{\sqrt{1 - A/B^2}}\right) e^{-yB/A} \\ &+ \left(\cosh(\delta_1 y) + \frac{\sinh(\delta_1 y)}{\sqrt{1 - A/B^2}}\right) \frac{B}{A} e^{-yB/A}\Big] \end{aligned} \tag{3.4}$$

where $\delta_1 = \frac{B}{A}\sqrt{1 - A/B^2}$

3.3.1.1 Stress Components

From these base functions, we can determine the horizontal and vertical stress components. The horizontal stress σ_x is calculated as,

$$\sigma_x(x, y) = \frac{S_f(y)}{\mu} + \frac{b^{h+1} - x^{h+1}}{b^h(h+1)} S'_f(y) \tag{3.5}$$

The vertical stress $\sigma_y$is given by,

$$\sigma_y(x, y) = \alpha(x, y) \left[\frac{S_f(y)}{\mu} + \frac{1}{b^h(h+1)} S'_f(y)(b^{h+1} - x^{h+1})\right] \tag{3.6}$$

where $\alpha(x, y)$ is the stress ratio coefficient,

$$\alpha(x, y) = \frac{1}{\cos^2\phi}\left(1 + \sin^2\phi + 2\sin\phi\sqrt{1 - \frac{\beta^2}{\tan^2\phi}}\right) \tag{3.7}$$

where ϕ is the internal angle of friction.

This equation is based on the Mohr-Coulomb failure criterion, and as a result there exist some limitations that should be noted here but will be discussed later in Section 5.1.

3.3.1.2 System Parameters

For this particular application, the model requires two key parameters, A and B, which are determined using equations 3.8 and 3.9. Rogers defined other cases, but they are not relevant here and are unphysical. These are described mathematically as,

$$B = \frac{b}{2\mu\cos^2\phi}\left[1+\sin^2\phi+\frac{2\sin\phi}{(h+1)\sqrt{1-\mu^2/\tan^2\phi}}\left(1-\frac{\mu^2}{\tan^2\phi}+hF\sqrt{1-\frac{\mu^2}{\tan^2\phi}}\right)\right] \tag{3.8}$$

$$A = \frac{2\mu b}{h+1}B - \frac{1}{b^h(h+1)\cos^2\phi}\left[\frac{b^{h+2}}{h+2}(1+\sin^2\phi)+2\sin\phi q\right] \tag{3.9}$$

Where q is determined through numerical integration,

$$q = \int_0^b x^{h+1}\sqrt{1-\left(\frac{x}{b}\right)^{h+1}\frac{\mu^2}{\tan^2\phi}}dx \tag{3.10}$$

And F is the hypergeometric function,

$$F = {}_2F_1\left(\frac{1}{2},\frac{1}{2h},\frac{2h+1}{2h},\frac{\mu^2}{\tan^2\phi}\right) \tag{3.11}$$

3.3.1.3 Numerical Implementation

Let us now consider how these equations were implemented in the DT. Using the model described above, the pressure distribution was computed on a grid of 101 × 101 (x_i,y_j)that spanned the bin radius and height. An odd number of points was chosen so that the exact bin centre would be defined,

$$x_i \in [0,b], \quad i = 1,\ldots,101 \tag{3.12}$$

$$y_j \in [0, H], \quad j = 1, \ldots, 101 \tag{3.13}$$

Where b is the radius of the bin and H is the total grain height.

The stress fields at each point (x_i, y_j) was calculated using eq.3.5, 3.6,the necessary system parameters (eqs. 3.8 and 3.9), and the alpha value (eq. 3.7).

For compaction, the 101 × 101 stress grid was computed using a common exponential approach [2, 3, 4]. This is described mathematically as,

$$\Delta\rho_k(x_i, y_j) = a_k \cdot \exp(b_k \cdot MC_k) \cdot \left[\frac{\sigma_y(x_i, y_j)}{1000}\right]^{c_k} \tag{3.14}$$

where the empirical coefficients $[a_k, b_k, c_k]$ are commodity-specific as given in Table 3.1.

Table 3.1: Commodity-specific compression parameters [2, 3, 4].

Commodity	a	b	c
Hard Wheat	-0.488	6.59	0.0203
Soft Wheat	-0.8034	8.0876	0.039415
Corn	-1.29693	7.11178	0.078701
Rice	-0.7580	8.9355	0.0499

Note that the Janssen compaction data (discussed more in Section 5.2) used a differential slice approach, which produced better results compared to traditional approaches [169, 168].

3.3.1.4 Multi-layer Implementation

With the DT, there's a possibility that grain from various locations of a farmer's field, each with potentially different properties, would be placed on top of each other, creating a non-homogeneous interface. For bins containing multiple grain layers, the model maintained the continuity of stress across the interfaces of the layers while accommodating different material properties. This meant that first, the pressure remains continuous across layer boundaries; the pressure at the bottom of one layer must equal the pressure at the top of the layer below it. Secondly, the density changes are accounted for at layer transitions. When a new grain type experiences

pressure from the layers above, its density increases from its initial value based on the specific compressibility of that layer's properties. Finally, the total pressure at any point is calculated by considering only the effects of the layers that are actually above that point. This builds up the complete pressure profile layer-by-layer through the entire bin.

3.3.1.5 Boundary Conditions

The model implements two boundary conditions. At the wall boundary ($r = b$), the shear stress equals the product of the coefficient of friction and the radial stress ($\tau_w = \mu\sigma_r$). Additionally, at the grain surface ($y = 0$), the vertical stress equals zero ($\sigma_y = 0$). These conditions are used so that the model accurately represents the physical behaviour of the stored grain while maintaining mathematical consistency.

3.3.2 Drying Model

The phenomenon of grain drying has two main factors: moisture transfer and heat transfer [203]. These factors work together as moisture either evaporates and diffuses out of the grain kernels or the kernels absorb moisture using air as a medium. Heat is required to evaporate moisture supplied by air or grain. The rate of moisture evaporation depends on three main factors, ignoring more nuanced phenomena such as tortuosity: the rate of heat supply, the moisture content of the grain, and the difference in the moisture content between the air and the grain. The rate of heat transfer depends on the air flow rate, the temperature of the air, and the temperature difference between the air and the grain. This entire process occurs over time, and as a result, different fronts develop, which is shown in Figure 3.11.

'Zone A' represents the dry grain in equilibrium with the ambient air being pulled into the bin by the fan. 'Zone B' represents the grain in the drying process, where the moisture content and temperature are changing. 'Zone C' is wet grain. In practice, its temperature and moisture content would change due to moisture moving from Zones A and B and depositing into this region, but for this ideal case,

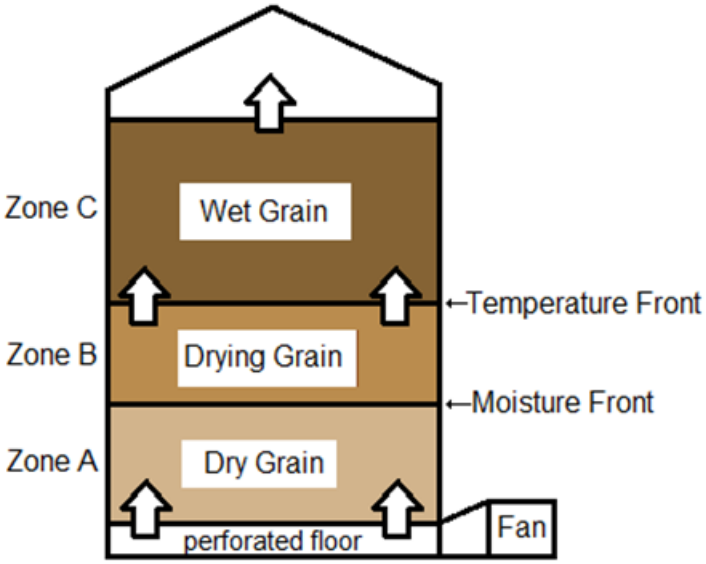

Figure 3.11: In-bin grain drying zones (A-C) showing the progression of temperature and moisture fronts through the grain mass, with airflow direction indicated by arrows. The darker colour represents a higher moisture content.

it is the original temperature and moisture content. The moisture front is when the moisture begins to rise again towards the initial moisture content (MC). Finally, the temperature front is where the temperature of the grain reaches its starting value. Different transport phenomena occur depending on MC and the heat of the grain and the ambient temperature.

To model this process, there are three main types of grain drying models, each with its own shortcomings and drawbacks. The first is a non-equilibrium model that uses four partial differential equations to describe the exchange of moisture. These models are more detailed and require complex algorithms to solve the equations because they cannot be solved analytically, but provide better results for heated air drying as they do not assume an equilibrium state [204]. The second is equilibrium-based and will be discussed more in-depth below, but it makes the assumption that air and the grain are at equilibrium. The final is logarithmic and is not often used due to its low accuracy (Jian et al., 2019). This work used an equilibrium-based model inspired by Thompson's work [205, 202, 206, 207].

3.3.2.1 Drying Equations

This work's approach to in-bin drying simulation is an equilibrium model and is based on J. Lawrence et al. (2015) [206]. It drew upon the work done by V. K. Jindal, both of which are fundamentally based on T.L. Thompson's model [205, 207, 202]. Furthermore, a dissertation completed in 2015 on the topic "A Simulation Platform for Accurate Prediction of In-bin Drying and Storage of Rough Rice" by H. Zhong was a beneficial resource for approaching this type of equilibrium model, although in the context of rice [208].

This model attempted to capture real physical phenomena using equations and 6 simplifying assumptions, which are articulated in Appendix A.2. The core simplifying assumption is that there will be a grain-air equilibrium when air enters a section of the bin, with regard to both moisture content and thermal energy. The model used seven equations, each of which is defined below, and each variable within the equation will be further defined in the Appendix A.3.

The grain mass was divided into multiple layers of thickness dx. Air enters and exits the layer with different characteristics. Based on Assumptions 5 and 6, the following energy conservation was used to describe each layer of the grain,

$$c_a T_o + H_o(h_v + c_v T_o) + c_g T_o R + c_w T_o(H_f - H_o) = c_a T_f + H_f(h_v + c_v T_f) + c_g T_f R \tag{3.15}$$

Where T_g was the grain temperature, H_o, H_f were the absolute humidity of the air that existed and entered the grain, and T_o, T_f were the initial and final temperatures of the air moving through the grain.

The first term described the initial enthalpy of the dry air that entered the layer. The second described the enthalpy of the water vapour entering the layer of grain. The third term is the initial enthalpy of the grain mass of the layer. The final term on the left-hand side of the equation described the change in moisture content of

the layer because of absolute humidity differences and the resulting enthalpy change. The three terms on the right-hand side of the equation are analogous to the first three on the left only described the air that exited the layer.

From this first equation, other supplementary equations were created to describe the terms in the equation,

The change in absolute humidity to the change in moisture content of the commodity was related using the following equation,

$$H_f - H_o = \frac{(M_o - M_f)R}{100} \tag{3.16}$$

The following was used to represent the dry matter to air ratio, which could also be understood as the grain-air mass ratio within the layer thickness. This equation also contained the time step (t).

$$R = \frac{\rho_g \times dx \times dmf}{\rho_a \times v_a \times t} \tag{3.17}$$

Eq. 3.17 was important to the overall functioning of the model and is discussed in more detail in Section 4.2.4.

The partial vapour pressure of the water vapour defined by the ASABE standard and equations 5, 6 [209] and shown below,

$$P_v = \frac{101325}{0.6219 + AH} \tag{3.18}$$

The saturation pressure of water vapour is described by the following empirical equation,

$$P_s = K \times e^{\frac{A+B\times T^2+C\times T^3+D\times T^4+E\times T^5}{F\times T-G\times T^2}} \tag{3.19}$$

Where the values for A, B, C, D, E, F, G, and K are found in the ASABE standard [209].

The mathematical definition of relative humidity (RH) is,

$$RH = \frac{P_v}{P_{ps}} \tag{3.20}$$

Finally, the RH of air when it was in equilibrium with the grain, assumption 5, is found below,

$$RH_{Chung} = e^{[\frac{-A}{(T+C)} \times e^{(-B \times MC)}]} \tag{3.21}$$

Where the values for A, B, and C were found in the ASABE standard [210].

3.3.2.2 Numerical Implementation

The numerical model employed an iterative layer-by-layer approach to simulate grain drying dynamics. This was a common approach covered in many publications [205, 202, 206, 207]. The algorithm solved a system of coupled equations for each thin layer of grain, incorporating the heat and mass transfer principles discussed in Section 3.3.2.1. As shown in Figure 3.12, it iteratively adjusted the absolute humidity of the exit air (H_f) until the relative humidity equilibrium between the grain and the air was achieved ($RH_{air} = RH_{grain}$).

The simulation progressed vertically through the grain bed, using the output conditions of each layer as input for the next layer. The discretization approach, illustrated in Figure 3.13, divided the grain bed into thin layers to model progressive changes in moisture content and temperature. At each time step, the model updated the moisture content and temperature profiles based on previous iterations. Key input parameters included ambient conditions (temperature, humidity), initial grain properties (moisture content, temperature, bulk density), and system specifications (bin dimensions, airflow rate). The model output the grain moisture content and temperature of each differential slice over time.

The simulation code was built upon Thompson's 1972 paper, and implemented his equilibrium-based approach with improved numerical methods enabled by modern computational resources[202] and overviewed in Figure 3.12.

The code took the known inputs collected from the DT, such as grain moisture

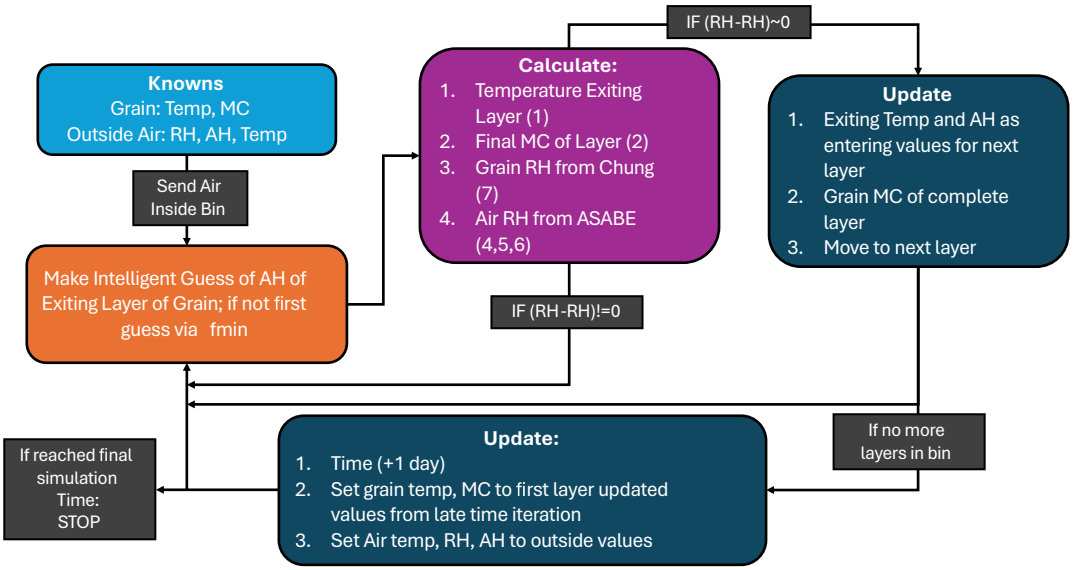

Figure 3.12: Flow chart of the grain drying algorithm showing the iterative process of calculating equilibrium conditions for each grain layer. The algorithm progressed through initial conditions, layer-by-layer calculations, and time step updates until reaching the final simulation time. The variables are defined in Table A.1.

content, temperatures, densities, and air conditions. These were indicated in the blue "Knowns" box in the flow chart from Figure 3.12. The `guess_h_out` functions implemented the "Make Intelligent Guess of AH" logic shown in the orange box. Using this guess the algorithm could calculate a number of grain and air properties found in the purple "Calculate" box: the temperature exiting layer (calculated as `Ta_out`), the final MC of layer (calculated as `MC_f`), grain RH using Chung's equation (`RH_from_g = chung(MC_f, Ta_out)`), air RH from ASABE standards (`RH_from_a = get_rh(H_out, Ta_out)`). These properties were assuming that the air and the grain were in equilibrium: $RH_air = RH_grain$.

This assumption allowed us to use the optimization `minimize ()` in the function `run_simulation`, which implemented the "equilibrium" check loop (`IF (RH-RH)=0`) that verified when the relative humidity difference between the grain and air approached zero. This was accomplished by searching for the optimal value of air absolute humidity (`H_out`) that minimized this difference.

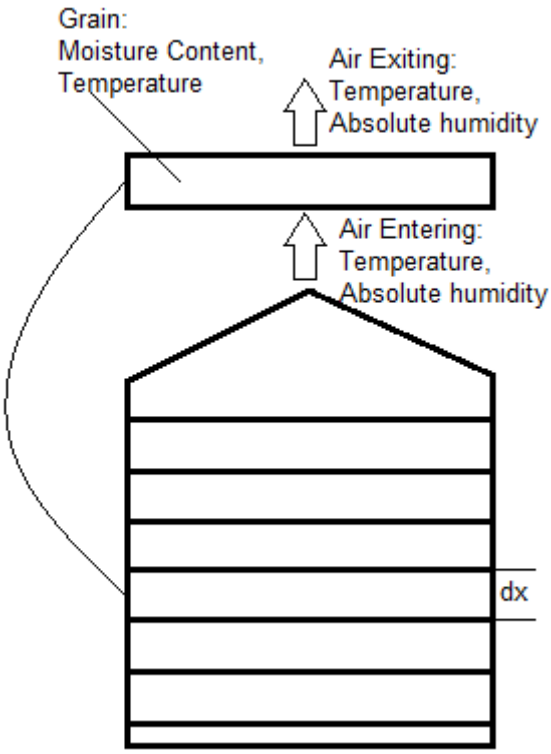

Figure 3.13: Representation of the discretized grain bed model showing thin layers (dx) with associated air and grain properties. Each layer exchanges heat and moisture with the passing air, where entering air conditions are determined by the exit conditions of the previous layer.

Once this was accomplished, the grain differential slice was updated. The exit temperature and the RH values were updated as the entering values. This was repeated for each layer until the top layer was reached, after which the time increment increased (+1 day). Please note that this was how frequently the ambient conditions updated, which drove the simulation, and was the time period for which the drying effects were averaged. This whole process was repeated until the final time was reached.

3.3.2.3 Model Validation

This mechanistic model was originally developed by this author as a MATLAB script to describe rice drying in grain bins. This work was rewritten in Python, and described the drying of rice, as mentioned above. In the original form, the simulation results were compared with a controlled laboratory experiment published

in literature. The model produced a drying simulation of the moisture content with an R^2 value of 0.9606 vs the data set and 0.9842 versus the model of the literature. This means that the model could account for 96% of the variation in the data, there was a strong correlation between the data and the model's predictions, and the residuals are relatively small compared to the overall variation in the data. With this being said, these results are not the main focus of this research and are therefore found in the Appendix A.4

Chapter 4

Results

The results from the triaxial sensor and the DT's client—and server-side development are presented in the following chapter.

4.1 Tri-Axial In-Situ Sensor

This section presents the results of the calibration process and the data collected in a full-scale pilot grain silo at the University of Kentucky.

4.1.1 Calibration

The data used to calibrate the sensors was processed using MATLAB. The results showed that each sensor demonstrated a linear relationship between weight and counts. The calibration with the lowest R^2 value is presented in Figure 4.1. The other calibration curves had equal or better linearity, which means all the sensors had a good correlation between readings and pressure.

4.1.2 Sensor Results

The sensor data gathered from experiments 1 and 2 are presented in Figure 4.2. The dashed line represents the results of the Janssen equation, with Table 4.1 detailing the parameters used to generate it, which matched the silo and material properties

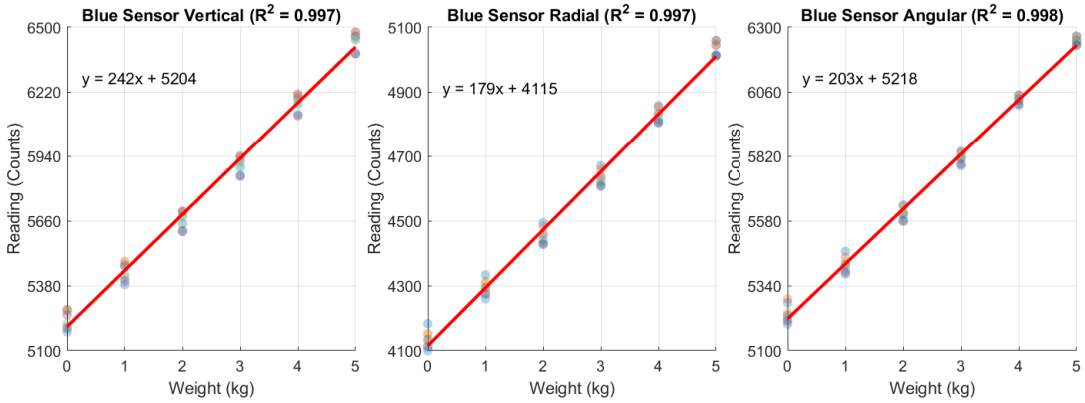

Figure 4.1: The "least linear" calibration example. All other calibrations had equal or better linearity. The sensor name corresponds with Figure 3.8a and 3.8b, and was the sensor positioned at the wall.

of the commodity used (wheat). Each colour corresponds to a different sensor, as shown in Figure 3.8a and 3.8b. For example, the green line with circle markers in Figure 4.2 shows the readings from the first experiment obtained by the sensor labelled White as a function of grain height, which was located at the wall of the bin.

Parameter	Value	Unit
Bulk Density (ρ)	780	kg/m^3
Lateral-to-Vertical Pressure Ratio (k)	0.4	n/a
Coefficient of Friction (μ)	0.4	n/a
Diameter	1.8	m
Hydraulic Radius (R)	0.45	m

Table 4.1: The parameters used in the Janssen equation visualization used to generate Figure 4.2. The bulk density was determined experimentally using a cox funnel and 0.5L test weight cup. Lateral-to-Vertical Pressure ratio and coefficient of Friction were taken from the ASABE guidelines [5]. The diameter was that of the silo used, and the hydraulic radius was determined mathematically from this.

Figure 4.2 shows that vertical pressure generally aligns with the expected results of the Janssen equation, although pressures often exceeded Janssen's estimates. It has long been known that the Janssen equation typically underestimates the vertical pressure. An explanation is its inability to account for the compaction of bulk solids, an issue addressed in some research using the differential form and density packing [180, 169, 142]. It should be noted that because many standards are based on Janssen's model, there are practical implications of reality exceeding this model's

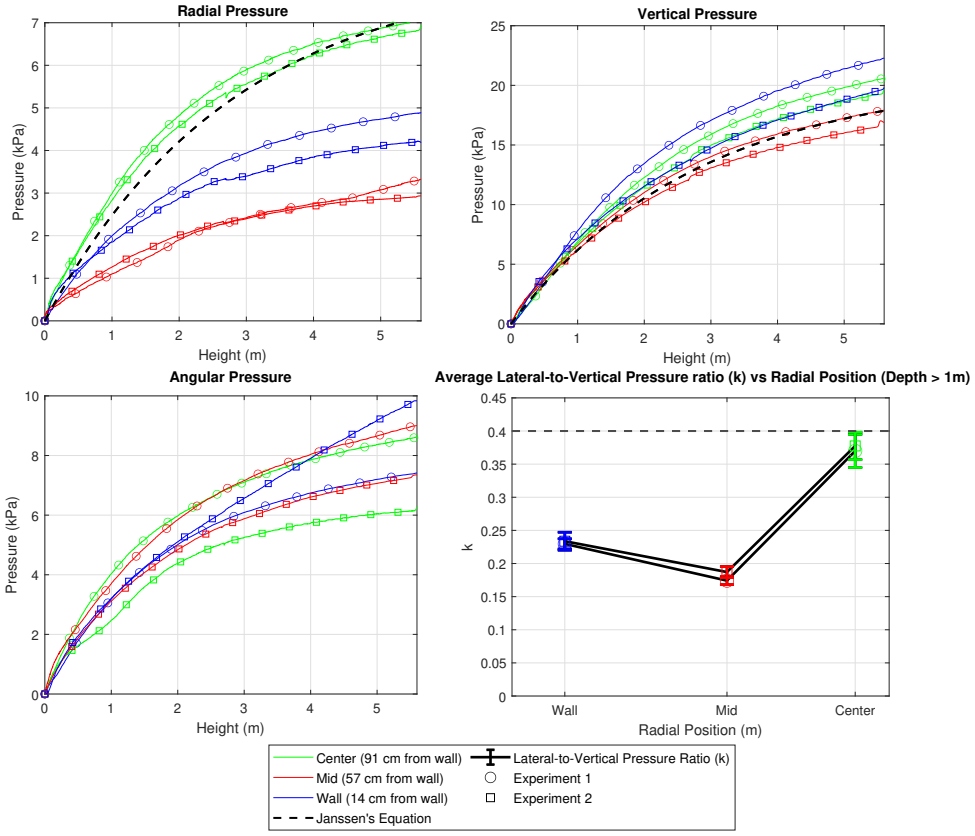

Figure 4.2: Results from two silo experiments showing pressure distributions and lateral-to-vertical pressure ratios in stored wheat. Data from three sensor positions are shown: Wall (Blue; 14 cm from wall), Mid (Red; 62 cm from wall), and Center (Green; 91 cm from wall), with measurements from Experiment 1 (circles) and Experiment 2 (squares). The dashed black lines represent Janssen's theoretical predictions. The lateral-to-vertical pressure ratio subplot includes a dashed reference line at k=0.4, showing significant variation in k-values across the silo width for fill depths greater than 1 m.

predictions, such as for inventory estimations, but most notably structural soundness of storage containers.

The vertical data showed that the pressure at the centre was consistently the lowest, within 5±% of Janssen's results. The wall sensor recorded significantly higher pressures in experiment 1, approximately +25% above Janssen's predictions. Similarly, the centre sensor also exceeded Janssen's predictions by approximately +15%, resulting in a 10% difference between the two.

In experiment 2, the vertical pressures at the wall and the center were closer, showing only minor differences. Both locations produced vertical pressures approximately +10% greater than the estimated Janssen values, though no clear stratification pattern emerged in this case.

The radial pressure shown in the upper left panel of Figure 4.2, and each sensor position provided a distinct pressure difference. The centre sensor (green) showed the highest radial pressures, reaching approximately 7 kPa at maximum height in both experiments. The mid sensor (red) demonstrated the lowest radial pressures, reaching nearly 2.5 kPa at maximum fill height. Finally, the sensor positioned at the wall (blue) experienced pressure between the two, but with the most variation between the two trials, approximately 17%.

The angular data was not used in this analysis because the model itself, which is based on Janssen's formula and Roger's radial extension, is axisymmetric. This means it cannot account for radial variation in the angular direction. Nonetheless, despite the limited angular data, preliminary indications suggest potential variability in that dimension; however, additional data are required to substantiate this observation.

Note that spatial variations in radial pressure would not be detectable using conventional wall-mounted sensors, highlighting an advantage of the triaxial in-situ measurement approach. The ability to simultaneously measure vertical and radial pressures at the same location, but more importantly, the radial pressure at any point in the bin, whereas traditional sensor setups only allowed for radial

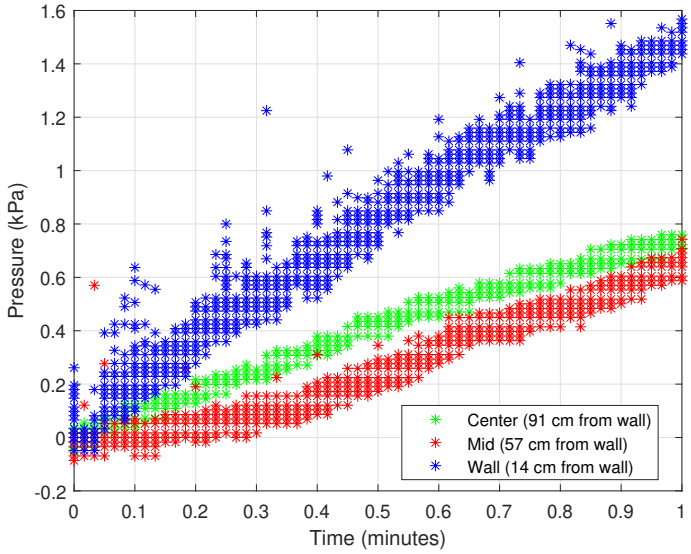

Figure 4.3: Fluctuation in unaveraged data, as a function of time. The sensors oversampled, and what appears to be a vertical row of data points shows extremely small increments in time; there is a horizontal spread within each vertical row. The data was averaged to allow for a clearer understanding and analysis that used a 1000-point moving window.

pressure to be measured at the bin wall, enables the empirical calculation of k at different positions within the grain mass. The empirical calculation of k is shown in the bottom right panel of Figure 4.2. The radial pressures showed, relatively, more variation than vertical pressures, which mathematically contributed to more variation in k.

The calculated error for the sensor measurements was ± 0.35 kPa. This indicated that the sensors were less reliable at lower measurement levels because the noise they produced was the same magnitude as the readings. However, the final sensor readings were significantly above this margin of error, allowing for smoother and more consistent results after a depth of 1 m of grain. The dynamic nature of the grain could also be a factor for readings under 1 m. The data was cleaned and analyzed, averaging each data set from over a million points to 10,000 points using a moving window. Figure 4.3 shows a sample of the unaveraged data.

4.2 Digital Twin

The DT had three main functions: bin management, pressure model, and drying simulation. The first served as the foundation that produced an accurate picture of the current inventory status, where the inventory was accurately catalogued, as well as the storage structure(s) used. The pressure model used inventory data to calculate density changes in the bin due to compression based on the work of Rogers et al. (2025) [1]. Finally, a drying simulation was created as an early proof-of-concept prototype, which was based on the popular theoretical equilibrium drying model theorized by T.L. Thompson [202]. The effects of variable density on the drying model are also investigated. The application was made accessible as a Streamlit application and found at `https://grain-bin-digital-twin.streamlit.app/`

The three functions were selected for strategic reasons. Bin management serves two purposes: it provides users with an up-to-date snapshot of their inventory (a simple yet essential requirement), and it ensures accurate data input for simulations like pressure and drying. Thereby, avoiding the 'garbage in, garbage out' phenomenon. Pressure was included because it influences many bin processes such as compaction, flow, and drying. Finally, the drying function offers farmers predictive insights. For example, advising them on optimal fan operation timing and whether ambient air will suffice for drying or if heated air would be necessary for safe storage.

4.2.1 Bin Management

The first section of the DT contains a profile/user selection tool and a bin visualization tool, as shown in Figure 4.4. The left side contains the "Bin Management" controls, detailed in Figure 4.5. The dropdown menu "Select User ID" enables selection of grouped silos, allowing users to create different profiles representing different farms, locations, or users. Below this, the "Bin Action" selector (highlighted in red in Figure 4.5) lets users choose their desired action. Users can perform three main actions on this page: select a specific bin to view/modify its contents, add a new bin to their profile (requiring radius, height, and building material specifications),

or modify the geometric and material properties of existing bins within their profile.

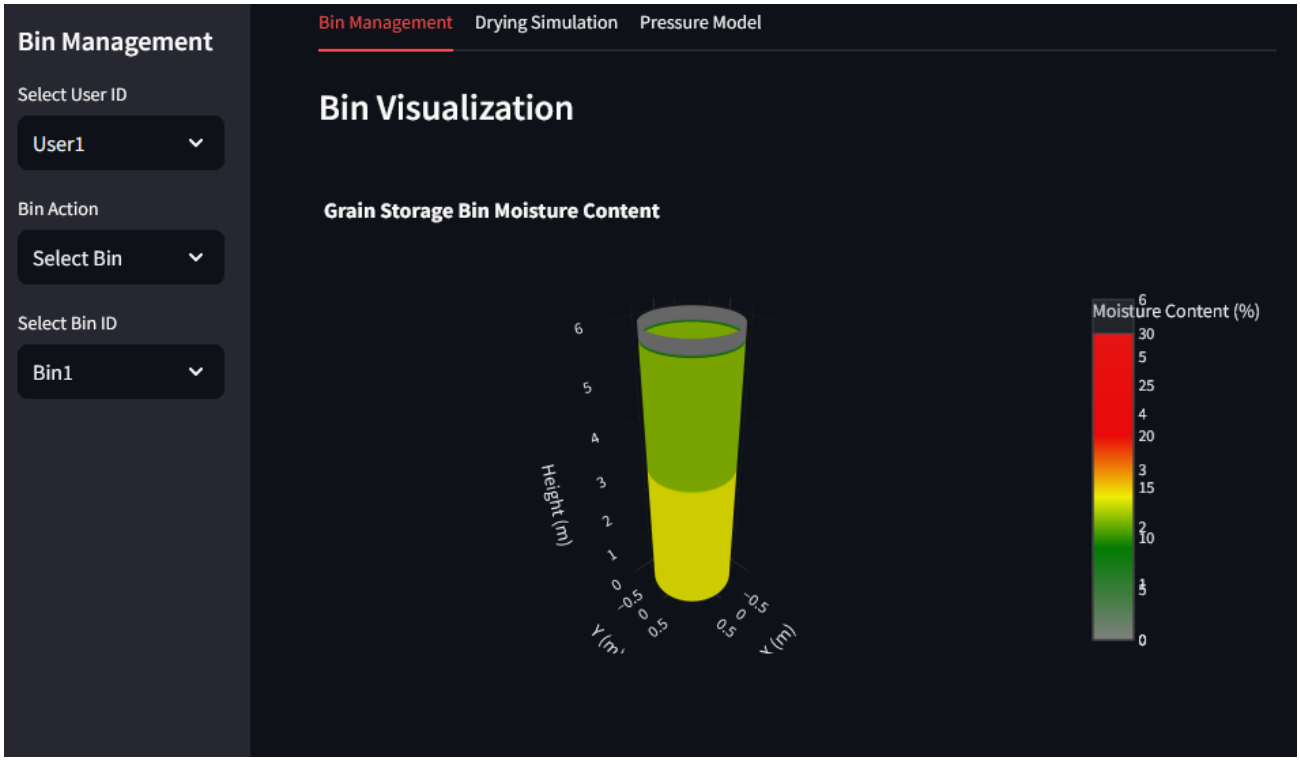

Figure 4.4: Interactive DT bin management interface showing two main components: (left) a control panel with dropdown menus for user profile selection, bin actions, and bin selection; (right) a cylindrical bin visualization displaying grain level and moisture content through a colour-coded heatmap. The visualization shows a partially filled storage bin with moisture content indicated by a vertical gradient scale ranging from red (high) to green (low).

The right side of the interface displays a 3D bin visualization of the currently selected bin, featuring a colour-coded representation of moisture content using a heatmap gradient. The visualization shows both the current grain fill level and the moisture distribution, with red indicating high moisture content and green representing lower levels, as shown in the legend, and can be seen in Figure 4.4. Moisture content was selected as the default display because the tool specifically gathered this data, while temperature information was not collected. Additionally, moisture content serves as a critical safety parameter for grain storage. While temperature is also crucial (as it can accelerate spoilage rates, especially in combination with high moisture), moisture provides the more fundamental indicator of storage safety. The visual emphasis on moisture content could allow farmers to quickly identify poten-

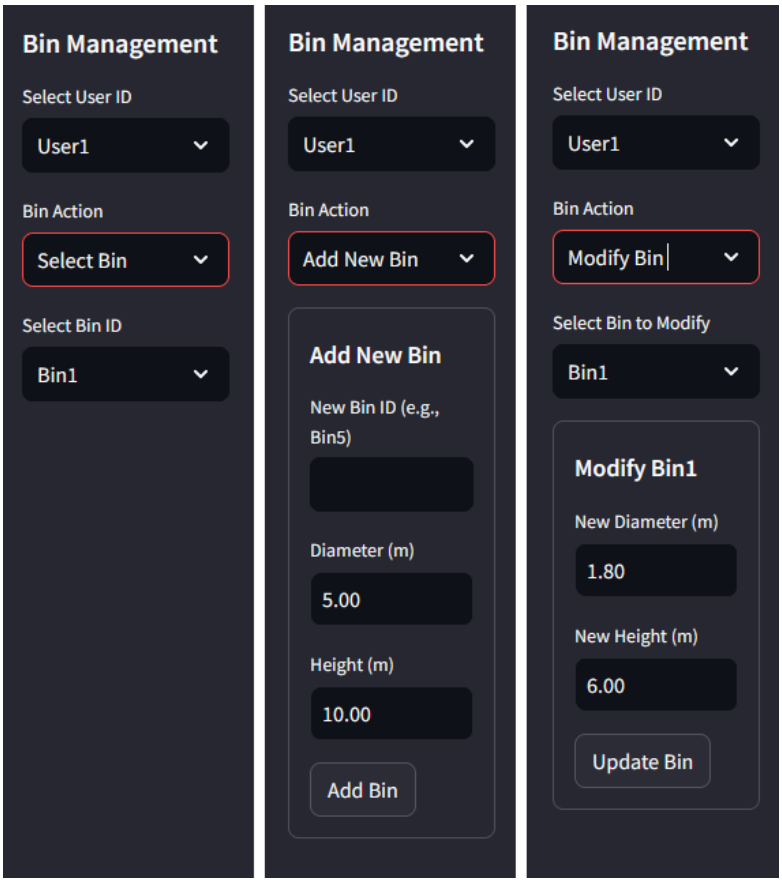

Figure 4.5: The three possible bin management interfaces which populate the left hand side of Figure 4.4: (left) bin selection panel allowing users to choose existing bins from their profile, (middle) new bin creation interface with input fields for diameter and height measurements, and (right) bin modification panel for updating the dimensions of existing bins. Each panel includes a user profile dropdown menu at the top and specific bin action controls below, which will apply the action to the specific profile.

tial problems in their stored grain, and potentially use the DT to help determine appropriate drying strategies.

The contents of the selected silo are described by six main parameters: layer number, date of addition, height $[m]$, mass $[tonnes]$, moisture content [%], bulk density $[kg/m^3]$. The collection of these data for each bin, organized by layer, is summarized in a table shown in Figure 4.6. This dynamic table can be sorted based on each of these parameters. By default, it is sorted by layer number ordering from bottom to top. The bin's geometric data, current grain height, total capacity, current fill height, and fill percentage, along with total mass and average moisture content summaries.

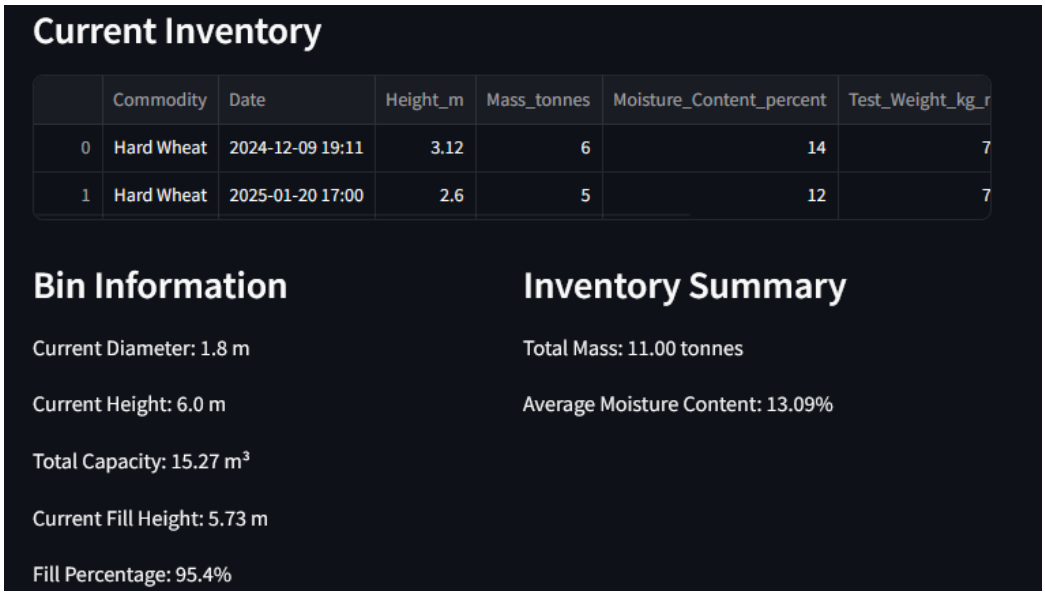

Figure 4.6: The silo inventory tracking interface displaying three main sections: (top) Current Inventory table showing grain layers with details including commodity type, date, height, mass, moisture content, and test weight; (bottom left) Bin Information panel showing physical parameters including diameter, height, capacity, fill height, and fill percentage; (bottom right) Inventory Summary section providing aggregate data including total mass and average moisture content of stored grain.

The contents of each selected silo can be added and removed using the grain addition and unloading form shown in Figure 4.7. For additions, the type of commodity must be selected from a drop-down (hard wheat, soft wheat, corn, rice), along with the mass, test weight, and moisture content. This new grain layer is added to the top of the bin's contents. These properties are stored in the database associated with the user, the silo, and the transaction time. Grain removals are much simpler and are automatically taken from the bottom layer. The current mass was displayed above the form to remind the user. Both additions and removals are automatically reflected in the table shown in Figure 4.6. Finally, these records were moved to an "Unloaded Grain History" section at the bottom of the first tab, so the farmer still has access to historical data, as shown in Figure 4.8

4.2.2 Pressure Simulation

The pressure simulation is a very simple front-end that requires the user to enter some technical values, which would not be known to the average user. These are all

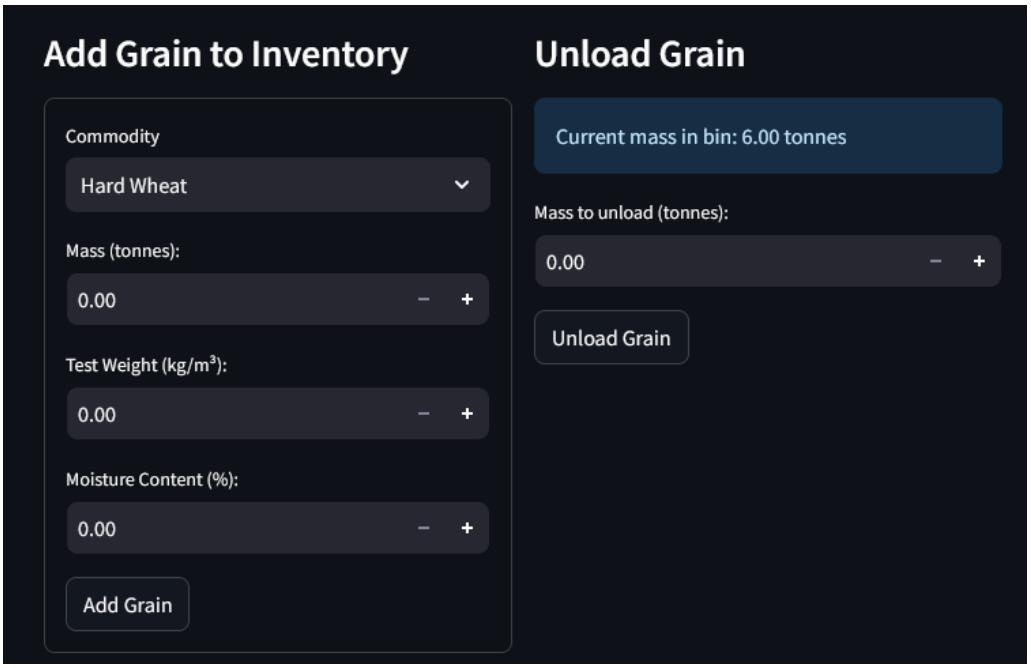

Figure 4.7: The grain inventory control interface with two main sections: (left) "Add Grain to Inventory" panel with input fields for commodity selection (Hard Wheat dropdown shown), mass in tonnes, test weight (kg/m^3), and moisture content (%), with increment/decrement controls; (right) "Unload Grain" section displaying current bin mass (6.00 tonnes) and controls for specifying the mass of grain to be unloaded.

parameters used in Rogers simulation, and would be hidden in future iterations of the DT only allowing the advanced user to tune these. Currently, they are visible for educational purposes. For future iterations, these would be determined experimentally for the grain bin and commodity type.

The simulation is run by pressing the 'Run Pressure Model' button and produces three figures. The first is Figure 4.10 and how the pressure distribution is a function of radius $[m]$ and height $[m]$. The corresponding pressure $[kPa]$ is displayed as a colour map, with blue representing low pressure and yellow high pressure. The 2D pressure distribution is then used to calculate the density change. Figure 4.11 shows the user the density change at the centre of the bin (radius = 0 m.) Figure 4.12 provides the user with a 2D density change heat map of the entire bin.

The simulation is applied to the current selected bin and takes into account the commodity, moisture content, and original bulk density, as well as the different layers of grain that have been stored, which could have different properties.

Figure 4.8: After grain is removed from a silo, the entries are not deleted but rather moved to a new collapsible table. These can represent bills of sale or other operations that require the user to remove grain, and retain all information initially given to these layers or partial layers.

4.2.3 Drying Simulation

The drying simulation has a number of adjustable parameters, presented in the left panel of Figure 4.13. The script is capable of pulling local weather to run the simulation based on current conditions by checking the "Use Live Weather Data for Winnipeg" option box. Winnipeg was hard-coded as the location because there was reliable data available that could be verified, as the author of this manuscript is located here. If the user chose to input their own parameters, this would include the ambient temperature [°C, dry bulb], and the ambient relative humidity [%]. Parameters the user must set, but currently autofilled to average values, are air flow $[(L/s)/m^2]$ and initial grain temperature [°C]. Finally, the number of simulation days can be set between 1 and 100.

In the right panel of Figure 4.13, the visualization setting could be adjusted for each simulation to allow better viewing. The specific days to be visualized on the 2D graph could be chosen using a dropdown, as shown in Figure 4.14. For 3D plotting the user could choose between moisture content and temperature, as well as select the time data set graphed using a slider, which is shown in Figure 4.16.

The simulation interface was straightforward, which featured a "Run Drying Simulation" button along with the dimensions of the currently selected bin. The processing time depended on the number of days simulated, with progress shown on a progress bar. The results plotted in Figures 4.15 and 4.16 for example took about

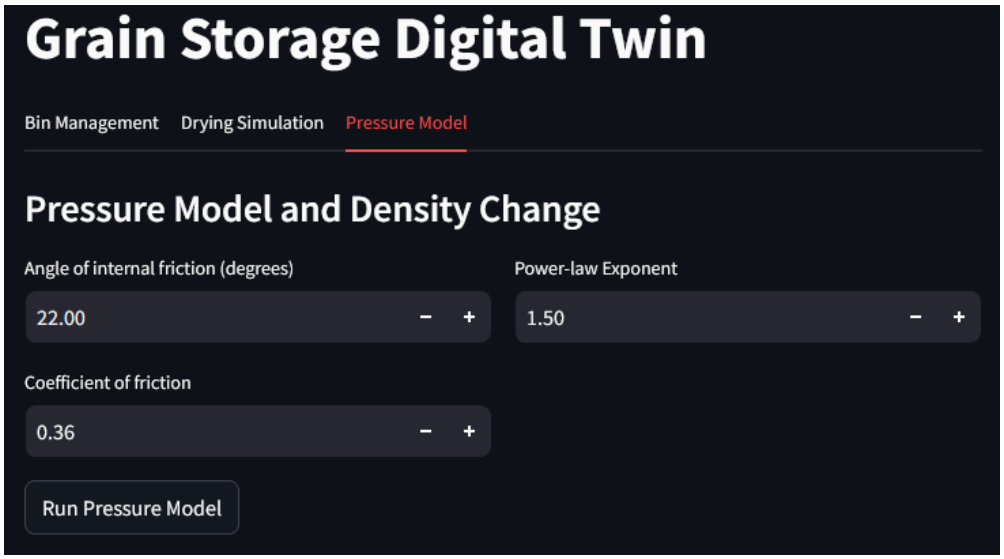

Figure 4.9: Implementation of the mathematical model of Rogers et al. (2025) with adjustable parameters, featuring interactive controls for the angle of internal friction (degrees), the power-law exponent and the coefficient of friction[1]. Current parameters are set to typical values of 22.00deg, 1.50 and 0.36, respectively, for grain storage pressure modelling.

10 s. The corresponding numerical results are published in a table, reproduced as Figure 4.17. The table was organized by day, showing the average/min/max moisture content and the average/min/max temperature of the grain, which could be downloaded as a CSV file.

4.2.4 Integrating Variable Density with Grain Drying Simulation

An additional feature of the DT is to perform the drying simulation using the compressed density as the density of each differential slice, as shown in Figure 4.12. The change in density directly affects the grain dry matter-to-air ratio (R) as described in Eq 3.17, which is an essential term for the model [202, 207]. Fundamentally, it is a dimensionless engineering parameter and not a physical property. In physical terms, R represents the mass of dry grain matter $[kg]$ relative to the mass of dry air $[kg]$ passing through the grain over a given period of time. In more concrete terms, it represents how much grain each unit of drying air must process. The parameter combines the effects of layer thickness, airflow rate, and time step into a single

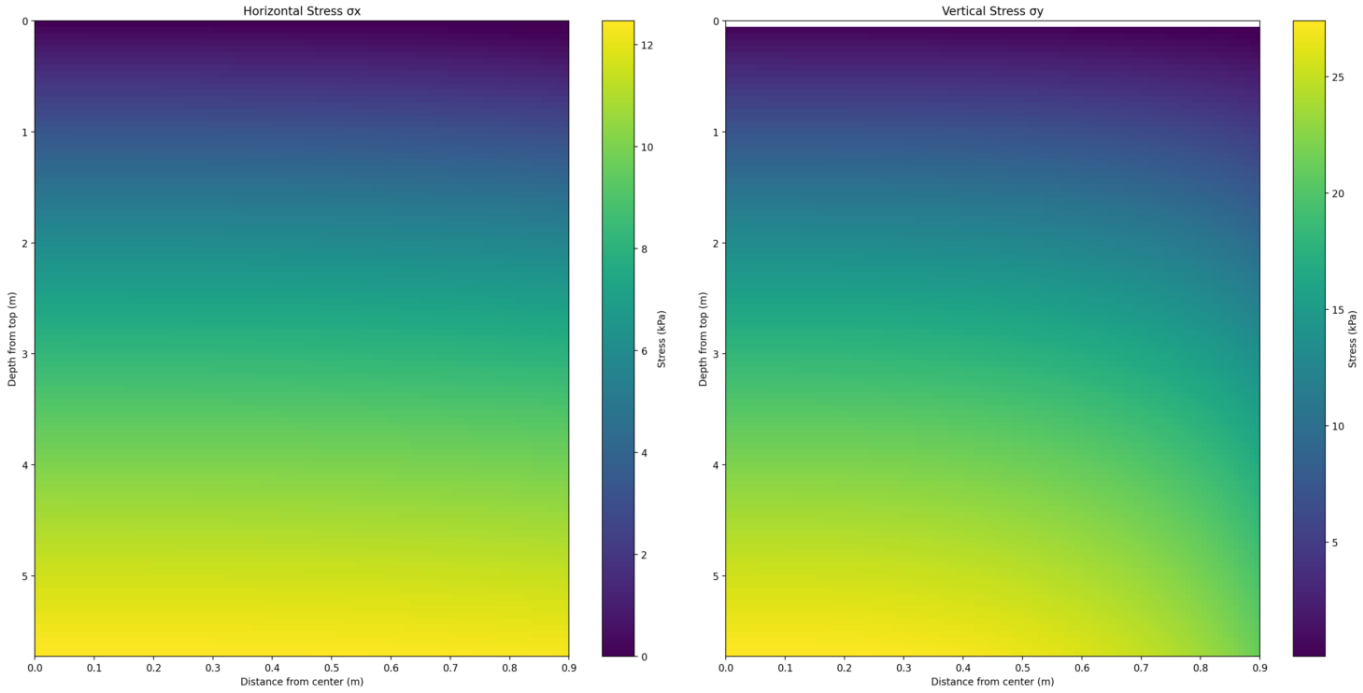

Figure 4.10: DT output showing calculated horizontal (σ_x)(left) and vertical (σ_y) (right) pressure distributions based on current selected inventory data shown in Figures 4.4 and 4.6. The pressure is a function of the radius (x) and depth (y), and is defined by a heatmap to the right of each graph. Blue represents low pressure and yellow high pressure. These pressure data are used for density calculations.

parameter that predicts drying performance. This is discussed further in Section A.4.

When density changes are incorporated into the drying simulation, the returned results show a clear difference. The DT provides a comparison between simulations that use a compacted and uncompacted density, which can be found in Figure 4.18. In it, variable density (solid orange line) showed less drying in the bottom 1 m followed by a plateau at approximately 13. 5% to 3.5 m height, after which the moisture content decreases to 12%. In contrast, constant density conditions (dashed blue line) maintained a low moisture content (10%) in the lower half of the bin, followed by a gradual increase that peaks at approximately 13.5% near the 5 m mark. These distinct moisture profiles demonstrate the significant influence of grain compaction on drying simulation. Further, the DT offers an average difference in moisture content, and a maximum difference, which were 2.3% and 3.8% respectively. The 3D visualization of the same bin, but day 17, the same as the uncompacted

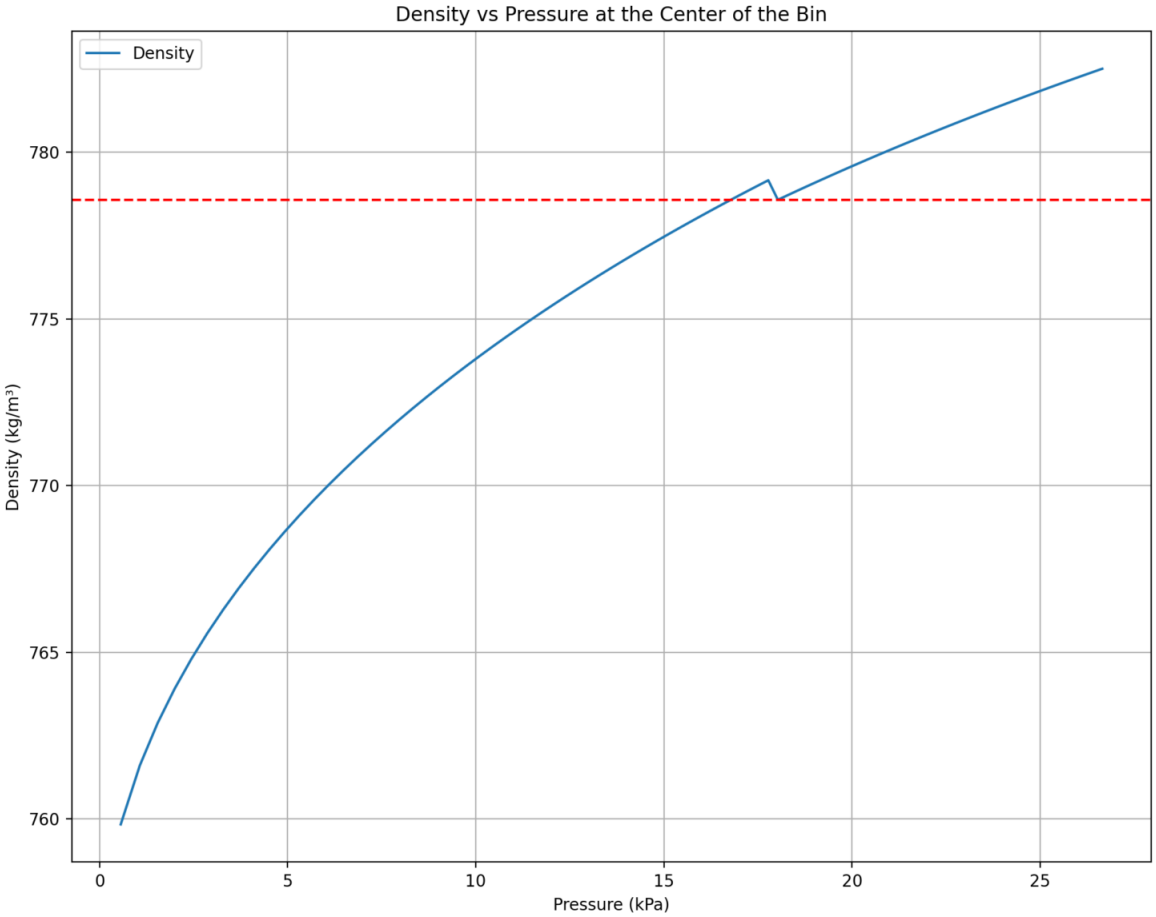

Figure 4.11: This output took the predicted pressure output at the centre of the bin and uses packing equation and parameters to predict the change in bulk density. The initial bulk density is taken from the inventory shown in Figures 4.4 and 4.6. The red dashed line marks the interface between layers.

drying found in Figure 4.16, is presented in Figure 4.19.

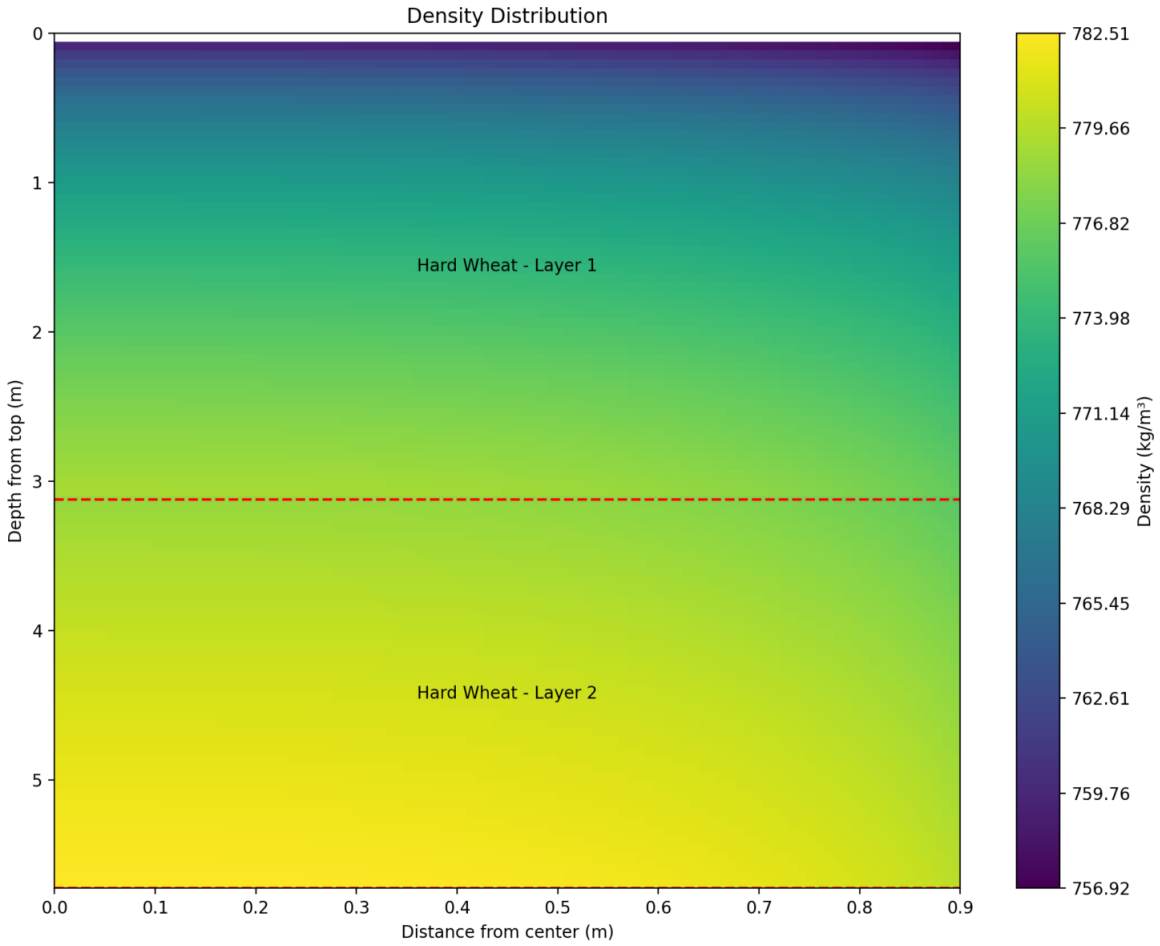

Figure 4.12: This output took the predicted pressure output (σ_y) of the entire bin, in both horizontal and vertical directions, as shown in Figure 4.9, and calculated the compressed bulk density distribution. This was based on current inventory data. The red dashed line marks the interface between layers, showing two distinct layers of hard wheat.

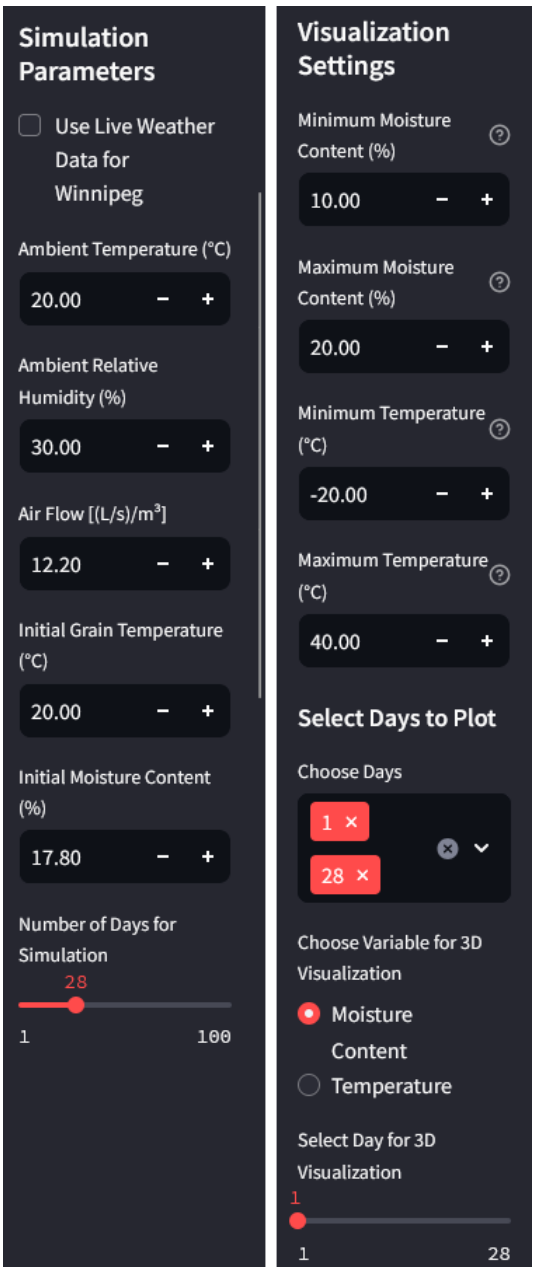

Figure 4.13: The DT drying simulation interface divided into two panels. The left panel shows Simulation Parameters, including options for live Winnipeg weather data input and manual settings for ambient conditions (temperature: 20°C, relative humidity: 30%), airflow rate (12.20 L/s/m^3), initial grain conditions (temperature: 20°C, moisture content: 17.80%), and simulation duration (1-100 days). The right panel contains Visualization Settings with adjustable ranges for moisture content (10-20%) and temperature (-20°C to 40°C), day selection for plotting (currently days 1 and 28 selected), and options for 3D visualization variables (moisture content or temperature) with a day selection slider.

Figure 4.14: DT interface header showing the drying simulation tab selected for a grain storage bin with dimensions of 1.8 m diameter and 6.0 m height, which corresponds to the bin selected as overviewed in Figure 4.5. The button 'Run Drying Simulation' initiates the simulation process, defined by the parameters described in Figure 4.13 and is applied to the inventory of the defined bin.

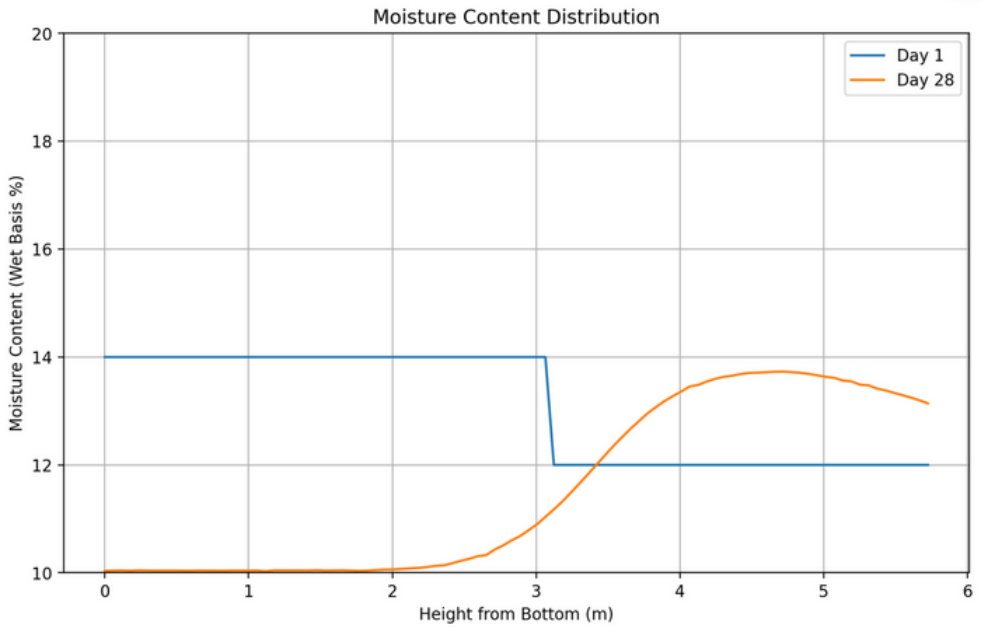

Figure 4.15: Two-dimensional plot comparing moisture content distribution across bin height between selected dates, from the interface shown in Figure 4.13. Day 1 (blue line) and Day 28 (orange line) were selected in this specific case. The graph shows the vertical moisture content profile over the height of the bin from 0 to 6 m, highlighting the changes in moisture distribution over the simulation period, with a distinct step change at approximately 3 m marking the interface between grain layers. This simulations suggests that the grain will not be completely dried over the 4 weeks, and clearly shows the movement of the moisture front across that time.

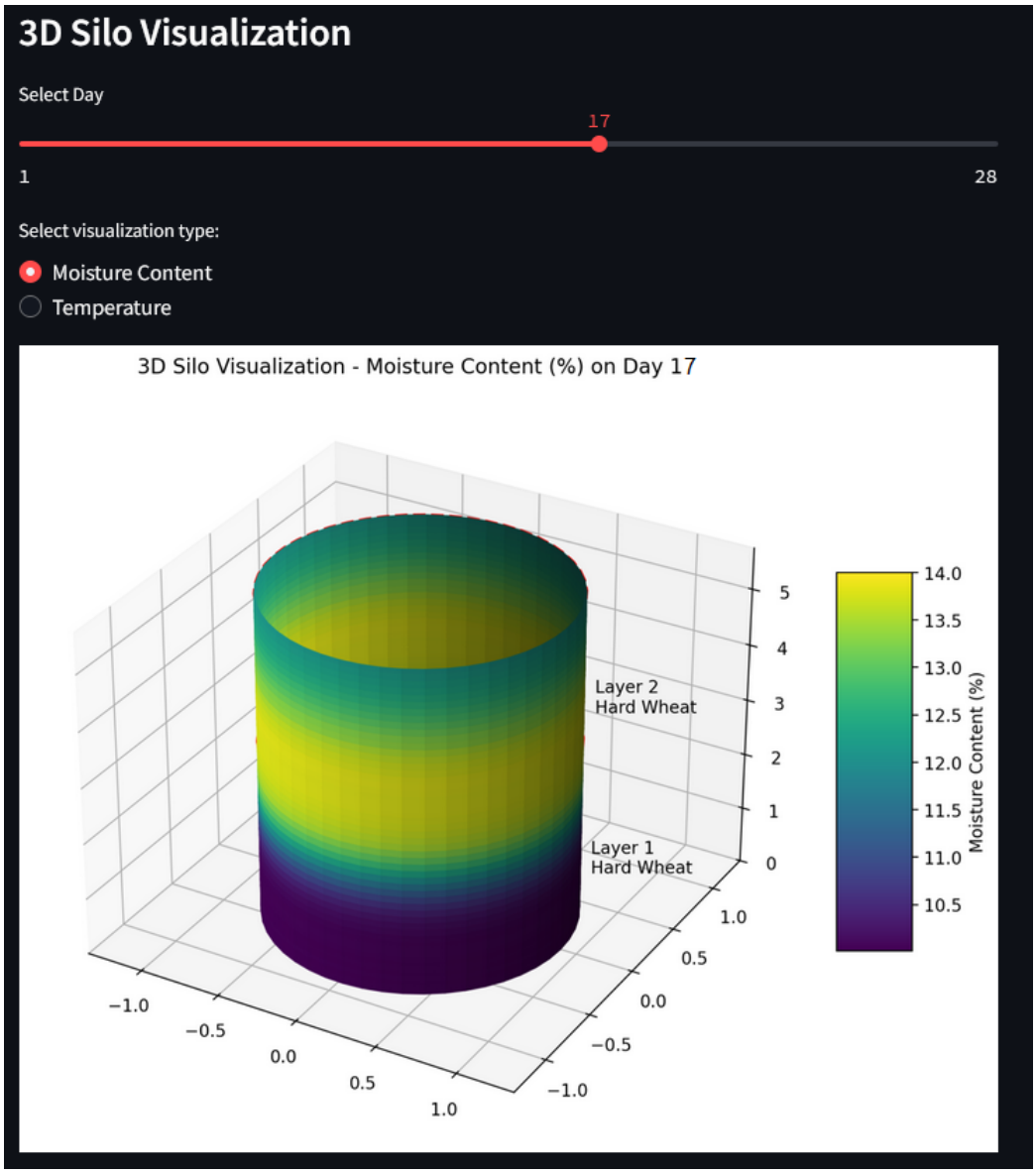

Figure 4.16: Three-dimensional visualization of moisture content distribution within the grain storage bin on Day 17, showing two distinct layers of hard wheat. The moisture content is represented by a colour gradient from 10.5% (purple) to 14.0% (yellow), with the interface between layers clearly marked. Interactive controls allow for day selection and visualization type toggle between moisture content and temperature.

Numerical Results

	Day	Average MC (%)	Min MC (%)	Max MC (%)	Average Temp (°C)	Min Temp (°C)	Max Temp (°C)
0	1	13.08	12	14	20	20	20
1	2	12.97	11.1	13.92	18.45	16.15	20.1
2	3	12.88	10.34	13.85	17.36	15.61	19.56
3	4	12.81	10.12	13.83	16.84	15.49	19.87
4	5	12.76	10.06	13.86	16.67	15.45	19.97
5	6	12.71	10.05	13.86	16.66	15.43	19.99
6	7	12.66	10.04	13.84	16.69	15.43	20
7	8	12.62	10.04	13.86	16.75	15.43	20
8	9	12.57	10.04	13.84	16.8	15.43	20
9	10	12.53	10.04	13.86	16.86	15.44	20

Figure 4.17: Numerical results table showing the progression of grain moisture content and temperature over the defined days of simulation, and can be expanded to see all dates. The table displays daily averages, minimums, and maximums for both moisture content (%) and temperature (°C), demonstrating the gradual reduction in average moisture content from 13.08% to 12.53%.

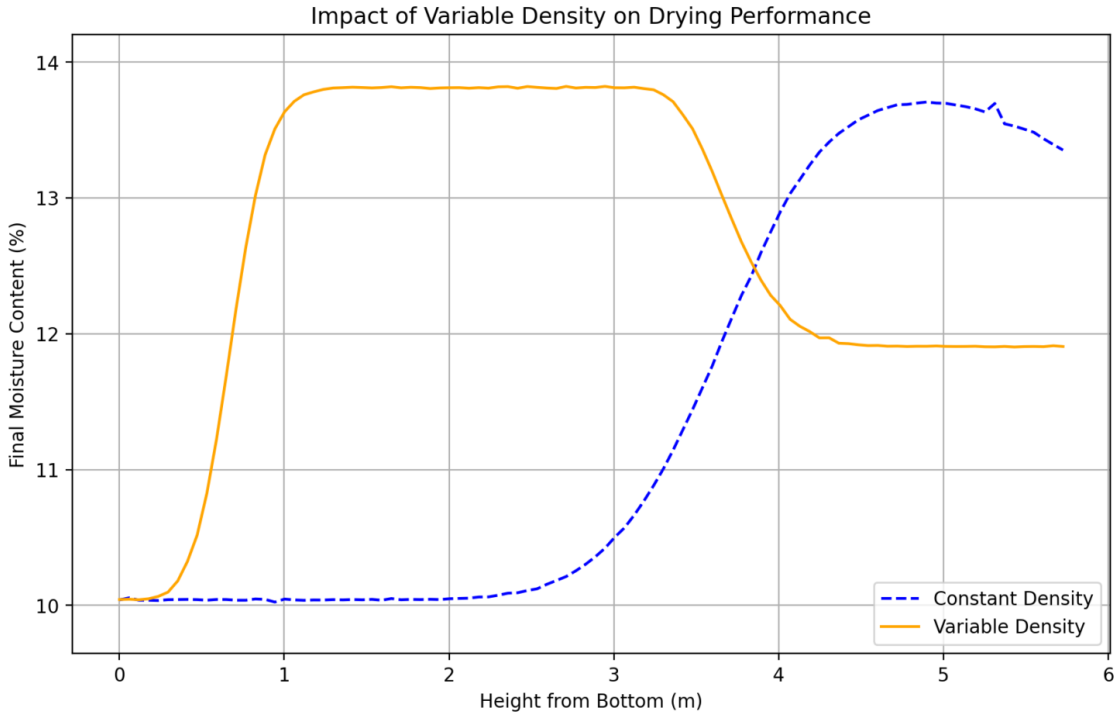

Figure 4.18: Impact of compaction on moisture content distribution in a grain bin drying simulation after 30 days. The simulation used a constant ambient temperature of 20°C, relative humidity of 30%, a flow rate of 12.2 $(L/s)/m^3$, and an initial grain temperature of 20°C. The bin had a diameter of 1.8 m and a height of 6.0 m, and corresponded to the inventory found in Figure 4.6. The graph displays final moisture content (%) as a function of height from the bottom of the bin (m).

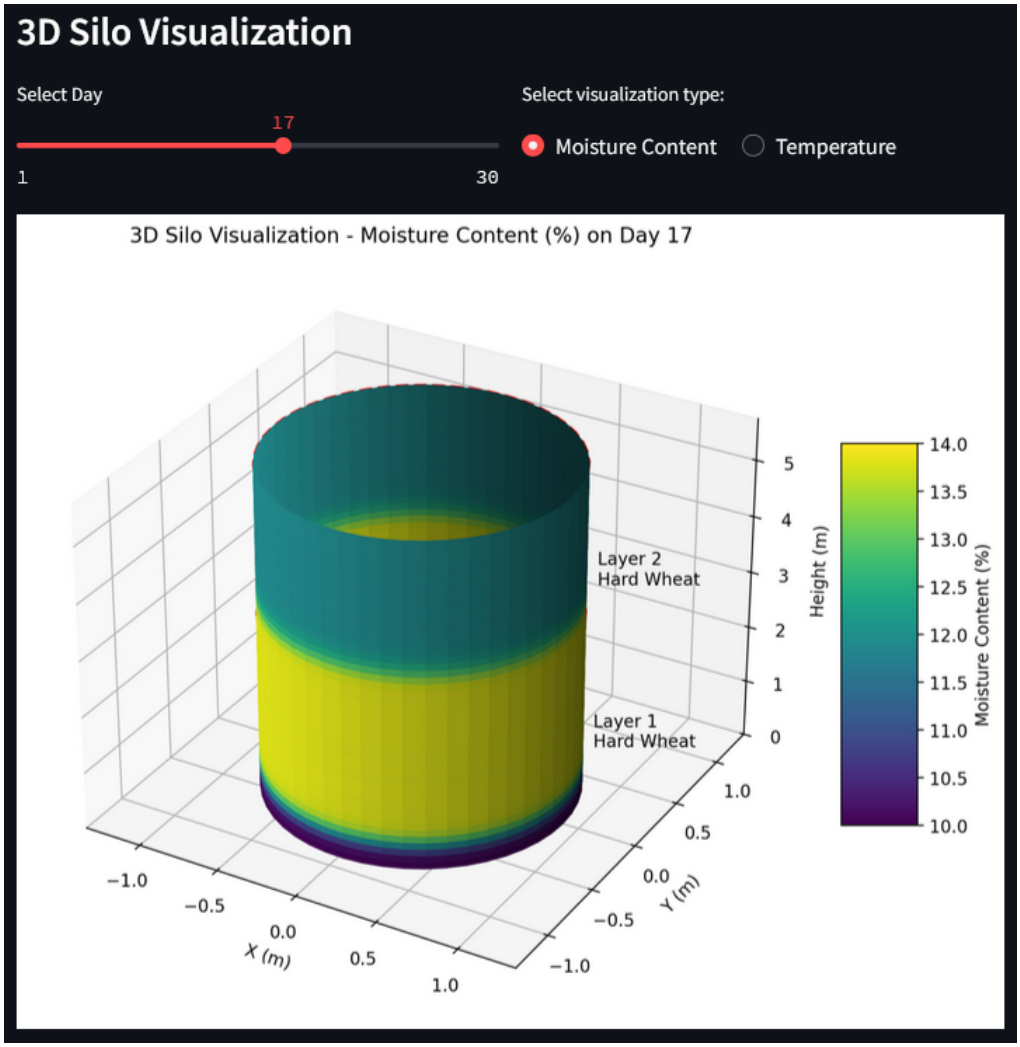

Figure 4.19: Variable density caused by compaction used in the drying simulation, which uses the same parameters (barring density) of the uncompacted simulation, in Figure 4.16. This is the resulting 3D visualization of moisture content distribution on Day 17, showing two distinct layers of hard wheat. The moisture content is represented by a colour gradient from 10.0% (purple) to 14.0% (yellow), with the interface between layers marked. Interactive controls allow for day selection (1-30) and visualization type toggle between moisture content and temperature.

Chapter 5

Discussion

5.1 In-Situ Pressure Sensor

In the past, modelling pressure distributions was crucial for optimizing grain silo design and ensuring structural integrity. The Janssen equation, shown below, was the traditional approach to modelling pressure within a grain bin,

$$\sigma_{vert} = \frac{\rho g R}{k\mu}(1 - \exp(-\frac{k\mu h}{R})) \tag{5.1}$$

$$\sigma_{rad} = k\sigma_{vert} \tag{5.2}$$

Where σ_{vert} represents the vertical pressure (Pa), σ_{rad} is the radial (horizontal) pressure (Pa), ρ is the bulk density of the material (kg/m^3), g is gravitational acceleration (9.81 m/s^2), R is the hydraulic radius of the silo, equal to cross-sectional area divided by perimeter (m), k is the ratio of horizontal-to-vertical pressure, μ is the coefficient of friction between the bulk solid and the silo wall (steel friction), and h is the depth below the grain surface (m).

Table 4.1 describes the parameters of this equation. Traditional approaches to pressure distribution assume k to be constant across the radius of the bin, and therefore, no radial pressure variation exists. However, this has been experimentally known not to be the case since Janssen's time. To investigate the radial pressure distribution mathematically, we used two approaches.

The preliminary data suggested that k varies radially within the silo, with measured values of 0.22 near the wall, 0.19 at mid-radius, and 0.37 at the centre as shown in Figure 4.2. This variation in k challenged the traditional assumption of constant k across the silo radius in the Janssen model. To explore these observations further, we used a MATLAB script with an optimization algorithm to find parameter values (within bounds established by industry standards and literature) that best fit our experimental data for R, and μ.

Figure 5.1 displays the interactive tool for tuning the model, which allowed users to adjust parameters corresponding to their specific grain and silo properties. This functionality enables users to calibrate the model by testing different values of μ, R, and ϕ based on their actual grain and storage infrastructure, generating an accurate model for the DT that reflects the real asset. Figures 5.2 and 5.3 show the measured pressure data alongside model curves generated with this data tool, for experiments 1 and 2, respectively.

One set of optimized parameters can be viewed in Table 5.1, but there is a range of choices that fall within an arbitrarily similar RMSE. The model curves used the experimentally determined k values, which were calculated as the ratio of the radial and vertical pressure gathered from the sensor data, and previously shown in Figure 4.2.

Our initial sensor data suggests that assuming a uniform k value across the silo radius may oversimplify the complex pressure distribution within bulk solids. Future research using this sensor technology could explore how factors such as filling methods, grain properties, and silo dimensions influence these radial variations, potentially leading to more accurate pressure models. However, these initial results should be interpreted cautiously as they represent a limited dataset intended primarily to demonstrate the functionality of our triaxial pressure sensor system rather than provide definitive conclusions about granular behaviour.

Our initial sensor data suggests that assuming a uniform k value across the silo radius may oversimplify the complex pressure distribution within bulk solids. Fu-

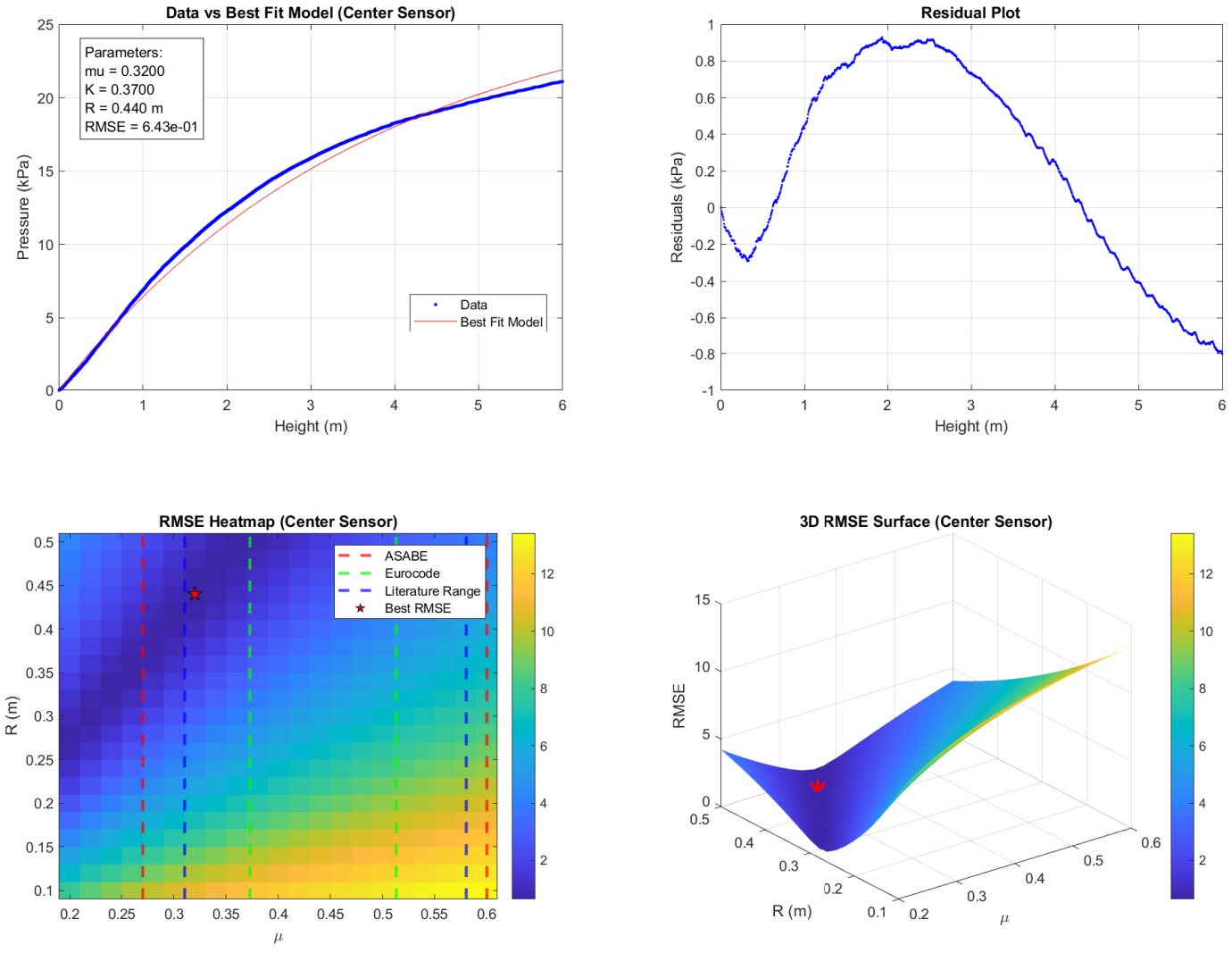

Figure 5.1: Model optimization interface for experiment 1 (centre sensor) using variable k: (top-left) best-fit model vs experimental data, (top-right) residual plot, (bottom-left) RMSE heatmap with industry standards, and (bottom-right) 3D RMSE surface visualization. This optimization used empirically determined k values while varying μ and R. The heatmap was interactive, which allowed users to select an R and μ value by clicking directly on the graph, which automatically updates the other three graphs.

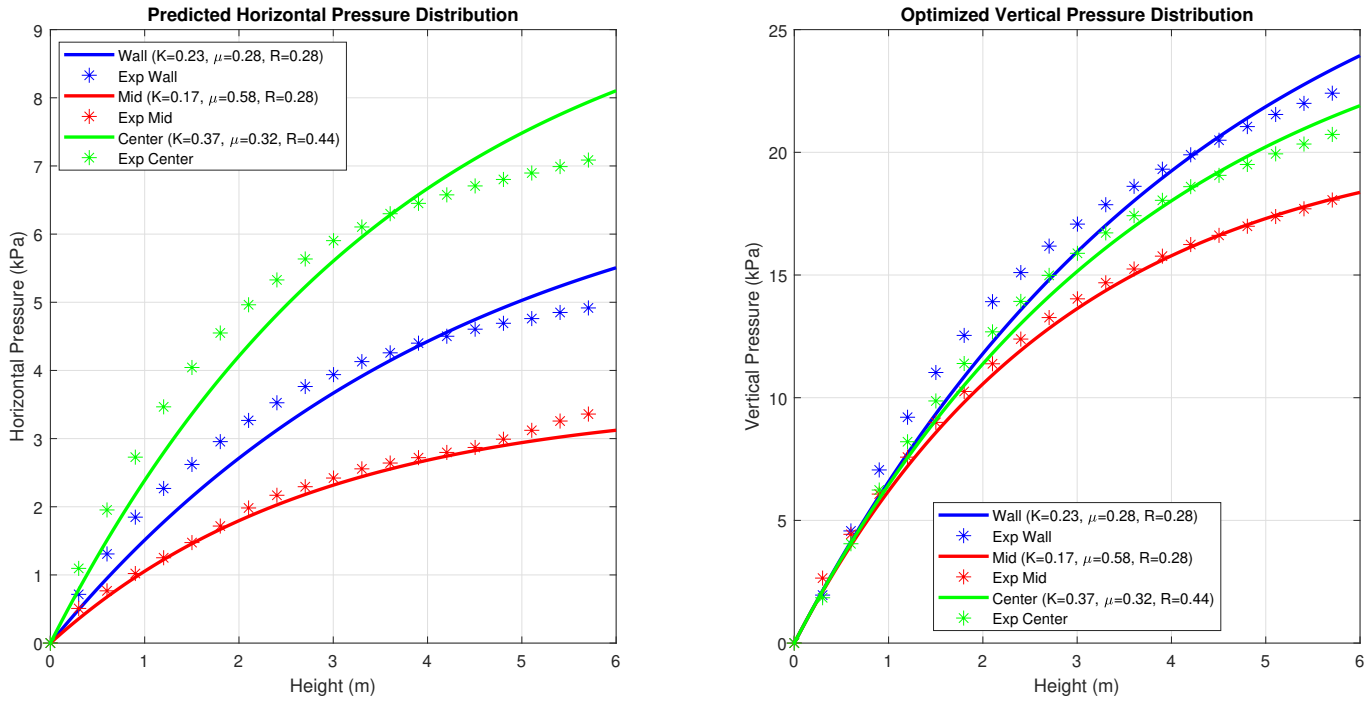

Figure 5.2: Predicted Horizontal and Optimized Vertical Pressure Distributions for Experiment 1 data using empirical k, where the model parameters (ϕ and R) were determined by RMSE minimization within literature-based bounds to best fit the experimental data.

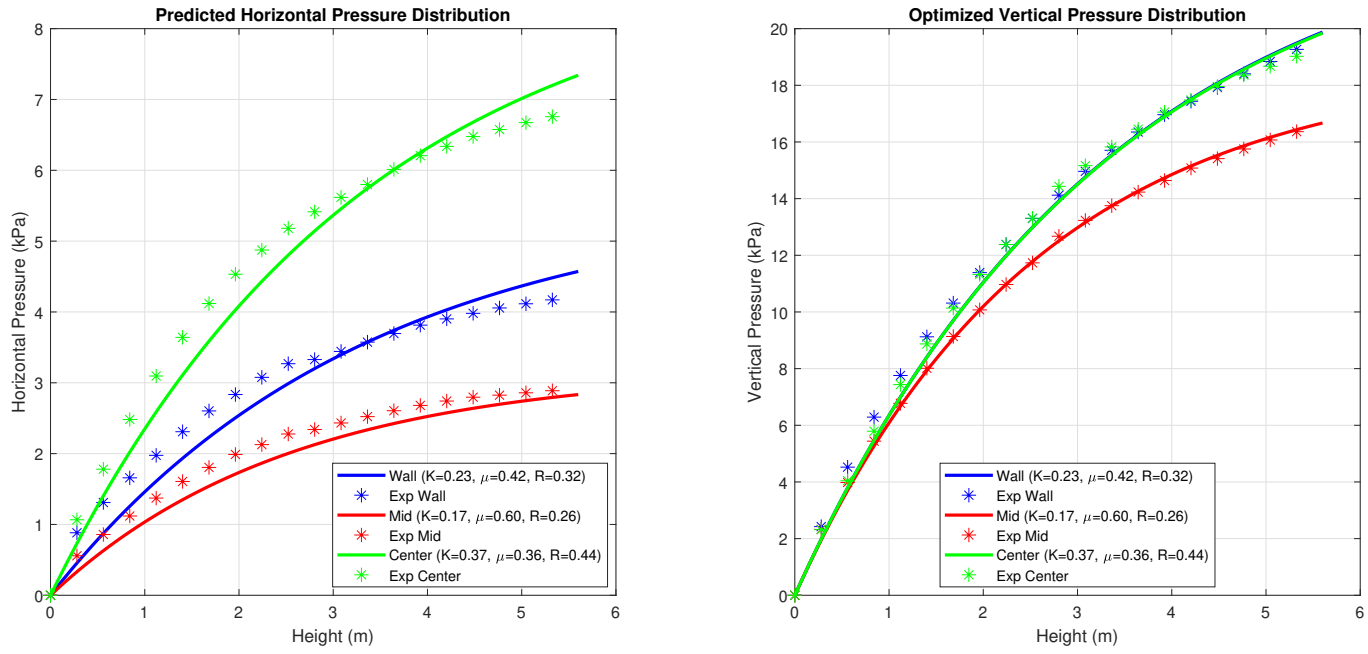

Figure 5.3: Predicted Horizontal and Optimized Pressure Distributions for Experiment 2 data using empirical k, where the model parameters (ϕ and R) were determined by RMSE minimization within literature-based bounds to best fit the experimental data.

Position	k	**Experiment 1**		**Experiment 2**	
		μ	R	μ	R
Wall	0.23	0.38	0.28	0.42	0.32
Mid	0.17	0.58	0.28	0.60	0.26
Center	0.37	0.32	0.44	0.36	0.44

Table 5.1: Optimized Model Parameters for Experiments 1 and 2

ture research using this sensor technology could explore how factors such as filling methods, grain properties, and silo dimensions influence these radial variations, potentially leading to more accurate pressure models. However, these initial results should be interpreted cautiously as they represent a limited dataset intended primarily to demonstrate the functionality of our triaxial pressure sensor system rather than provide definitive conclusions about granular behaviour.

5.1.1 Design Considerations and Potential Improvements

The sensor design described in Section 3.1.1 presented several challenges inherent to measuring stress within granular materials. While measuring stress in bulk solids remains a challenging open problem, design elements that may have affected measurement accuracy were identified and possible improvements to address these limitations were considered.

The sensor design aimed to minimize its influence on the grain's stress distribution. However, the presence of the sensor in the bulk solid might have acted as an inclusion, altering the local stress distribution. Jalil et al. (2012) showed that rigid inclusions could act as stress concentrations in clay (powder), which led to stress heterogeneity in the surrounding area. Depending on the inclusion orientation and force direction, they could cause a local increase or decrease in stress. When the inclusions were arranged horizontally (perpendicular) to the load direction, there was a significantly less pronounced volumetric strain distribution than vertically (parallel) [211]. Antony et al. (2015) reported that granular materials distributed stress more uniformly around an inclusion than powders with loading, in part due to cohesion effects [212]. Antony and Ghadiri (2020) showed that when the surrounding

particles were at least 10 times smaller than the inclusion (a size ratio > 10), the stress distribution became more consistent and uniform around the inclusion [213].

Next, it has been noted that the stiffness of the pressure plate is crucial for accurate measurements [191]. Theoretical calculations based on Askegaard's error formula [195] suggest that the aluminum disc used in this design should result in a minimal error due to deflection, as covered in Appendix A.1. Furthermore, the higher friction coefficient of aluminum compared to galvanized steel [214] would alter the normal stress, as described by Janssen's equation. This could potentially be addressed by coating the plate with a material that more closely matched the grain's properties, as was done by Askegaard et al. (1998) [196] or rubbing the surface to impart parts of the bulk solid, such as waxes for agricultural commodities, on the surface. Next, the small 1 mm recess of the pressure plate could be problematic, as is the case of sensors mounted to the wall of a silo which causes force shielding [191, 192]. Although in a wall-mounted context, the sensor's surface sits behind the plane of the silo wall, and this is not the same condition as in-mass sensors. Finally, imperfect orientation with gravitational force [194, 196] is also a potential error, but the experimental procedure attempted to counteract this. The magnitude of these effects should be studied in future work.

Compared to previous triaxial sensor designs [200, 187, 194, 196], the current design offers a larger sensing surface and a novel piston system for better stress averaging. Moreover, our device was put in a large-sized storage silo. This was a real-world environment, and the data reflected real-world conditions. In contrast, the other triaxial sensor studies used much smaller enclosures of questionable dimensions and might not provide adequate mass to achieve the "Janssen Effect." A potential improvement to the piston system would be to investigate a diaphragm-style sensor system, such as Martinák et al. (2004), which could provide more sensitivity to readings [200].

5.1.2 Sensor Performance and Experimental Limitations

To evaluate the performance of our triaxial sensor system in real-world conditions, we first considered the accuracy of the measurement. As established during calibration, the sensors have an estimated error of ±0.35 kPa. This resulted in a relative error of approximately 11% at a grain depth of 1 m. At greater grain depths (6 m), where the pressure is higher, there is a significantly lower error of approximately 5%. As the grain depth increased, the relative error decreased.

During data collection, we observed some potentially interesting preliminary pressure results. The measurements in Figure 4.2 indicate differences in pressure readings at different radial positions within the silo. These preliminary observations suggest potential spatial variations in k, though additional experimental runs would be necessary to establish the statistical reliability of these patterns.

The patterns we observed have some similarities to those reported in previous research. For context, Molenda et al. (1996) investigated pressure variations across the radius of a smaller experimental silos and noted that the lowest pressures were often recorded at mid-radius positions, and theorized variation in k as the reason [183]. While our experimental conditions differed significantly in terms of silo dimensions, and wall characteristics, one of the filling method (centre) was the same. The preliminary data from our triaxial sensors provided an initial demonstration of the measurement capabilities and potential of this new system, which should be explored in future research.

During experiment 1, we observed an interesting phenomenon during a pause in filling (between 17.8 and 20.6 minutes) when grain flow was stopped to record grain height. During this static period, the sensors continued to record data, as shown in Figure 5.4. The pressure readings showed a general downward trend in all directions, with a slight increase occurring at 19.5 minutes, despite the grain mass remaining constant. This drift was most pronounced in the vertical direction (5.2% decrease), compared to radial and angular measurements. While this change falls within the estimated error of the sensor, it resembles the grain settling process

described by Ruiz et al. (2012) [215]. Their research found that during static conditions, grain undergoes a settling process with a distinctive pattern: a gradual reduction in pressure followed by a sudden spike, then another reduction. As shown in their findings, these pressure fluctuations occur in 'surges', with progressively increasing lengths of time between them. The slight pressure reduction we observed in Figure 5.4 could correspond to the beginning of Ruiz et al.'s relaxation cycles. Since all our other measurements were taken during dynamic filling conditions, the implications of this observation for the overall dataset require further investigation.

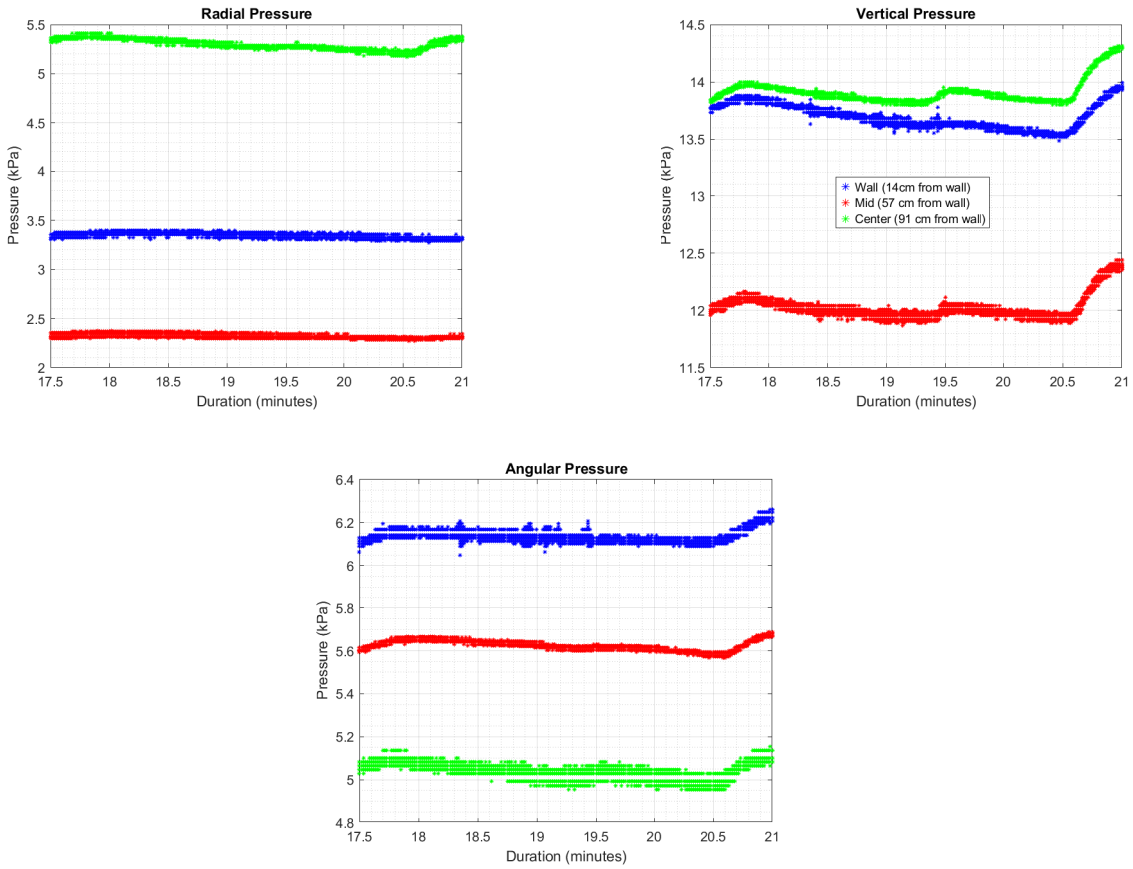

Figure 5.4: Pressure measurement during a static period in experiment 1. The data shows an unexpected decline in pressure readings across all directions over a 3-minute interval, despite constant grain mass. This systematic drift requires further investigation.

Several limitations affect the quality and interpretation of the sensor data collected in this study. First, our dataset is based on a limited number of experimental runs, which limits the statistical soundness of our findings and prevents definitive conclusions about pressure distribution patterns. Second, the measurements were

obtained using one grain type (soft red winter wheat at 13.5% moisture content) under one particular filling method (centre, small inlet), which limits the generalizability of our observations to other materials and filling conditions. Third, while the sensor design aimed to minimize disruption to the grain mass, the presence of the sensor itself may have introduced some localized alterations to the stress field, potentially affecting measurement accuracy. The aluminum material used in the piston design has a different friction coefficient than the silo wall, which could influence the stress transmission at the sensor interface. Furthermore, during our static measurement period, we observed a slight drift in pressure readings (approximately 5.2% decrease in vertical pressure over a 3-minute interval) despite constant grain mass, suggesting either grain relaxation effects or minor measurement instability that warrants further investigation and should consider the work done by Ruiz et al. (2012) by extending periods of rest. These limitations, while not invalidating our proof-of-concept demonstration, emphasized the preliminary nature of our findings and the need for more extensive experimentation in future research.

5.2 Digital Twin

This section examines the effectiveness of the pressure/packing and drying model. It compares the current implementation of the "sensorless monitoring" via DTs, as described in this investigation, with the current state-of-the-art. Finally, it describes limitations and short- and long-term improvements that can be made to the model.

5.2.1 Drying Simulation and Compaction

Integrating variable density into the drying simulation fundamentally altered the grain dry matter-to-air ratio (R), an important parameter associated with each differential slice. This dimensionless parameter, which represented how much grain each unit of drying air must process, changed throughout the vertical profile of the bin as grain density increased from top to bottom due to compaction. Traditional

drying models assumed a constant density throughout the bin, which oversimplified the physical reality. The variable density approach to drying simulation addresses this limitation by accounting for compression effects on airflow and moisture transfer, which has been highlighted in other work [201]. This is the first work to put these two features together in a general tool.

The R parameter provides the theoretical foundation that explains why density variations significantly impact drying performance. As shown by Jindal et al. (1994), R directly represents how much grain each unit of drying air must process during the drying operation [207]. Their study set up various PVC columns to measure and calculate R, noting that grain density, airflow rate, depth, and duration all affected the value. Eq 3.17 was reproduced below for ease of reading.

$$R = \frac{\rho_g \times dx \times dmf}{\rho_a \times v_a \times t} \tag{5.3}$$

In regions with higher compaction –the bottom layers– the increased density created a higher R that required more air to dry the same amount of grain. This can be thought of as a reduced drying efficiency. The change in drying efficiency had a drastic effect, as shown in Figure 4.18. R must be tuned for the model to work reliably, setting dx and t to appropriate values. Corrected density for compression significantly changed the drying simulation results (2.3% average, 3.8% maximum), showing that R was a critical parameter affecting moisture distribution. The simulations will not provide accurate results if density is not adequately considered.

The drying simulation presented here has not yet been validated with experimental drying data, which is an important limitation of the current model. Further parameter tuning would be necessary before applying this model in practice, as highlighted in literature [207, 205, 202, 216, 217]. Specifically, the proper use of R in drying simulations requires a more finely calibrated experimental value, which would account for specific operating conditions. A variable R would provide an approach that reflects the mechanisms of reality during simulation.

DTs' application to drying has been abstractly predicted in literature [201, 218].

Concretely, this work suggests that by accounting for the spatial variability of R due to compaction, the DT can provide a more mechanistically accurate representation of moisture transfer physics within the context of this equilibrium model. Density effects should be investigated in deep grain bins where pressure gradients substantially influence drying performance. A variable R provided an approach that better reflected the physical mechanisms during simulation, even though the results presented are numerically unlikely.

5.2.2 Current State of the Art for Grain Management

This work must be positioned within the existing technology available on the market. The solution to inventory management adopted by farmers varies greatly depending on the size of their operations. Smaller operations rely on memory or physical checks to monitor grain bin contents. In contrast, more complex commercial systems include detailed spreadsheet-like programmes that provide inventory logs, transactions, and contracts. Although these systems typically rely on farmer input rather than sensor data, they can be integrated with sensors that measure bin fill levels. These sensor systems can work independently or be incorporated into inventory management software.

Information on these products is limited to the company-provided literature, which is fundamentally marketing material. One can easily see why there could be a disparity between what a product claims and what it actually does 'under the hood.' Some products sell ideas more than functionality, and the claims of these products to be 'precision/digital agriculture' should be questioned. Furthermore, the academic literature supports this skepticism. For example, the accuracy of cable monitoring is highly suspect because grain is an insulator. This is confirmed by academic studies which show that cables can provide a false sense of security [9, 10]. The error of fill level sensors has been shown to be significant [12]. It should also be noted that there is a lack of pricing information, likely due to scalability; product costs vary depending on the user, their operation size, and each company's relationship

with its clients. As a result, it is difficult to compare the costs associated with this research's proposed solution to these industrial ones. The following discussion explores the range of products currently available.

AgriChain provided software for farmers called Growers that focuses on tracking and visualization capabilities [219]. Bin levels, GPS tracking, stock mixing, and contract management are displayed through remote access. With no clear pricing beyond "free to try," this suggests a purely software-based approach without sensor requirements.

Greenstone Solutions offered an unbundled product suite (AGRIS, CINCH, oneWeight, myGrower) [220]. Each software handles distinct aspects: AGRIS for inventory and resource planning, CINCH for financial flows, oneWeight for scale automation, and myGrower for agribusiness management. These products, primarily designed for grain elevators, rely on worker inputs rather than automated data collection.

CompuWeight aimed to digitise traditional whiteboard approaches to grain inventory management [221]. It provided bin level and quality displays, basic blending calculations, and identity preservation features. Although sensor integration is possible, the software functions primarily through user data input.

BinMaster's suite included multiple platforms (BinCloud, BinView, AgriView, Binventory) integrated with their proprietary sensors [222]. Their sensor range includes continuous monitoring types (non-contact radar, 3D sensing, guided wave radar) and contact sensors. At $60/year for BinCloud, it represents the only product with transparent pricing, although sensor costs are not disclosed.

Cimbria's system represented the closest approach to a DT, although without simulation capabilities. It combines laser-based monitoring with comprehensive quality tracking, recording grain transfers, and maintaining detailed histories [223]. The system appears designed for elevators managing multiple grain sources, emphasizing quality preservation for mixing capabilities.

There were two general trends in the products covered above. The first was tracked changes in input from the user or sensors. These changes can be inventory

levels, financial transactions, or even physical shipments and the resulting contracts. Secondly, they provided data visualization, which can generate summaries (i.e., reports) that can help a grain manager make decisions. The Cimbria product was a noteworthy example because quality and grading criteria are also considered in the information they track. However, this software-hardware suite was still simply a tracking tool.

Returning to the idea of the "Digital Shadow" as discussed in Section 2.3.1 will provide a framework to determine what is and is not a DT. The literature has defined the steps from a manual system to a proper DT, although in reality, they are not as discrete. A 'Digital Model' represents the most basic form of digital representation, requiring manual data entry to reflect any changes in the physical system. A "Digital Shadow" incorporates automated one-way data flow, where changes in the physical system automatically update its digital counterpart without human intervention. The most advanced form, a DT, builds on the capabilities of 'Digital Shadow' by adding automated two-way communication, allowing both automatic updates from physical to digital and the ability of the digital representation to automatically initiate changes through simulations in the physical system [224]. For this reason, the Cimbria system would represent a step between a digital model and a digital shadow and is not a DT. This is because the product seems to be a manual and automatic data entry/tracking hybrid, offering no simulations (besides simple blending tools already present in 'whiteboard replacements' like CompuWeight).

A proper DT will provide a historical record of the data gathered and present simulation data on what-if scenarios. For example, is there a potential that this specific grain would spoil under current conditions? Is it worth turning on my dryer even though it is currently raining? DTs do not simply display data but provide new data through simulations. They are proactive instead of reactive, and the industry solutions to inventory management covered above are at best reactive. This DT goes beyond passive monitoring to deliver actionable insights through its preliminary drying simulation. The infrastructure developed from this research could

serve as a platform for implementing numerous future applications, from safe storage predictions to market analysis.

5.2.3 Key Differences with Research's Digital Twin

The key difference between this research's DT approach to inventory management and current industry solutions lies in its simulation capabilities and structured database architecture designed specifically for simulation purposes. While existing commercial solutions like BinMaster, CompuWeigh, and Cimbria provide inventory tracking functionality, they primarily serve as Digital Models, focusing on monitoring and recording stock levels rather than enabling predictive/proactive simulation.

These systems (usually intended for grain elevator operations) lack the bidirectional data flow and simulation capabilities that characterize proper DT implementations, as well as a detailed database specifically set up for such operations. Their functionality is limited to inventory management and does not extend to dynamic modelling and predictive capabilities that would enable the optimization of grain handling operations through simulation-based decision support.

This DT visualized grain container inventory levels through a layer-based representation, as shown in Figure 4.4. Although record keeping was common among industry tools, this research uniquely provided farmers with 3D-layer-based information containing specific local data. These layers tracked important parameters such as moisture content and density, as shown in Figure 4.6, allowing for complex simulations. This system maintained a complete record of grain movement in and out of bins, supporting analysis, sales documentation, and regulatory compliance. Furthermore, using a first-in-first-out mass-flow assumption, the DT can trace grain loads from field to market by correlating harvest and sales data.

The moisture content scale integrated into the 3D visualization distinguished this research's interface from others. It could be calibrated to the safe storage guidelines of the Canadian Grain Commission, and alert farmers to potential problems like spoilage or over-drying. Unlike systems that relied on averages, this DT provided

layer-based measurements throughout the bin, which was crucial because spoilage typically occurred at specific points rather than uniformly. The layered data structure allowed for accurate compilation and drying simulations, which were detailed with their numerical implementation in Section 3.3.

Detailed inventory management was the foundation for pressure and drying simulations, enhancing operator decision-making. The compaction model helped users better understand density changes and volume, while the drying simulation optimized drying strategies based on weather data and best safe storage practices. Furthermore, the enhanced compaction data could be used in drying simulations. Unlike sensor-based systems like Cimbria, this approach did not require expensive hardware or maintenance.

For example, the database stored both the material properties of layers of grain as well as their time of addition, and spoilage is a function of time, temperature, and moisture content. Since the database kept a record of the time of addition, safe storage guidelines could be automated to apply. Providing management advice on storage time, cooling, or drying based on local weather data. This cost-effective solution could make advanced grain management accessible to smaller operations while maintaining the capability to scale to larger facilities. By focusing on accurate record-keeping and simulation-based predictive capabilities, the system enabled proactive management decisions based on predicted conditions and potential scenarios rather than just reactive monitoring.

5.2.4 Limitations

This was a first attempt at creating a digital representation of a grain bin and a limited amount of work that can fit the scope. Currently, the capabilities and features of the grain bin DT are idealized and based on synthetic data with little validation. The limitations outlined here serve as guidance for future work.

First, turning attention to record-keeping and the pressure model. One of the most significant blind spots of record keeping is the lack of the grain hysteresis ef-

fect, where a partially filled bin contains more mass when unloaded from full than when filled to the same volume from empty. Despite being a relatively well-known phenomenon, there is a lack of literature on the topic. Horabik et al. (1999) conducted a significant study on the topic that examined how vertical wall load related to total grain mass during fill and unload cycles. [225]. They found that the hysteresis effect was strongest during initial unloading and stabilised after 4-5 cycles, with each succeeding cycle producing a hysteresis loop several times smaller than the first. This effect resulted from irreversible grain rearrangement during fill/unload cycles. They observed that grain behaviour during bin unloading mirrored triaxial compression tests, where plastic deformation caused particle rearrangement. Two main mechanisms drove this phenomenon: particles rearranged in denser configurations and grain deformation due to increased pressure from dynamic movement. Standard design codes failed to account for these effects, which vary based on grain type, moisture content, bin geometry, and loading history. This effect is particularly relevant to the farming practices of turning grain for quality maintenance. Another related limitation was the assumption of mass flow in bins, which simplified data organization. This is the idea that the grain follows a "first-in-first-out" principle.

Roger's model implemented the Mohr-Coulomb failure assumption, which cannot account for the empirical values of k collected by the triaxial sensor. This limited the accuracy of the current model, which could be tuned more closely to the data gathered. Furthermore, the pressure simulation displayed advanced values that the user could access, which have little meaning without understanding the model. Ultimately, this should be preset to the bin in question, but the limits of the model's current assumptions prevent this. Finally, the current model is axisymmetric. While necessary for applying Roger's extension of Janssen's formula, this framework cannot account for pressures in the angular direction. As a result, a portion of the data collected during the study could not be used. While the angular data is limited, it does suggest that variation could exist in that direction, though more data is needed to substantiate this hypothesis.

The fundamental assumptions and the implementation of the drying model have some limitations. First, the user input ambient and weather data was not time-based and was set to one value for each input instead of the fluctuating temperature and humidity of the ambient conditions over hours and days, as would naturally occur. Moreover, when weather data was pulled, it was hard-coded for Winnipeg. Furthermore, the parameters used in the drying equations might not reflect the specific species of commodities used in the simulation. Finally, the model was an equilibrium-based simulation, which assumed that as air moved across each layer in the bin, the air and the grain were in equilibrium. In reality, this cannot be the case. For example, when the airflow was high or when the incoming air temperature was significantly higher or lower than the temperature of the grain, such as in heated drying [217]. However, such an assumption is seen as acceptable for near-ambient aeration/drying situations [216]

The server and client-side implementations also had some limitations. The database had no security measures implemented. It is publicly accessible and open to anyone, which was done to allow interested parties to access it. Furthermore, the client-side development lacked a human factors perspective when implementing, meaning the layout might not be intuitive for all users.

5.2.5 Improvements to this Research's Digital Twin

Below are changes that could be implemented to improve the work, but extend beyond its current scope.

Basic moisture diffusion models could be included to validate the state of grain in weeks or months, and if the farmer should be advised to turn the grain to accelerate moisture diffusion, displaying the potential future moisture content. Furthermore, heat transfer models could be implemented to predict the change in the silo's temperature gradient, which would be necessary for the moisture diffusion models and aeration/drying models.

The specificity of various parameters and models should be investigated. Further

developing Roger's model and changing the Mohr-Coulomb failure criterion to the Drucker-Prager approach would allow the data from the triaxial sensor to be applied to this model.

Grain relaxation models could be added to better simulate long-term storage effects such as loading/unloading hysteresis. A DT is well suited to account for this phenomenon, as the physics of it are based on the history of the transactions, which are all saved. Sawicki (1994) and Sawicki et al. (1995) have developed models to account for grain bulk plastic deformation based on a loading history [226, 227]. Furthermore, a relaxation model of the grain's ability to bounce back from compaction would nuance the model, which could improve the accuracy of density and pressure predictions; this can be thought of as the grain's sponginess.

A non-equilibrium-based model would be more accurate for heated air drying, a common practice that farmers use. This approach would be useful for farmers to determine whether heated air drying is needed to drop the moisture content to a safe level or whether the operation can be performed by near-ambient drying/aeration. Such improvements could also reduce costs and prevent overdrying. Furthermore, the parameters used in equations should be investigated, as they are currently based on many different sources in the literature. For the drying simulation, the value of R must be validated for large bins and how compaction affects it, as discussed in Sections 4.2.4 and 5.2.1. The system should integrate real-time weather data for any location, rather than relying on hard-coded data. Moreover, forecasted and seasonal averages could be used during simulations for future predictions and running scenarios.

A key potential use of DTs identified was the application of the data collected to inform decisions, as well as create and refine models. The integration of sensors such as the triaxial sensor, temperature and moisture content, and ambient conditions could be used to track relevant data that might be used to predict future conditions. Furthermore, the possibility of non-mass flow, such as funnel flow or rat holing, should be a possibility while emptying, and the DT's state should be able

to reflect this. This could be based on the data available to the DT: moisture content, commodity type, and bin dimensions. Finally, all data should be protected by integrating the built-in Firebase password feature to protect user data and profiles.

5.2.6 Future Possibilities and Speculation

There are more distant possibilities for DTs in farm operations, which are not a simple extension of scope, but an entirely new collection of work far beyond what is presented here. They will be mentioned to point towards potential directions and maybe spark interest. First, DTs could be used to track grain from the field to the elevator, including details such as soil chemistry, texture, and chemical use, to provide farmers with valuable yield and quality information. This could change the role agricultural services provide, such as seed dealers, agronomists, chemical sales, and even farmers' equipment retailers. Alternatively, it has been argued that these new digital technologies in agriculture will not disrupt markets, but rather further reinforce existing oligopolistic market structures [228], which will be discussed in Section 5.2.7

Furthermore, a harvest could be simulated entirely 'in silico' ahead of time based on weather forecasts, equipment, moisture content of the field, drone data, etc. One could imagine trying out additional vehicles and operators for the harvest while looking at the costs associated with them to fine-tune the operation. This advanced planning could potentially reduce operational costs and improve harvest efficiency. The harvest route taken and the time of day could be taken into account to fill a grain bin to optimise drying and aeration activities. The grain bins could communicate their needs to the grain carts and also to the harvester in real-time, but also before any machine was turned on. The interconnected farm provides optimizations for processes that are typically performed by brute force, long, continuous hours, and hard work. Many of the hazards identified with farming are present most during harvest, and it is a very dangerous time for operators [229]. Having a DT suggest optimal operations during a stressful and dangerous time could not only improve

farm functions but also mitigate some of the dangers of harvest.

5.2.6.1 Traceability

In the past two decades, many countries have enforced regulatory policies to highlight the importance of traceability of agri-food supply chains. Traceability in this context can be defined as '... the ability to trace and follow a food, feed, animal or ingredients that produce food, through all stages of production and distribution' as in EC Regulation 178/2002 [230]. The United States has the Bioterrorism Act of 2002 [231], which outlined the need for food traceability. Furthermore, a Food Safety Modernization Act is currently being created, which will clearly articulate rules for food traceability. The Safe Food for Canadians regulations for Canada were updated in 2019 to require food businesses to track the movement of their food [232]. In Europe, the General Food Law was updated in 2002 to incorporate traceability [230]. The International Organization for Standardization (ISO) also produced Standard 9000/9001 that relates to implementing traceability and quality management systems [233, 234].

The common characteristic between all these acts and standards is the one-step-up and one-step-down rule: information on where a commodity came from and where it went must be documented. The traceability of food products is considered essential for the food industry. Currently, there is no legal requirement to implement larger internal and external traceability (going beyond the one-step rule). As technology develops and as the demand for consumer safety, confidence, and knowledge increases, a more comprehensive framework for traceability will be developed to provide proper traceability and communication. These small changes in consumer interest and demand can significantly affect the supply chain in terms of fluctuation in inventory and orders; this phenomenon is the bullwhip effect and can be appropriately managed by sharing information along the supply chain [235]. To achieve this information sharing, Regattieri et al. (2007) suggested a general framework that should be developed on four pillars: product identification (physical

characteristics), data to trace (information to manage), product routing (product life along the supply chain), and traceability tools (technology like radio frequency identification) [236].

An application of this can be found in a terminal elevator in Mariupol, Ukraine., which developed a traceability software based on the EC Regulation 178/2002 and ISO 9001 standards [237]. Although this software primarily focused on inventory management, it lacked integration of grain quality information. The developers proposed that combining real-time grain quality sensors with their inventory management platform could significantly improve the decision-making processes. This improved system would offer comprehensive inventory data, including information on intake, weighing, sample selection, unloading, placement, and shipment. As described in Section 5.2.2, the Mariupol project has created a 'digital shadow' of their inventory, surpassing the capabilities of the Cimbria system discussed earlier. By integrating the DT concept presented in this research, the system could generate data for simulations and data-driven decision-making. Moreover, this enhanced traceability would allow operators to have improved operations and the ability to transmit crop data along the supply chain if required, addressing critical food safety and quality assurance needs.

DTs could be used to pass a digital fingerprint of a commodity through the supply chain, increasing the traceability of the commodity. This has been suggested in previous work by this author [13]. Currently, there is an increase in global demand for traceability in regard to monitoring quality, food safety, biosecurity, or even GMO status [75]. As grain moves along the supply chain, its traceability is reduced, resulting in a disconnect between consumers and producers. Farmers are well positioned to implement digital technologies that can trace the origin of their crops in the field and track various factors throughout the growing season, including soil health, nutrient levels, crop health, chemicals used, pest management, yield, and all unit operations that occur in their inventory to pass to grain elevators if needed. This information could be passed on to the next link in the supply chain if

needed.

Unlike conventional approaches to traceability, limited to one-step-up and one-step-down, a DT approach would enable end-to-end visibility with a comprehensive digital fingerprint of grain. For example, while the Mariupol terminal's systems focus on basic transaction records, this research's DT maintains a continuous digital fingerprint incorporating spatial moisture distribution, pressure modelling, and quality parameters throughout storage. Future implementations could track growing conditions, pesticide use, and other qualities to create a complete profile of the stored grain. This surpasses traditional traceability by tracking critical factors affecting grain value and safety, not just location data. The DT's ability to simulate future conditions provides predictive insights that static systems cannot offer, allowing proactive decision-making rather than simply documenting past movements. There is substantial literature predicting DTs will serve as a key technology within Industry 4.0, enabling intelligent interconnection throughout supply chains [238, 239, 240, 241].

5.2.7 Broader Implications

All technology needs to be accepted by its users, and the farming community is usually reluctant to adopt new gadgets because it is a practice based on tradition. Many works have empirically studied this phenomenon, which has been suggested to be caused by several barriers: socio-economic [242], communication [243], and skepticism of technological dependencies [244], among many other possibilities.

As mentioned in Section 2.1, Norbert Wiener was the father of cybernetics and a great proponent of technological advancement, but he was also skeptical of its neutrality. In chapter ten of his book, "The Human Use of Human Beings: Cybernetics and Society," he notes that cybernetic systems have been able to produce "automatic machines", which he calls the 2nd Industrial Revolution: the automatic age. He says that while this era will have many benefits for humanity, it is practically certain it would lead to "ruin and despair" because of our "freedom to exploit." In

a widely cited passage, Wiener says, "The world of the future will be an even more demanding struggle against the limitations of our intelligence, not a comfortable hammock in which we can lie down to be waited upon by our robot slaves" [245]. This contains many ideas. It calls the reader to consider the indelible nature of the struggle. It examines how human agency participates in technological use and the dangers of over-reliance. Wiener emphasizes the continuous thought needed in technology application, the treatment and "rights" of future technology, and the balance of technology with human nature.

This is not an abstract claim, and Wiener's insights can be grounded in the history of grain storage. S. Martin (2016) writes that the advancement of grain storage technology has profoundly influenced the agricultural commodity sector [246]. Technology has transformed grain into a versatile asset for leveraging credit, selling, and feeding the world's growing population. Specifically, Martin's research highlights the impact of warehouse receipts (a record of stock), moisture measurement devices, dryers, aeration technology, and other agricultural advancements in transforming grain stockpiles used for food into financial assets suitable for collateral and credit.

Currently, farms and grain elevators can secure finances based on their inventory status through warehouse receipts. These receipts provide stock validation for the grain handler and connect it with credit opportunities. During this process, grain audits are important to verify the authenticity of these receipts. This step is essential due to the long-standing issue of grain inventory fraud, as Martin documented. Governing bodies conduct these inspections in accordance with national standards that have evolved over the years.

With the adoption of these technologies, grain handlers have a better understanding of their inventory, which can help prevent undervaluation or overvaluation (i.e., fraud). Today, this phenomenon also participates in a push to utilize new technologies to improve food traceability. As discussed above, DTs have been shown to be a strong emerging technology to help achieve this [13]. Traceability allows for monitoring and documenting quality changes during processing (e.g., moisture change,

fumigation application) and shipping. On paper, this provides the consumer with even more nutritious food.

Martin's (2016) historical examination of grain storage technologies provides valuable insight into how new tools transform agricultural practices. Just as warehouse receipts and moisture meters changed grain from simply food into tradable financial assets, DTs have the potential to introduce a similar transformation. The practical concern involves how food is managed and transformed through such systems. Decision-makers might unintentionally prioritize optimizing the model's parameters (as opposed to hidden ones). This happens because digital parameters become the language the market uses. In this environment, the virtual takes precedence over the real. For example, operators might focus on growing food that maximizes financial benefits while ignoring what food fundamentally means in different contexts: a source of nutrition for consumers, a cultural product tied to taste preferences and traditions, a political object subject to government regulation, or an environmental factor with long-term impacts. This shift from physical to virtual management parallels historical patterns observed by Martin, where food becomes more abstract, and it is turned into an asset. These technological innovations altered fundamental relationships between farmers, their grain, and the market. Ultimately, these changes transform what society determines "food" to be. This extension of Martin's work into the cyber-physical dualism DTs present can be grounded in a look at how modern agriculture and big tech collaborate to reinforce their existing market dominance, which in turn privileges the digital realm and their parameters, abstracting 'food' further into the virtual.

Digital platforms have transformed traditional markets that remained stable for many years. Key examples include transportation (Uber), accommodations (Airbnb), education (Coursera), and news distribution (Facebook/Google). These platforms have reorganized economic structures and changed how value is created across these sectors, illustrated by what van Dijck et al. describe as the "Platform Society" [247]. Sauvagerd et al. (2024) noted that agriculture provides an inter-

esting contradiction to this. Unlike in other industries where new technologies or companies typically disrupt existing markets, in agriculture, established multinational agribusinesses (BAYER, John Deer, AGCO) and Big Tech (Google, Apple, Meta, Amazon and Microsoft) companies collaborate to reinforce existing oligopolistic market structures [228].

Sauvagerd et al. (2024) work showed that this was caused by three main forces. The first is "Datafication", where agricultural data is collected and circulated but remains fragmented in competing "silos" controlled by different agribusinesses, preventing full interoperability. The second is "Selection", where platforms use algorithms to make farm management recommendations, often creating information imbalances that favour the platform owner's products (such as seeds or chemicals) and vendor lock-ins that tie farmers to specific products. The final is "Commodification", where established agribusinesses and Big Tech companies collaborate to transform farm data into marketable products and services that strengthen their existing market positions rather than disrupt them. Often, farmers' data are turned into profitable services, offering analytics that optimize processes such as harvest or chemical use, with the goal of centralizing the farming services onto one hub [228]. These three forces illustrate how digital representations increasingly dominate physical farming realities. When agricultural decisions are mediated primarily through digital platforms, the optimization of digital parameters can eclipse concern for the material world.

Sauvagerd's work explicitly highlighted DTs' role on farms and how they used real-time data to inform decision-making and optimize farming operations, a 'Digital Platform' that the work addressed. Depending on how it is applied, future versions of the technology developed in this research could contribute to each of Sauvagerd's three forces.

This could be an issue for the farmer because it makes them reliant on products and services they do not have the expertise or rights to fix. It could turn the farmer from a traditionally skilled professional to just an operator of applications

which were built on their expertise and sold back to them, with few alternatives as these systems become standard. This could leave the farmer economically vulnerable. They become locked into proprietary product markets where input costs are increasingly determined by platform providers rather than competitive markets. Additionally, as agricultural knowledge becomes embedded in algorithms rather than farming communities, the resulting information asymmetry further diminishes farmers' bargaining power and decision-making autonomy. This shift toward data-driven agriculture risks privileging what can be measured and modelled digitally over what farmers observe physically in their fields. The DT, initially designed to represent the physical world, begins to define what aspects of that world are deemed important.

As Wiener cautions us in his analysis of the 2nd Industrial Revolution, the advancement of the 4th Industrial Revolution (or DTs) may also be a double-edged sword. Applying 'Industry 4.0' in agriculture will undoubtedly increase the quantity and quality of grains. However, there is also a risk that it could transform food, a resource referred to in academic papers as "vital for feeding a growing global population," into a digital asset to be optimized and exploited along with farmers themselves.

Reflecting on how DTs might alter the grain and farmers' role, as Martin and Sauvagerd's have shown, is essential. The privileging of digital representation also risks creating systems where what cannot be easily digitized, such as local ecological knowledge, cultural farming practices, or complex environmental interactions, become increasingly marginalized in agricultural decision-making.

If the creators of these technologies fail to consider these implications in their research, the resulting innovations, despite their potential to do so much good in the world, such as 'feed a growing population,' will almost certainly lead to unforeseen consequences [248, 249] such as the challenging of farmer's right to repair [78], power inequality [250], disappearance of independent farms [251], data ownership and protection [250], subscription economy [248], and hunger to name a few.

With all this said, this research is very hopeful and enthusiastic about improv-

ing food production and the farmers' experience. However, in the spirit of Wiener's skepticism of his work, any good critique should include a critique of itself. Otherwise, it is doomed to repeat the failures that an improvement seeks to address.

Chapter 6

Conclusion

This work addressed the lack of proactive and innovative grain storage management tools. The primary research question guiding this work was "How can one develop a high-fidelity virtual model with minimal input data that accurately represents real-world conditions and inventory statuses of grain storage bins?" By exploring this question through theoretical, experimental, and practical efforts, this research aimed at the conceptual development of a DT framework and its practical application.

This research employed the concept of "sensorless monitoring" as its foundational approach. This approach represents a significant departure from conventional methods that rely heavily on expensive and potentially unreliable sensor technology. By requiring only minimal input data that most farmers already have access to, the DT framework makes sophisticated grain management tools available regardless of farm scale or resources. This accessibility is particularly important given the challenges to global food security identified in Section 1.2. This approach emphasizes predictive solutions rather than traditional reactive monitoring that merely alerts users to problems after they occur. This predictive capability fundamentally distinguishes it from other management systems.

The theoretical work looked at the history of computer control systems, their application to agriculture, various mathematical models that would be essential to studying grain storage, and finally, sensors that could help develop and validate mathematical models. The topics of computer-controlled systems discussed cyber-

netics (2.1), expert systems (2.2), and DTs (2.3). The applications of these were connected to the agricultural sector, showing a historical desire to add computer control and decision-making capacity. This work suggested that DTs could provide solutions to the failures of previous attempts to digitize control and expertise, to help grain storage inventory management and decision-making. This was mainly due to their use of mathematical modelling and modern computing power.

The mathematical model this research was focused on was the pressure theory of bulk solids, namely the Janssen model (2.4.2). This would help to quantify the pressure experienced by the bulk, causing compression, which would affect more advanced simulations, such as drying. While the Janssen equation makes simplifying assumptions required by this work, Rogers et al. implemented necessary modifications to the model, which this author contributed to developing (§2.4.3). The compression equations used are one type commonly used in the literature and follow an exponential relationship. The model uses moisture content, pressure, and original bulk density as input, along with empirically determined constants that are commodity-specific. Additionally, the DT included a proof-of-concept drying simulation based on Thompson's equilibrium air drying model.

An instrument was required to experimentally determine the pressure in the bin, which was studied to validate the new model. There was a notable gap in the availability of sensors to determine how the pressure changed across the radius of a bin. The work documented the design, calibration, and use of a novel tri-axial in-situ pressure sensor specifically calibrated for grain storage applications, in a wheat-filled silo at the University of Kentucky. This measurement system was capable of capturing the three-dimensional stress state at different locations within bulk solids, which is a capability that advances beyond traditional wall-mounted sensors. The sensor design, with its larger sensing surface and piston system, addresses several limitations of previous triaxial sensors while providing measurements in a large-scale silo environment, and can investigate variable k-values. Our initial measurements indicated differences in pressure readings at different radial positions within the

silo. From the limited dataset, the calculated k-values were 0.22 near the wall, 0.19 at mid-radius, and 0.37 at the centre. While these preliminary observations suggest potential variations in k across the silo radius, we emphasize that additional experimental runs would be necessary to establish statistical reliability of these findings. The observed patterns align with trends reported by Molenda et al. (1996), but our study's limited scope prevents definitive conclusions about radial pressure distribution [183].

This work was brought together in the development of a grain bin DT, an implementation of the sensorless monitoring concept. It was a single-page web application that consisted of a database to store information, a logic layer to handle data, a user interface to input data, as well as to view both historical and simulated data. The main functions of the tool were bin management for accurate inventory tracking, a pressure model that calculates density changes due to compression based on Rogers et al. (2025), and a prototype drying simulation based on Thompson's equilibrium model. It could process the bin with constant and variable density, which was done to demonstrate how pressure distribution models directly inform practical grain management through their application to simulate drying processes. The application's code was hosted on a GitHub repository as a Streamlit application, where the back-end was handled by Google's Firebase NoSQL server.

The goal of the DT was to create a framework that used only basic farmer-accessible data, that would eventually have the capacity to predict potential inventory spoilage problems instead of reacting to their presence once it was too late, as traditional systems do. This approach was a key advantage over current state-of-the-art grain management systems, providing early detection capabilities.

6.1 Objectives Achieved

This work fulfilled its stated objectives, which are articulated in Section 1.4.1. The relevance and application of DT technology to grain storage management were established through a comprehensive literature review in Section 2, identifying a clear

gap in existing industry and academia, which was further developed in Section 5.2.2 (Objectives 1–2). Analytic mathematical models of the pressure distribution within grain bins were developed and experimentally tested in Sections 3 and 4, providing new insights into grain behaviour with minimal input (Objectives 3-4). A functional DT platform, integrating these validated models with a user interface that required minimal input, was successfully implemented and reported in Section 4 (Objective 5). Finally, the theoretical potential for greater integration with other agricultural systems and the significant social implications for global food traceability were explored, highlighting future possibilities and wider impacts in Section 5.2.7 (Objectives 7–8). Furthermore, the scope was expanded to include a drying simulation, which was able to use the calculated bulk compression as an input 4.2.4.

Each of the above objectives provided valuable information used to answer the question of how to develop a virtual model of a grain storage bin, both conceptually and practically. Together, they integrated high-level conceptual development, sensor development, experimental data collection, and mathematical modelling, which ultimately resulted in a practical DT solution that addressed the research gap identified.

6.2 Significance

This work establishes a fundamental digital representation of a grain bin that uniquely captures both vertical and horizontal variations within storage bins, setting it apart from conventional inventory management tools. While other tools reviewed in Section 5.2.2 track basic data such as commodity type, fill levels, and moisture content, this DT approach distinguishes itself through the form of the data: spatial data. This enhanced dimensional understanding enables not just improved user awareness but also simulation capabilities, setting up an entirely different approach to inventory management.

While this work does not directly predict spoilage, it provides the essential foundation upon which such predictions could be built. The concept of “sensorless mon-

itoring" developed in this work represents a substantial departure from conventional approaches, the significance of which has already been discussed above.

Additionally, the mathematical models and sensors used to investigate them in this research provided insights into grain behaviour. These findings and scientific tools contributed to a broader understanding of the behaviour of bulk materials in storage, which can inform industrial and academic research. Understanding spatial pressure variations is essential for optimizing silo designs, reducing structural failures, and improving grain storage management. Enhanced pressure sensors and distribution models could lead to more efficient use of materials in construction while maintaining structural integrity. Furthermore, these insights into how stress propagates through grain masses contribute to our understanding of related phenomena such as compaction, aeration dynamics, and moisture migration.

This work established the required platform to create a predictive approach to grain management and implement a few rudimentary simulations. To the knowledge of this author, such a tool has never been created for grain storage, positioning this research as a pioneering effort in the application of DTs to post-harvest grain management.

6.3 Limitations and Future Directions

This research has created a foundational DT for grain storage management, which focused on pressure distribution, compaction modelling, and an early implementation of a drying simulation. However, several limitations exist that should be addressed in future work.

6.3.1 Sensor Design and Experimental Limitations

The triaxial pressure sensor developed for this research faced several limitations and challenges inherent in measuring stress in granular materials. First, the sensor itself may have acted as an inclusion in the grain mass, potentially altering the local

stress distribution. The 1 mm recess of the pressure plate could cause force shielding effects. There is a potential for misorientation with gravitational force. An anomaly in pressure readings was observed during static measurement periods, suggesting possible grain relaxation, sensor error, or more fundamental design limitations under sustained loads. Finally, while the aluminum disc should theoretically result in minimal error due to deflection, the higher friction coefficient of aluminum compared to galvanized steel could alter the force measurements.

Additionally, this experiment has several limitations. First, it was limited to a single grain type (soft red winter wheat at 13.5% moisture content) and a specific filling method (center, small inlet). Moreover, the number of experimental runs was restricted, which limits the statistical robustness of the findings.

6.3.2 Mathematical Model Limitations

Several phenomena challenge the model's immediate applicability to grain storage environments. Grain hysteresis during loading/unloading, where partially filled bins contain more mass when unloaded from full than when filled to the same volume from empty. Furthermore, the "sponginess" of grains and their relaxation over time affect density and pressure predictions. The model also employed mass flow assumptions that, while simplifying data organization, may not have accurately reflected grain behaviour in scenarios such as funnel flow or rat holing during bin emptying. Additionally, the current pressure model failed to address the angular pressure measurements collected by the sensor because the model was planar.

The drying model currently implemented had several inherent limitations. First, both user-input ambient conditions and weather data were set as static values rather than time-varying parameters that would reflect natural fluctuations. Weather data was hard-coded to Winnipeg, which limited applicability to other regions. The equilibrium-based simulation assumed that air and grain reached equilibrium as air moves across each layer, which was unrealistic in situations with high airflow or significant temperature differentials, such as heated-air drying. The parameters used

in the drying equations may not accurately reflect the specific commodity species used in the simulations.

6.3.3 Digital Twin Implementation Limitations

The current implementation of the DT faced several limitations. A database security concerns existed, as the system is currently publicly accessible and not password protected. Furthermore, the user interface design lacked a human factors design, which could limit intuitive use.

6.3.4 Future Research Directions

The following could be investigated to address the above limitations. The main design improvement for the sensor was to explore a diaphragm-style sensor, which may provide greater sensitivity and enhance sensor design. Furthermore, more experimental runs should be conducted with the sensor to provide statistically significant results.

With regards to the experimental application of the sensor, future research should include conducting multiple experimental runs with the same configuration to establish statistical reliability, investigating how different grain types, moisture contents, and filling methods affect pressure distributions. Extending the rest period for grain to consider the effect of the relaxation of grains. Frictional (internal and external) properties of grain and silos should be further investigated as they are important factors in this topic. Furthermore, the sensor data should be compared to traditional sensor systems. The different test configurations, paired with the traditional sensor data, should be used to determine if the sensors are significantly affecting the stress field as inclusions.

Regarding mathematical models, refinement could include the implementation of the Drucker-Prager failure criterion in Rogers et al.'s (2024) work. New three-dimensional, non-axisymmetric models should be developed to enable the use of angular sensor data. This would provide a more complete and accurate representa-

tion of the true stress state within the bulk solid. Non-equilibrium models could be used for heated air drying, and important drying parameters for the existing drying equations investigated. Implementation of moisture diffusion and heat transfer models to predict long-term grain conditions. Finally, the open problem of loading/unloading hysteresis needs to be investigated. This is an enormous research project in itself, as the literature currently does not provide clear answers.

There are immediate and distant research directions regarding the DT. Considering immediate research, the use of location-specific real-time weather and forecasts to improve simulation accuracy is possible with the current Python library used. Next, a human factors engineering study would help create a more ergonomic experience. This study could also determine which features a farmer would find most useful and least useful, potentially leading to a more intuitive interface, which increases accessibility for operators and operations. For example, whether the current button layout is confusing, how they prefer receiving information on safe storage, continuous gradients or warning zones, or how long the grain can currently be stored safely for (with a countdown). Finally, integrating the DT with existing sensor array technology, such as cable technology, would allow another data input. They would not become a requirement but would offer another data input, maintaining the philosophy of "sensorless monitoring".

More distant research directions include an expansion of the DT framework to address additional aspects of (post-)harvest management, potentially creating a comprehensive farm management system. For example, developing a future farm where combines, chaser bins, and storage bins communicate with each other during harvest, taking into account many real-time factors such as weather, crop moisture content, fleet size, market value, and energy demand to determine best practices. One could simulate how beneficial a specific type of harvester or an additional storage bin could be before purchasing them. Furthermore, investigating the potential of the DT frame to improve grain traceability could contribute to increased food safety standards and greater transparency within the supply chain, a growing concern for

most governments.

This research established the essential foundation for grain storage DTs, and addressing the above limitations and exploring these future directions will further enhance the theoretical contributions and practical value of this work. The technologies that come from this could offer tremendous potential for improving grain management and reducing waste. With this being said, they also stand to generate complex implications for farming communities and consumers. The history of agricultural innovation shows that new technologies can fundamentally transform how grain is valued and traded. By developing solutions that prioritize farmer autonomy and practical knowledge, this work aims to contribute to a future where DTs enhance rather than exploit agricultural communities and food systems, addressing concerns about data ownership and the potential transformation of food into merely financial assets.

6.4 Final Remarks

This research took on the challenge of creating a DT for grain bins, an idea completely absent from both the academic literature and industry at the beginning of this work. In doing so, the project exemplified the essence of engineering. It integrated high-level conceptual work, novel sensor development, experimental data collection, and mathematical modelling, all synthesized into a practical final product. This comprehensive approach highlights the interdisciplinary integration of science, technology, engineering, and mathematics (STEM) needed to address a complex real-world challenge like managing grain inventory effectively and sustainably. This work required these different disciplines' skills and perspectives to approach the initial theoretical problem. The solution created is an integrated approach to a real-world problem that provides value to the end-user: farmers!

Looking ahead, this DT framework has the potential to implement proactive grain management with predictive monitoring capabilities. Future development should focus on preserving the minimal input philosophy that makes this technol-

ogy valuable to farmers regardless of their scale or resources. Furthermore, DTs should be designed with farmers' real-world requirements in mind, helping to prevent waste and optimize farm-wide processes. As digital agriculture advances, the approach established in this research could provide a foundation for further innovations that respect farmer knowledge and autonomy. This balance of technological innovation with pragmatic implementation could address increasingly complex demands in global food systems, while genuinely serving the needs of farmers.

References

Bibliography

[1] Adam Rogers, George Dyck, Qiang Zhang, Kurt Hildebrand, and Jitendra Paliwal. A general continuum modelling approach for variable shear stress as a separable function in stored bulk solids. *Powder Technology*, 434(December 2023):119331, 2024.

[2] S G Mcneill, R G Maghirang, and J M Boac. S 3-4 2. 61(2):747–757, 2018.

[3] Josephine M. Boac, Rumela Bhadra, Mark E. Casada, Sidney A. Thompson, Aaron P. Turner, Michael D. Montross, Samuel G. McNeill, and Ronaldo G. Maghirang. Stored Grain Pack Factors for Wheat: Comparison of Three Methods to Field Measurements. *Transactions of the ASABE*, 58(4):1089–1101, aug 2015.

[4] Aaron P Turner, Michael D Montross, and Samuel G Mcneill. Modeling the Compressibility Behavior of Hard Red Wheat Varieties. *Transactions of the ASABE*, 59(3):1029–1038, jun 2016.

[5] ASABE Standards. ASAE D272.3: Resistance to airflow of grains, seeds, other agricultural products, and perforated metal sheets. *ASAE Standards*, 1996:1–7, 2016.

[6] Jonathan A. Foley, Navin Ramankutty, Kate A. Brauman, Emily S. Cassidy, James S. Gerber, Matt Johnston, Nathaniel D. Mueller, Christine O'Connell, Deepak K. Ray, Paul C. West, Christian Balzer, Elena M. Bennett, Stephen R. Carpenter, Jason Hill, Chad Monfreda, Stephen Polasky, Johan Rockström, John Sheehan, Stefan Siebert, David Tilman, and David P.M. Zaks. Solutions for a cultivated planet. *Nature*, 478(7369):337–342, 2011.

[7] Food and Agriculture Organization. The state of food and agriculture 2019 in brief: Moving forward on food loss and waste reduction. Report, Food and Agriculture Organization of the United Nations, Rome, 2019. Retrieved from https://www.fao.org/3/ca6122en/CA6122EN.pdf.

[8] Deepak Kumar and Prasanta Kalita. Reducing Postharvest Losses during Storage of Grain Crops to Strengthen Food Security in Developing Countries. *Foods*, 6(8), 2017.

[9] K. E. Ileleji, D. E. Maier, C. Bhat, and C. P. Woloshuk. DETECTION OF A DEVELOPING HOT SPOT IN STORED CORN WITH A CO2 SENSOR. *Applied Engineering in Agriculture*, 22(2):275–289, 2006.

[10] Benjamin Plumier and Dirk Maier. Effect of Temperature Sensor Numbers and Placement on Aeration Cooling of a Stored Grain Mass Using a 3D Finite Element Model. *Agriculture*, 11(3):231, mar 2021.

[11] Rani Puthukulangara Ramachandran. Integrated approach on stored grain quality management with CO2 monitoring-A review. *Journal of Stored Products Research*, 96(August 2021):101950, 2022.

[12] A. P. Turner, M. D. Montross, J. J. Jackson, S. G. McNeill, M. E. Casada, J. M. Boac, R. Bhadra, R. G. Maghirang, and S. A. Thompson. Error Analysis of Stored Grain Inventory Determination. *Transactions of the ASABE*, 59(3):1061–1072, jun 2016.

[13] George Dyck, Eric Hawley, Kurt Hildebrand, and Jitendra Paliwal. Digital Twins: A novel traceability concept for post-harvest handling. *Smart Agricultural Technology*, 3(February 2022):100079, 2023.

[14] Christos Pylianidis, Sjoukje Osinga, and Ioannis N. Athanasiadis. Introducing digital twins to agriculture. *Computers and Electronics in Agriculture*, 184(July 2020):105942, 2021.

[15] Warren Purcell and Thomas Neubauer. Digital Twins in Agriculture: A State-of-the-art review. *Smart Agricultural Technology*, 3(January 2022):100094, 2023.

[16] Heiner Lasi, Peter Fettke, Hans Georg Kemper, Thomas Feld, and Michael Hoffmann. Industry 4.0. *Business and Information Systems Engineering*, 6(4):239–242, 2014.

[17] Norbert Wiener. *Cybernetics or Control and Communication in the Animal and the Machine*. MIT Press, 2019.

[18] Yanbo Huang and Qin Zhang. *Agricultural Cybernetics*. Springer, Berlin/Heidelberg, Germany, 2021.

[19] Fuji Jian and Digvir S. Jayas. The Ecosystem Approach to Grain Storage. *Agricultural Research*, 1(2):148–156, 2012.

[20] A. Toosi, A. G. Bottino, B. Saboury, E. Siegel, and A. Rahmim. A brief history of ai: How to prevent another winter (a critical review). *PET Clinics*, 16(4):449–469, 2021.

[21] P. Jackson. *Introduction to Expert Systems*. Addison Wesley, Boston, Massachusetts, United States, 1986.

[22] Frederick Hayes-Roth, Donald A. Waterman, and Douglas B. Lenat. *Building Expert Systems*. Addison-Wesley Longman Publishing Co., Inc., USA, 1983.

[23] Gunnar Johannsen and James L. Alty. Knowledge engineering for industrial expert systems. *Automatica*, 27(1):97–114, 1991.

[24] Luc Steels. Second generation expert systems. *Future Generation Computer Systems*, 1(4):213–221, 1985.

[25] L. A. Zadeh. The role of fuzzy logic in the management of uncertainty in expert systems. *Fuzzy Sets and Systems*, 11:199–227, 1983.

[26] Hubert L. Dreyfus, Hubert L. Dreyfus, and Stuart E. Dreyfus. From socrates to expert systems. In *Skillful Coping*, chapter 6, pages 25–43. 2014.

[27] Shu Hsien Liao. Expert system methodologies and applications-a decade review from 1995 to 2004. *Expert Systems with Applications*, 28(1):93–103, 2005.

[28] Stephen I Gallant. / t vt A }. 32(2), 1988.

[29] Bimal K. Bose. Expert system, fuzzy logic, and neural networks in power electronics and drives. *Power Electronics and Variable Frequency Drives: Technology and Applications*, 82(9402594):559–630, 1996.

[30] Jiří Šíma. Neural expert systems. *Neural Networks*, 8(2):261–271, 1995.

[31] Andrew Basden. On the application of expert systems. *International Journal of Man-Machine Studies*, 19(5):461–477, 1983.

[32] Samuel H. Huang and Hong Chao Zhang. Neural-expert hybrid approach for intelligent manufacturing: A survey. *Computers in Industry*, 26(2):107–126, 1995.

[33] Youngohc Yoon and George Swales. Integrating artificial neural networks with rule-based expert systems *. 11:497–507, 1994.

[34] Wr Becraft, Pl Lee, and Rb Newell. Integration of neural networks and expert systems for process fault diagnosis. *Proceedings of the 12th International . . .*, pages 832–837, 1991.

[35] Byungwhan Kim and Gary S. May. Real-time diagnosis of semiconductor manufacturing equipment using a hybrid neural network expert system. *IEEE transactions on components, packaging and manufacturing technology. Part C. Manufacturing*, 20(1):39–47, 1997.

[36] Riccardo Poli, Stefano Cagnoni, Giuseppe Coppini, and Guido Valli. A Neural Network Expert System for Diagnosing and Treating Hypertension. *Computer*, 24(3):64–71, 1991.

[37] D. L. Hudson, M. E. Cohen, and M. F. Anderson. Use of neural network techniques in a medical expert system. *International Journal of Intelligent Systems*, 6(2):213–223, 1991.

[38] Karl Bergerson and Donald C. Wunsch. A commodity trading model based on a neural network-expert system hybrid. *Proceedings. IJCNN-91-Seattle: International Joint Conference on Neural Networks*, pages 289–293, 1991.

[39] A Vellido, P J G Lisboa, and J Vaughan. Neural networks in business : a survey of applications (1992 – 1998). 17:51–70, 1999.

[40] Robert J. McQueen, Stephen R. Garner, Craig G. Nevill-Manning, and Ian H. Witten. Applying machine learning to agricultural data. *Computers and Electronics in Agriculture*, 12(4):275–293, 1995.

[41] Israel Broner and Carlton R. Comstock. Combining expert systems and neural networks for learning site-specific conditions. *Computers and Electronics in Agriculture*, 19(1):37–53, 1997.

[42] D. Rosa, F. Mayol, J. A. Moreno, T. Bonsón, and S. Lozano. An expert system/neural network model (ImpelERO) for evaluating agricultural soil erosion in Andalucia region, southern Spain. *Agriculture, Ecosystems & Environment*, 73(3):211–226, 1999.

[43] D. S. Jayas, J. Paliwal, and N. S. Visen. Multi-layer neural networks for image analysis of agricultural products. *Journal of Agricultural Engineering Research*, 77(2):119–128, 2000.

[44] Pratesh Jayaswal, S. N. Verma, and A. K. Wadhwani. Development of EBP-Artificial neural network expert system for rolling element bearing fault diagnosis. *JVC/Journal of Vibration and Control*, 17(8):1131–1148, 2011.

[45] Dac Khuong Bui, Tuan Nguyen, Jui Sheng Chou, H. Nguyen-Xuan, and Tuan Duc Ngo. A modified firefly algorithm-artificial neural network expert system for predicting compressive and tensile strength of high-performance concrete. *Construction and Building Materials*, 180:320–333, 2018.

[46] S. Dubey, R. K. Pandey, and S. S. Gautam. Literature review on fuzzy expert system in agriculture. *International Journal of Soft Computing and Engineering*, 2(6):289–291, 2013.

[47] Konstantinos G. Liakos, Patrizia Busato, Dimitrios Moshou, Simon Pearson, and Dionysis Bochtis. Machine learning in agriculture: A review. *Sensors (Switzerland)*, 18(8):1–30, 2018.

[48] J. M. McKinion and H. E. Lemmon. Expert systems for agriculture. *Computers and Electronics in Agriculture*, 1(1):31–40, 1985.

[49] R. Doluschitz and W. E. Schmisseur. Expert systems: Applications to agriculture and farm management. *Computers and Electronics in Agriculture*, 2(3):173–182, 1988.

[50] Robert N Coulson, L Joseph Folse, and Douglas K Loh. Artificial Intelligence and Natural Resource Management Published by : American Association for the Advancement of Science Linked references are available on JSTOR for this article : Artificial Intelligence and Natural Resource Management. *Science*, 237(4812):262–267, 1987.

[51] J. W. Jones, Pierce Jones, and P. A. Everett. Combining Expert Systems and Agricultural Models: a Case Study. *Transactions of the American Society of Agricultural Engineers*, 30(5):1308–1314, 1987.

[52] Pierce Jones. Agricultural applications of expert systems concepts. *Agricultural Systems*, 31(1):3–18, 1989.

[53] M. Evans, R. Mondor, and D. Flaten. Expert Systems and Farm Management. *Canadian Journal of Agricultural Economics/Revue canadienne d'agroeconomie*, 37(4):639–666, 1989.

[54] S. R. Harrison. Validation of agricultural expert systems. *Agricultural Systems*, 35(3):265–285, 1991.

[55] Robert E White. *Computional Mathematics Matlab*. 2004.

[56] S. Shenoi, C. S. Chang, H. H. Converse, and L. T. Fan. Expert system for grain elevator hazard prevention. *Applied Engineering in Agriculture*, 7(6):701–704, 1991.

[57] A. Ndiaye. Study of an Expert System on Preservation of the Quality of Post-Harvest Grain: Planning of Storage Technical Route. *IFAC Proceedings Volumes*, 28(6):85–93, 1995.

[58] T. Denne. *An Expert System for Stored Grain Pest Management*. Phd dissertation, Silwood Centre for Pest Management, Imperial College, London, United Kingdom, 1988. Unpublished.

[59] Barry C. Longstaff. Decision tools for grain storage pest management. *Journal of Stored Products Research*, 33(2):99–114, 1997.

[60] D. D. Mann, D. S. Jayas, N. D.G. White, W. E. Muir, and M. S. Evans. A grain storage information system for Canadian farmers and grain storage managers. *Canadian Agricultural Engineering*, 39(1):49–56, 1997.

[61] T. H. Jones, J. D. Mumford, J. A.F. Compton, G. A. Norton, and P. S. Tyler. Development of an expert system for pest control in tropical grain stores. *Postharvest Biology and Technology*, 3(4):335–347, 1993.

[62] P. W. Flinn, D. W. Hagstrum, C. R. Reed, and T. W. Phillips. Stored Grain Advisor Pro: Decision support system for insect management in commercial grain elevators. *Journal of Stored Products Research*, 43(4):375–383, 2007.

[63] P. M. N. Rani, T. Rajesh, and R. Saravanan. Expert systems in agriculture: A review. *Journal of Computer Science and Applications*, 3(1):59–71, 2011.

[64] C. B. Singh, D. S. Jayas, J. Paliwal, and N. D. G. White. Detection of insect-damaged wheat kernels using near-infrared hyperspectral imaging. *Journal of Stored Products Research*, 45(3):151–158, 2009.

[65] Y. Q. Xiang, Q. H. Zhang, P. Han, and M. Y. Chen. Research of early-warning expert system for security of grain storage based on uncertain inference. *Applied Mechanics and Materials*, 536–537:437–442, 2014.

[66] Fei Tao, Jiangfeng Cheng, Qinglin Qi, Meng Zhang, He Zhang, and Fangyuan Sui. Digital twin-driven product design, manufacturing and service with big data. *International Journal of Advanced Manufacturing Technology*, 94(9-12):3563–3576, 2018.

[67] Cor Verdouw, Bedir Tekinerdogan, Adrie Beulens, and Sjaak Wolfert. Digital twins in smart farming. *Agricultural Systems*, 189(January):103046, 2021.

[68] Juuso Autiosalo, Jari Vepsalainen, Raine Viitala, and Kari Tammi. A Feature-Based Framework for Structuring Industrial Digital Twins. *IEEE Access*, 8:1193–1208, 2020.

[69] David Jones, Chris Snider, Aydin Nassehi, Jason Yon, and Ben Hicks. Characterising the Digital Twin: A systematic literature review. *CIRP Journal of Manufacturing Science and Technology*, 29:36–52, 2020.

[70] Michael Grieves. Digital Twin : Manufacturing Excellence through Virtual Factory Replication - A Whitepaper by Dr . Michael Grieves. *White Paper*, (March):1–7, 2014.

[71] Fei Tao, Meng Zhang, and A.Y.C. Nee. *Digital Twin Driven Smart Manufacturing*. 2019.

[72] Michael W. Grieves. Product lifecycle management: the new paradigm for enterprises. *International Journal of Product Development*, 2(1-2):71–84, 2005.

[73] Cor Verdouw and Jan Willem Kruize. Digital twins in farm management : illustrations from the FIWARE accelerators SmartAgriFood and Fractals Digital twins in farm management : illustrations from the FIWARE accelerators SmartAgriFood and Fractals. (October), 2017.

[74] Chad Matthew Laux and Charles R Hurburgh. The impacts of a formal quality management system: A case study of implementing ISO 9000 at Farmers Cooperative Co., Iowa. 3274884:174, 2007.

[75] Maitri Thakur, Bobby J. Martens, and Charles R. Hurburgh. Data modeling to facilitate internal traceability at a grain elevator. *Computers and Electronics in Agriculture*, 75(2):327–336, 2011.

[76] T. Defraeye, G. Tagliavini, W. Wu, K. Prawiranto, S. Schudel, M. Assefa Kerisima, P. Verboven, and A. Bühlmann. Digital twins probe into food cooling and biochemical quality changes for reducing losses in refrigerated supply chains. *Resources, Conservation and Recycling*, 149(April):778–794, 2019.

[77] Air Defence and Forces Academic. 1 2. 537(2014):437–442, 2021.

[78] Laurens Klerkx, Emma Jakku, and Pierre Labarthe. A review of social science on digital agriculture, smart farming and agriculture 4.0: New contributions and a future research agenda. *NJAS - Wageningen Journal of Life Sciences*, 90-91(November):100315, 2019.

[79] Sjaak Wolfert, Lan Ge, Cor Verdouw, and Marc-jeroen Bogaardt. Big Data in Smart Farming – A review. *Agricultural Systems*, 153:69–80, 2017.

[80] Matthew J. Smith. Getting value from artificial intelligence in agriculture. *Animal Production Science*, 60(1):46–54, 2019.

[81] Joel Novek. The automation of grain-terminal elevators in canada. In Ian Varco, Maureen McNeil, and Steven Yearley, editors, *Deciphering science and technology: The social relations of Expertise*, chapter 6, pages 155–176. MacMillan, 1990.

[82] Charles Nwaizu and Qiang Zhang. Computational modeling of heterogenous pore structure and airflow distribution in grain aeration system. *Computers and Electronics in Agriculture*, 188(July):106315, sep 2021.

[83] Manuel O. Binelo, Vanessa Faoro, Oleg A. Kathatourian, and Bulat Ziganshin. Airflow simulation and inlet pressure profile optimization of a grain storage bin aeration system. *Computers and Electronics in Agriculture*, 164(April), 2019.

[84] Jeferson C.da Rocha, Ricardo S. Pohndorf, Volnei L. Meneghetti, Maurício de Oliveira, and Moacir C. Elias. Effects of mass compaction on airflow resistance through paddy rice grains. *Biosystems Engineering*, 194(1973):28–39, 2020.

[85] O. A. Khatchatourian and M. O. Binelo. Simulation of three-dimensional airflow in grain storage bins. *Biosystems Engineering*, 101(2):225–238, 2008.

[86] G. H. L. Hagen. Über den druck und die bewegung des trocknen sandes. *Bericht über die zur Bekanntmachung geeigneten Verhandlungen der Königlich Preussischen Akademie der Wissenschaften zu Berlin*, pages 35–42, 1852.

[87] Brian P. Tighe and Matthias Sperl. Pressure and motion of dry sand: Translation of Hagen's paper from 1852. *Granular Matter*, 9(3-4):141–144, 2007.

[88] Matthias Sperl. Experiments on corn pressure in silo cells - Translation and comment of Janssen's paper from 1895. *Granular Matter*, 8(2):59–65, 2006.

[89] I. Roberts. *Determination of the Vertical and Lateral Pressures of Granular Substances*. The Royal Society Publishing, 1884.

[90] M Ketchum. The design of walls, bins and grain elevators. 1911.

[91] European Committee for Standardization. Eurocode 1: Actions on structures - part 4: Silos and tanks. European Standard EN 1991-4, CEN, Brussels, 2006.

[92] ASABE. Tower Silos : Unit Weight of Silage and Silo Capacities. *ASABE Standard*, 1982, 2005.

[93] A.W. Roberts. 100 Years of Janssen. *Bulk solids handing*, Volumen 3(3):369–409, 1995.

[94] Zhijun Xu and Pengfei Liang. Modified lateral pressure formula of shallow and circular silo considering the elasticities of silo wall and storage materials. *Scientific Reports*, 12(1):1–10, 2022.

[95] George Dyck, Adam Rogers, and Jitendra Paliwal. A Review of Analytical Methods for Calculating Static Pressures in Bulk Solids Storage Structures. *KONA Powder and Particle Journal*, 41(July):108–122, 2024.

[96] M. Reimbert and A. Reimbert. *Silos: Theory and Practice*. Trans Tech Publications, 1976.

[97] D. Schulze. *Powders and Bulk Solids: Behaviour, Characterization, Storage and Flow.*

[98] M. Koenen. Berechnung des seiten- und bodendrucks in silozellen. *Centralblatt der Bauverwaltung*, 16:446–449, 1896.

[99] R. M. Nedderman. *Statics and Kinematics of Granular Materials*. Cambridge University Press, nov 1992.

[100] Wilfrid Airy. The Pressure of Grain. *Minutes of Proceedings Institution of Civil Engeieers*, 131:347–358, 1898.

[101] H.A. Janssen. On The Pressure of Grain in Silos. 1895.

[102] A. W. Jenike and J. R. Johanson. On the theory of bin loads. *Journal of Manufacturing Science and Engineering, Transactions of the ASME*, 91(2):339–344, 1969.

[103] A. W. Jenike, J. R. Johanson, and J. W. Carson. Bin loads - 2: Concepts. *Journal of Engineering for Industry, Transactions ASME*, 95(1):1–5, 1973.

[104] A. W. Jenike, J. R. Johanson, and J. W. Carson. Bin loads—part 3: Mass-flow bins. *Journal of Engineering for Industry*, 95(1):6–12, 1973.

[105] A. W. Jenike, J. R. Johanson, and J. W. Carson. Bin loads—part 4: Funnel-flow bins. *Journal of Engineering for Industry*, 95(1):13–16, 1973.

[106] Kurt Bräuer, Michael Pfitzner, Dmitry O. Krimer, Michael Mayer, Yimin Jiang, and Mario Liu. Granular elasticity: Stress distributions in silos and under point loads. *Physical Review E - Statistical, Nonlinear, and Soft Matter Physics*, 74(6), 2006.

[107] G. Ovarlez and E. Clément. Elastic medium confined in a column versus the Janssen experiment. *European Physical Journal E*, 16(4):421–438, 2005.

[108] Dominik Schillinger and Ramesh B. Malla. Analytical Elastic Solution Based on Fourier Series for a Laterally Confined Granular Column. *Journal of Engineering Mechanics*, 134(11):937–951, 2008.

[109] L Vanel, Ph Claudin, J Bouchaud, M E Cates, E Clément, J P Wittmer, and Université Paris Vi. Stresses in Silos : Comparison Between Theoretical Models and New Experiments. (1):1439–1442, 2000.

[110] S Xu, Q Zhang, and M G Britton. A Microscopic Theory for Predicting Loads in Storage Bins for Granular Materials. pages 253–259, 1996.

[111] A.J. Matchett. Stresses in a bulk solid in a cylindrical silo, including an analysis of ratholes and an interpretation of rathole stability criteria. *Chemical Engineering Science*, 61(6):2035–2047, mar 2006.

[112] J. F. Chen, J. M. Rotter, and J. Y. Ooi. Review of numerical prediction methods for silo wall pressures. *Advances in Structural Engineering*, 2(2):119–134, 1999.

[113] Renzo Di Felice and Carla Scapinello. On the interaction between a fixed bed of solid material and the confining column wall: The Janssen approach. *Granular Matter*, 12(1):49–55, 2010.

[114] Adrian Körzendörfer. Vibrations and ultrasound in food processing – Sources of vibrations, adverse effects, and beneficial applications – An overview. *Journal of Food Engineering*, 324(November 2021), 2022.

[115] Stefano Silvestri, Giada Gasparini, Tomaso Trombetti, and Dora Foti. On the evaluation of the horizontal forces produced by grain-like material inside silos during earthquakes. *Bulletin of Earthquake Engineering*, 10(5):1535–1560, 2012.

[116] Arthur Pascot, Naïma Gaudel, Sergiy Antonyuk, Jérémy Bianchin, and Sébastien Kiesgen De Richter. Influence of mechanical vibrations on quasi-2D silo discharge of spherical particles. *Chemical Engineering Science*, 224:115749, 2020.

[117] J. M. Buick, Pankaj, J. Y. Ooi, J. Chavez-Sagarnaga, A. Pearce, and G. Houghton. Motion of granular particles on the wall of a model silo and the associated wall vibrations. *Journal of Physics D: Applied Physics*, 37(19):2751–2760, 2004.

[118] Yann Bertho, Frédérique Giorgiutti-Dauphiné, and Jean Pierre Hulin. Dynamical Janssen Effect on Granular Packing with Moving Walls. *Physical Review Letters*, 90(14):4, 2003.

[119] C. R.K. Windows-Yule, Sebastian Mühlbauer, L. A.Torres Cisneros, P. Nair, V. Marzulli, and T. Pöschel. Janssen effect in dynamic particulate systems. *Physical Review E*, 100(2):1–7, 2019.

[120] I. Bratberg, K. J. Måløy, and A. Hansen. Validity of the Janssen law in narrow granular columns. *European Physical Journal E*, 18(3):245–252, 2005.

[121] Shivam Mahajan, Michael Tennenbaum, Sudhir N. Pathak, Devontae Baxter, Xiaochen Fan, Pablo Padilla, Caleb Anderson, Alberto Fernandez-Nieves, and Massimo Pica Ciamarra. Reverse Janssen Effect in Narrow Granular Columns. *Physical Review Letters*, 124(12):1–9, 2020.

[122] Loic Vanel, Daniel Howell, D. Clark, R. P. Behringer, and Eric Clément. Memories in sand: Experimental tests of construction history on stress distributions under sandpiles. *Physical Review E - Statistical Physics, Plasmas, Fluids, and Related Interdisciplinary Topics*, 60(5):5040–5043, 1999.

[123] Ekramul Haque. Estimating bulk density of compacted grains in storage bins and modifications of J anssen's load equations as affected by bulk density . *Food Science Nutrition*, 1(2):150–156, 2013.

[124] James W. Landry, Gary S. Grest, and Steven J. Plimpton. Discrete element simulations of stress distributions in silos: Crossover from two to three dimensions. *Powder Technology*, 139(3):233–239, 2004.

[125] S. Courrech Du Pont, P. Gondret, B. Perrin, and M. Rabaud. Wall effects on granular heap stability. *Europhysics Letters*, 61(4):492–498, 2003.

[126] Jie Tang, Haifeng Lu, Xiaolei Guo, and Haifeng Liu. Static wall pressure distribution characteristics in horizontal silos. *Powder Technology*, 393:342–348, 2021.

[127] D.M Walker. An approximate theory for pressures and arching in hoppers. *Chemical Engineering Science*, 22(3):486, 1966.

[128] K. Endo, K. Anki Reddy, and H. Katsuragi. Obstacle-shape effect in a two-dimensional granular silo flow field. *Physical Review Fluids*, 2(9):1–16, 2017.

[129] Q Zhang, Y Shan, and M G Britton. MEASURING MOISTURE-INDUCED LOADS IN A MODEL GRAIN BIN. *Transactions of the ASAE*, 41(3):813–817, 1998.

[130] Yangyang Chen, Cai Liang, Xin Wang, Xiuqi Guo, Xiaoping Chen, and Daoyin Liu. Static pressure distribution characteristics of powders stored in silos. *Chemical Engineering Research and Design*, 154:1–10, 2020.

[131] A. Lapko, M. Gnatowski, and J. A. Prusiel. Analysis of some effects caused by interaction between bulk solid and r.c. silo wall structure. *Powder Technology*, 133(1-3):44–53, 2003.

[132] J. Y. Ooi and J. M. Rotter. Elastic predictions of pressures in conical silo hoppers. *Engineering Structures*, 13(1):2–12, 1991.

[133] J K Walters. A theoretical analysis of stresses in silos with vertical walls. 28:13–21, 1973.

[134] F. Ayuga, P. Aguado, E. Gallego, and Á Ramírez. New steps towards the knowledge of silos behaviour. *International Agrophysics*, 19(1):7–17, 2005.

[135] Yuan Yuan Liu, Ding Li Zhang, Bei Bing Dai, Jie Su, Yanrong Li, and Albert T. Yeung. Experimental study on vertical stress distribution underneath granular silos. *Powder Technology*, 381:601–610, 2021.

[136] J. Jaky. Pressure in silos. In *Proceedings of the 2nd International Conference on Soil Mechanics*, volume 1, pages 103–107, 1948.

[137] D. B. McInnes. Stresses developed by granular material in cylindrical bins, 1968.

[138] S. B. Savage. Some considerations of flow of cohesionless granular solids, 1967.

[139] Ja.B. Lvin. Analytical evaluation of pressures of granular materials on silo walls. *Powder Technology*, 4(5):280–285, jul 1971.

[140] S. C. Cowin. The theory of static loads in bins. (September 1977):409–412, 1977.

[141] Olivier Millet, Jamila Rahmoun, and Géry De Saxcé. Analytic calculation of the stresses in an ensiled granular medium. *Comptes Rendus - Mecanique*, 334(2):137–142, 2006.

[142] Adam Rogers, George Dyck, Jitendra Paliwal, Kurt Hildebrand, Michael D. Montross, and Aaron P. Turner. The Janssen effect and the Chini ordinary differential equation. *Powder Technology*, 436(January):119493, 2024.

[143] Jamila Rahmoun, Olivier Millet, and Géry De Saxcé. A continuous media approach to modeling the stress saturation effect in granular silos. *Journal of Statistical Mechanics: Theory and Experiment*, 2008(6), 2008.

[144] Qijun Zheng and Aibing Yu. Why have continuum theories previously failed to describe sandpile formation? *Physical Review Letters*, 113(6):1–5, 2014.

[145] Jun Ai, Jian Fei Chen, and Jin Y. Ooi. Finite element simulation of the pressure dip in sandpiles. *International Journal of Solids and Structures*, 50(6):981–995, 2013.

[146] Yuan Yuan Liu, Albert T. Yeung, Ding Li Zhang, and Yan Rong Li. Experimental study on the effect of particle shape on stress dip in granular piles. *Powder Technology*, 319:415–425, 2017.

[147] Józef Horabik and Marek Molenda. Distribution of static pressure of seeds in a shallow model silo. *International Agrophysics*, 31(2):167–174, 2017.

[148] Yingguang Fang, Xiaolong Li, Lingfeng Guo, Renguo Gu, and Weizhou Luo. The experiment and analysis of the repose angle and the stress arch-caused stress dip of the sandpile. *Granular Matter*, 24(1):1–12, 2022.

[149] Yingguang Fang, Xiaolong Li, Lingfeng Guo, Renguo Gu, Weizhou Luo, and Ziwei Yan. The experiment and analysis of the stress dip underneath the granular silo. *Granular Matter*, 24(2):1–15, 2022.

[150] Xinxin Wang and Cheng Liu. Regional prediction of multi-mycotoxin contamination of wheat in Europe using machine learning. *Food Research International*, 159(March):111588, 2022.

[151] J. P. Wittmer, P. Claudin, M. E. Cates, and J. P. Bouchaud. An explanation for the central stress minimum in sand piles, 1996.

[152] A. W. Jenike. Gravity flow of bulk solids. Bulletin 108, Utah Engineering Experiment Station, University of Utah, 1961.

[153] P. A. Cundall and O. D. L. Strack. A discrete numerical model for granular assemblies. *Géotechnique*, 29(1):47–65, 1979.

[154] S. Rao. *The Finite Element Method in Engineering*. Elsevier Science, Netherlands, 2011.

[155] Tian Tian, Jinglin Su, Jinhui Zhan, Shujun Geng, Guangwen Xu, and Xiaoxing Liu. Discrete and continuum modeling of granular flow in silo discharge. *Particuology*, 36:127–138, 2018.

[156] V. Vidyapati and S. Subramaniam. Granular flow in silo discharge: Discrete element method simulations and model assessment. *Industrial and Engineering Chemistry Research*, 52(36):13171–13182, 2013.

[157] Bhanjan Debnath, V. Kumaran, and K. Kesava Rao. Dense granular flow through a flat-bottomed silo: Comparison of the DEM and continuum models with experiments. *Powder Technology*, 431(September 2023):119036, 2024.

[158] Yaxiong Zhang, Fuguo Jia, Yong Zeng, Yanlong Han, and Yawen Xiao. DEM study in the critical height of flow mechanism transition in a conical silo. *Powder Technology*, 331:98–106, 2018.

[159] Álvaro Ramírez-Gómez. The discrete element method in silo/bin research. Recent advances and future trends. *Particulate Science and Technology*, 38(2):210–227, 2020.

[160] C. J. Coetzee. Review: Calibration of the discrete element method. *Powder Technology*, 310:104–142, 2017.

[161] Józef Horabik and Marek Molenda. Parameters and contact models for DEM simulations of agricultural granular materials: A review. *Biosystems Engineering*, 147:206–225, 2016.

[162] J. Horabik, P. Parafiniuk, and M. Molenda. Stress profile in bulk of seeds in a shallow model silo as influenced by mobilisation of particle-particle and particle-wall friction: Experiments and DEM simulations. *Powder Technology*, 327:320–334, 2018.

[163] Haiyang Zhao, Xizhong An, Yongli Wu, and Quan Qian. DEM modeling on stress profile and behavior in granular matter. *Powder Technology*, 323:149–154, 2018.

[164] Marvin Carpena Petingco, Mark E Casada, Ronaldo G Maghirang, Sidney A Thompson, Aaron P Turner, Samuel G. McNeill, and Michael Montross. Discrete Element Method Simulation of Wheat Bulk Density as Affected by Grain Drop Height and Kernel Size Distribution. *Journal of the ASABE*, 65(3):555–566, 2022.

[165] Huili Yue. Food safety pre-warning system based on data mining for a sustainable food supply chain. *Food Control*, 2016.

[166] S. A. Thompson, S. G. McNeill, I. J. Ross, and T. C. Bridges. Packing factors of whole grains in storage structures. *Applied Engineering in Agriculture*, 3(2):215–221, 1987.

[167] A. P. Turner, S. G. McNeill, M. D. Montross, M. E. Casada, S. A. Thompson, R. G. Maghirang, and M. C. Petingco. Bulk compressibility behavior for select crops. *Applied Engineering in Agriculture*, 2023. In Press.

[168] R. Bhadra, A. P. Turner, M. E. Casada, M. D. Montross, S. A. Thompson, J. M. Boac, S. G. McNeill, and R. G. Maghirang. Pack Factor Measurements for Corn in Grain Storage Bins. *Transactions of the ASABE*, 58(3):879–890, jun 2015.

[169] S. A. Thompson, C. V. Schwab, and I. J. Ross. Calibration of a Model for Packing Whole Grains. *Applied Engineering in Agriculture*, 7(4):450–456, 1991.

[170] J. F. Labuz and A. Zang. Mohr–coulomb failure criterion. *Rock Mechanics and Rock Engineering*, 45:975–979, 2012.

[171] W. Rankine. On the stability of loose earth. *Philosophical Transactions of the Royal Society London*, pages 9–27, 1856.

[172] R. Rusinek. Experimental method for determination of the pressure distribution in granular solids. *Research in Agricultural Engineering*, 49(2):61–64, 2003.

[173] J. Horabik and R. Rusinek. Pressure ratio of cereal grains determined in a uniaxial compression test. *International Agrophysics*, 16:23–28, 2002.

[174] A. Qadir, H. Guo, X. Liang, Q. Shi, and G. Sun. Effect of the ratios of diameter of silo to bead on the pressure screening in granular columns. *European Physical Journal E*, 31(3):311–314, 2010.

[175] Shanshan Sun, Junhai Zhao, and Changguang Zhang. Calculation of silo wall pressure considering the Intermediate stress effect. *Advances in Civil Engineering*, 2018, 2018.

[176] Siqiang Wang, Ying Yan, and Shunying Ji. Transition of granular flow patterns in a conical hopper based on superquadric DEM simulations. *Granular Matter*, 22(4):1–16, 2020.

[177] J. Wiacek and M. Molenda. Effect of particle size distribution on micro-and macromechanical response of granular packings under compression. *International Journal of Solids and Structures*, 51(25):4189–4195, 2014.

[178] Q Zhang, M G Britton, and R J Kieper. INTERACTIONS BETWEEN WHEAT AND A. 37(3):951–956, 1994.

[179] Randy Back. Frictional effects on mass measurements in a column of glass beads. *Granular Matter*, 13(6):723–729, dec 2011.

[180] R. E. Clower, I. J. Ross, and G. M. White. Properties of Compressible Granular Materials As Related To Forces in Bulk Storage Structures. *Transactions of the ASAE*, 16(3 (MAY-JUNE, 1973)):478–481, 1973.

[181] A. O. Atewologun, G. L. Riskowski, and N. L. Buck. An In-mass Transducer for Measuring the Static Pressure Ratio (K) in Grain Storage Bins. *Transactions of the ASAE*, 35(5):1659–1664, 1992.

[182] Hakan Kibar. Multivariate analyses of selected mechanical properties of dry bean grain. *International Agrophysics*, 29(2):175–183, 2015.

[183] M. Molenda, J. Horabik, and I. J. Ross. Effect of filling method on load distribution in model grain bins. *Transactions of the ASAE*, 39(1):219–224, 1996.

[184] Yingguang Fang, Xiaolong Li, Lingfeng Guo, Renguo Gu, Weizhou Luo, and Ziwei Yan. The experiment and analysis of the stress dip underneath the granular silo. *Granular Matter*, 24(2):1–15, 2022.

[185] C V Schwab, I J Ross, G M White, and D G Colliver. Wheat Loads and Vertical Pressure. 37(5):1613–1619, 1994.

[186] Mengnan Liu, Shuiliang Fang, Huiyue Dong, and Cunzhi Xu. Review of digital twin about concepts, technologies, and industrial applications. *Journal of Manufacturing Systems*, 58(October 2019):346–361, 2021.

[187] G. J. Law, S. C. Negi, and J. C. Jofriet. Method for measurement of horizontal to vertical pressure ratios of wheat and barley in a circular bin. *Canadian Agricultural Engineering*, 35(1):45–49, 1993.

[188] A. O. Atewologun and G. L. Riskowski. Experimental determination of janssen's stress ratio by four methods for soybeans under static conditions. *Transactions of the American Society of Agricultural Engineers*, 34(5):2193–2198, 1991.

[189] S. A. Thompson, N. Galili, and R. A. Williams. Vertical floor pressures during filling of a full-scale grain bin. *Transactions of the American Society of Agricultural Engineers*, 39(3):1093–1100, 1996.

[190] Rômulo Marçal Gandia, Francisco Carlos Gomes, Wisner Coimbra de Paula, Estácio Antunes de Oliveira Junior, and Pedro José Aguado Rodriguez. Static and dynamic pressure measurements of maize grain in silos under different conditions. *Biosystems Engineering*, 209:180–199, 2021.

[191] A. Ramírez, J. Nielsen, and F. Ayuga. On the use of plate-type normal pressure cells in silos. Part 1: Calibration and evaluation. *Computers and Electronics in Agriculture*, 71(1):71–76, 2010.

[192] A. Ramírez, J. Nielsen, and F. Ayuga. On the use of plate-type normal pressure cells in silos. Part 2: Validation for pressure measurements. *Computers and Electronics in Agriculture*, 71(1):64–70, 2010.

[193] Sandpiles. 1997.

[194] V. Askegaard. Design and application of stress and strain cells with small measuring errors. *NDT International*, 14(5):271–277, 1981.

[195] V. Askegaard. Normal and shear stress on a silowall, and stress and strain state in a silo medium. In C. J. Brown and J. Nielsen, editors, *Silos: Fundamental of theory, behaviour and design*, pages 686–698. E. & FN Spon, Routledge, New York, 1998.

[196] Vagn Askegaard. Problems in connection with design, calibration and use of pressure cells. *Journal of Theoretical and Applied Mechanics*, 26(2):219–229, 1988.

[197] C. J. Brown, E. H. Lahlouh, and J. M. Rotter. Experiments on a square planform steel silo. *Chemical Engineering Science*, 55(20):4399–4413, 2000.

[198] Yusheng Lei, Qinwei Ma, and Qingfan Shi. Side-wall pressure distribution of cylindrical granular containers with flat bottom. *Powder Technology*, 353:57–63, 2019.

[199] Yuan Yuan Liu, Ding Li Zhang, Bei Bing Dai, Jie Su, Yanrong Li, and Albert T. Yeung. Experimental study on vertical stress distribution underneath granular silos. *Powder Technology*, 381:601–610, 2021.

[200] Lukáš Martinák, Aleš Oujezdský, and Aleš Slíva. Measurement of pressures in silos using strain gages. *IFAC Proceedings Volumes (IFAC-PapersOnline)*, 37(20):141–146, 2004.

[201] George Dyck, Adam Rogers, Michael D. Montross, Kurt Hildebrand, Aaron P. Turner, Jitendra Paliwal, Barry Farmer, and Carlos A. Jarro. Novel in-situ pressure sensors for bulk solids in silos: Design, calibration, data acquisition, and analysis. *Computers and Electronics in Agriculture*, 2025. Accepted.

[202] T. L. Thompson. Temporary storage of high-moisture shelled corn using continuous aeration. *Transactions of the ASABE*, 15(2):333–337, 1972.

[203] W. E. Muir. *Grain Preservation Biosystems 2000*. University of Manitoba: Biosystems Department, Winnipeg, 2000.

[204] Z. Naghavi, A. Moheb, and S. Ziaei-rad. Numerical simulation of rough rice drying in a deep-bed dryer using non-equilibrium model. *Energy Conversion and Management*, 51(2):258–264, 2010.

[205] T L Thompson, R M Peart, and G H Foster. Matllematical Simulation of Corn Drying A New Model. *ASAE*, 11(4), 1968.

[206] J. Lawrence, G. G. Atungulu, and T. J. Siebenmorgen. Modeling in-bin rice drying using natural air and controlled air drying strategies. *Transactions of the ASABE*, 58(4):1103–1111, 2015.

[207] V. K. Jindal and T. J. Siebenmorgen. Simulation of low temperature rough rice drying and re-wetting in shallow beds. *Transactions of the American Society of Agricultural Engineers*, 37(3):863–871, 1994.

[208] H. Zhong. *A Simulation Platform for Accurate Prediction of In-bin Drying and Storage of Rough Rice*. Phd thesis, University of Arkansas, Fayetteville, Arkansas, 2015. Unpublished.

[209] ASABE Standards. D271.2: Psychrometric data in SI units. Technical report, American Society of Agricultural and Biological Engineers, St. Joseph, Michigan, 1979.

[210] ASABE Standards. D245.6: Moisture relationships of plant-based agricultural products. Technical report, American Society of Agricultural and Biological Engineers, St. Joseph, Michigan, 1992.

[211] J. Jalili, M. K. Jafari, A. Shafiee, J. Koseki, and T. Sato. An investigation on effect of inclusions on heterogeneity of stress, excess pore pressure and strain distribution in composite soils. *International Journal of Civil Engineering*, 10(2):124–138, 2012.

[212] S. Joseph Antony, David Chapman, S. Judes Sujatha, and Thabit Barakat. Interplay between the inclusions of different sizes and their proximity to the wall boundaries on the nature of their stress distribution within the inclusions inside particulate packing. *Powder Technology*, 286:98–106, 2015.

[213] S. J. Antony, M. Al-Sharabi, N. Rahmanian, and T. Barakat. Shear stress distribution within narrowly constrained structured grains and granulated powder beds. *Advanced Powder Technology*, 26(6):1702–1711, 2015.

[214] Q. Zhang, V. M. Puri, and H. B. Manbeck. Model for Frictional Behavior of Wheat on Structural Materials. *Transactions of the American Society of Agricultural Engineers*, 31(3):898–903, 1988.

[215] A. Ruiz, A. Couto, and P.J. Aguado. Design and instrumentation of a mid-size test station for measuring static and dynamic pressures in silos under different conditions – part ii: Construction and validation. *Computers and Electronics in Agriculture*, 85:174–187, 2012.

[216] S. Pabis and D. S. Jayas. Deep-Bed Grain Drying - A Review of Particular Theories. *Drying Technology*, 11(7):1553–1582, 1993.

[217] Fuji Jian and Digvir S. Jayas. *Grains*. Number september 2016. CRC Press, Boca Raton, nov 2021.

[218] Defraeye Thijs and Daniel I. Onwude. The future of digital twins for drying. *Drying Technology*, 39(1):1–2, 2020.

[219] Grain inventory management & trading platform, 2024.

[220] Agribusiness software solutions, 2024.

[221] Gms inventory - grain management system, 2024.

[222] Bincloud inventory management software, 2024.

[223] Inventory management system, 2024.

[224] Werner Kritzinger, Matthias Karner, Guy Traar, Jan Henjes, and Wilfried Sihn. Digital twin in manufacturing: A categorical literature review and classification. *IFAC-PapersOnLine*, 51(11):1016–1022, 2018.

[225] J. Horabik, M. Molenda, and I. J. Ross. WALL LOADS IN A MODEL GRAIN BIN DURING FILL AND UNLOAD CYCLES. *Transactions of the ASAE*, 42(3):771–776, 1999.

[226] Andrzej Sawicki. Elasto-Plastic Interpretation of Oedometric Test, 1994.

[227] Andrzej Sawicki and Waldemar Swidzinski. Cyclic compaction of soils, grains and powders. *Powder Technology*, 85(2):97–104, 1995.

[228] Monja Sauvagerd, Maximilian Mayer, and Monika Hartmann. Digital platforms in the agricultural sector: Dynamics of oligopolistic platformisation. *Big Data & Society*, 11(4):20539517241306365, 2024.

[229] H. S. Chattha, K. W. Corscadden, and Q. U. Zaman. Hazard identification and risk assessment for improving farm safety on canadian farms. *Journal of Agricultural Safety and Health*, 23(3):155–174, 2017.

[230] European Parliament and Council of the European Union. Regulation (ec) no 178/2002 of the european parliament and of the council of 28 january 2002 laying down the general principles and requirements of food law, establishing the european food safety authority and laying down procedures in matters of food safety, 2002. Official Journal of the European Communities, L 31, 1.2.2002, p. 1–24.

[231] Department of Agriculture. Implementation of the public health security and bioterrorism preparedness and response act of 2002; establishment and maintenance of records for foods. Federal Register 149, Food Safety and Inspection Service, 2005. Available in the Federal Register, Vol. 70, No. 149.

[232] Government of Canada. Safe food for canadians regulations, 2018. SOR/2018-108.

[233] International Organization for Standardization. Quality management systems – fundamentals and vocabulary. International Standard ISO 9000:2015, ISO, Geneva, Switzerland, 2015.

[234] International Organization for Standardization. Quality management systems – requirements. International Standard ISO 9001:2015, ISO, Geneva, Switzerland, 2015.

[235] Aysegul Sarac, Nabil Absi, and Stphane Dauzere-Pérès. A literature review on the impact of RFID technologies on supply chain management. *International Journal of Production Economics*, 128(1):77–95, 2010.

[236] A. Regattieri, M. Gamberi, and R. Manzini. Traceability of food products: General framework and experimental evidence. *Journal of Food Engineering*, 81(2):347–356, 2007.

[237] F. A. TRISHYN. Automation of Traceability Process At Grain Terminal Llc " Ukrtransagro". *Grain Products and Mixed Fodder's*, 17(2):46–50, 2017.

[238] B. Tjahjono, C. Esplugues, E. Ares, and G. Pelaez. What does industry 4.0 mean to supply chain? *Procedia Manufacturing*, 13:1175–1182, 2017. Manufacturing Engineering Society International Conference 2017, MESIC 2017, 28-30 June 2017, Vigo (Pontevedra), Spain.

[239] Daniel Onwude, Flora Bahrami, Chandrima Shrivastava, Tarl Berry, Paul Cronje, Jade North, Nicola Kirsten, Seraina Schudel, Eleonora Crenna, Kanaha Shoji, and Thijs Defraeye. Physics-driven digital twins to quantify the impact of pre- and postharvest variability on the end quality evolution of orange fruit. *Resources, Conservation and Recycling*, 186:106585, 2022.

[240] Thijs Defraeye, Chandrima Shrivastava, Tarl Berry, Pieter Verboven, Daniel Onwude, Seraina Schudel, Andreas Bühlmann, Paul Cronje, and René M. Rossi. Digital twins are coming: Will we need them in supply chains

of fresh horticultural produce? *Trends in Food Science and Technology*, 109(January):245–258, 2021.

[241] Maitri Thakur and Charles R. Hurburgh. Framework for implementing traceability system in the bulk grain supply chain. *Journal of Food Engineering*, 95(4):617–626, 2009.

[242] J Blasch, B Van Der Kroon, P Van Beukering, R Munster, S Fabiani, P Nino, and S Vanino. Farmer preferences for adopting precision farming technologies : a case study from. 49(December 2020):33–81, 2022.

[243] Christopher M Raymond and Guy M Robinson. Factors affecting rural landholders ' adaptation to climate change : Insights from formal institutions and communities of practice. *Global Environmental Change*, 23(1):103–114, 2013.

[244] Brian C Campbell and Brian C Campbell. The Reluctant Farmer : The Role of Multimedia in America ' s 20th-Century Agricultural Transformation The Reluctant Farmer : The Role of Multimedia in America ' s 20th-Century Agricultural Transformation. *Visual Anthropology*, 32(3-4):240–264, 2019.

[245] Norbert Wiener. *The Human Use of Human Beings: Cybernetics and Society*. Number 320. Da Capo Press, 1954.

[246] Sarah Martin. Storage Matters: Managing Grain, Securing Finance, and Building Markets. 2016.

[247] José van Dijck, Thomas Poell, and Martijn de Waal. *The Platform Society*. Oxford University Press, New York, 2018.

[248] Michael Carolan. Publicising Food: Big Data, Precision Agriculture, and Co-Experimental Techniques of Addition. *Sociologia Ruralis*, 57(2):135–154, 2017.

[249] Emily Duncan, Alesandros Glaros, Dennis Z. Ross, and Eric Nost. New but for whom? Discourses of innovation in precision agriculture. *Agriculture and Human Values*, 38(4):1181–1199, 2021.

[250] Sarah Rotz, Emily Duncan, Matthew Small, Janos Botschner, Rozita Dara, Ian Mosby, Mark Reed, and Evan D.G. Fraser. The Politics of Digital Agricultural Technologies: A Preliminary Review. *Sociologia Ruralis*, 59(2):203–229, apr 2019.

[251] Alana Semuels. They're trying to wipe us off the map. small american farmers are nearing extinction. *TIME*, 27, November 2019.

[252] S. Ding, Ying Ji, Senbin Ye, J. M. Rotter, and Qi Li. Measurements of pressure and frictional tractions along walls of a large-scale conical shallow hopper and comparison with Eurocode 1991-4:2006. *Thin-Walled Structures*, 80:231–238, 2014.

[253] eFunda. Plate calculator – simply supported circular plate with uniformly distributed loading. Online calculator, n.d. Retrieved April 22, 2024, from `https://www.efunda.com/formulae/solid_mechanics/plates/calculators/cpS_PUniform.cfm#Results`.

[254] M. Khanali, S. Rafiee, and A. Jafari. Moisture-dependent physical properties of rough rice grain. *Mechanical Engineering*, 52:11609–11613, 2012.

[255] ASABE Standards. D243.4: Thermal properties of grain and grain products. Technical report, American Society of Agricultural and Biological Engineers, St. Joseph, Michigan, 2003.

[256] D. S. Suministrado. Some physical and thermal properties of rough rice. M.eng. thesis, Asian Institute of Technology, Bangkok, Thailand, 1979.

Appendices

A.1 Deflection Calculations

The sensor system consisted of a 3D printed plastic shell with three aluminium pistons housing compressive piezoelectric sensors. These pistons fit into recesses in the shell and were secured with 4 bolts. The main pressure plate measured 63.5 mm in diameter and 3.17 mm in thickness. The housing lip, which holds the pressure plate, was approximately 1 mm deep.

There is a great deal of literature on the error in plate-type normal pressure cells for the measuring of stress loads in silos. Ramrez et al. [191] provide both a review of the literature and an analysis of these sensors. They outline three criteria for accurate pressure cells: "(1) the stiffness of the cell plate, (2) the stiffness of the cell-to-wall fixing system, and (3) the accuracy with which the pressure cell is mounted flush with the silo wall." As criteria 2 and 3 do not apply to our sensor, we focus on the stiffness of the cell plate.

Ding et al. [252] used a piston-style pressure sensor to measure stresses in a silo's conical section sidewall during filling and discharge to validate Eurocode building codes. The front disc of the pressure piston, cut from the hopper itself, was 120 mm in diameter and 6 mm thick stainless steel.

Askegaard [196] provides a formula for the pressure error due to the bending of the average plate:

$$\frac{\Delta p}{p} = K\frac{E}{(1-\nu^2)}a\frac{\Delta w_{aver}}{p} \tag{1}$$

Where $\frac{\Delta p}{p}$ is the relative pressure error due to plate deflection, K is a constant depending on cell type (0.7 for a plate without fluid behind it), E and ν are the elastic modulus and Poisson's ratio for the granular material, p is the applied normal pressure, a is the radius of the plate and Δw_{aver} is the average plate deflection for this pressure.

A circular plate supported under a uniformly distributed load, the deformation at any point is given by [253]:

$$w(r) = \frac{pr_0^4}{64D(1+\nu)}[2(3+\nu)(1-(\frac{r}{r_0})^2) - (1+\nu)(1-(\frac{r}{r_0})^4)] \tag{2}$$

The average deformation is calculated as:

$$w_{aver} = \frac{1}{\pi r_0^2}\int_0^{r_0} w(r)2\pi r dr = \frac{(\nu+7)pr_0^4}{192D(\nu+1)} \tag{3}$$

For our aluminium disc ($E = 69$ GPa, $\nu = 0.33$, $p_{max} = 20$ kPa, $r_0 = 31.75$ mm,

$h = 3.17$ mm):

$$D = \frac{Eh^3}{12(1-\nu^2)} = 205.55 \text{ Nm}^2 \tag{4}$$

$$w_{aver} = 2.904 \times 10^{-6} \text{ m} \tag{5}$$

Using Askegaard's error formula with wheat properties ($E = 5000$ kPa, $\nu = 0.3$):

$$\frac{\Delta p}{p} = 0.001762 = 0.1762\% \tag{6}$$

This theoretical error due to disc rigidity is minimal. However, the actual deflection may differ due to the disc's centre support and spring-supported edges.

A.2 Drying Model Assumptions

The following assumptions about the system shall be made:

1. There will be only homogeneous grain in the system.
   (a) No dockage, insects, mites, or other "foreign" material
2. Constant ambient weather conditions: temperature, RH
3. No external transport phenomena are acting on the bin.
   (a) Solar radiation, wind, etc.
4. Uniform airflow rate throughout the entire bin
5. There will be a grain-air equilibrium when air enters a section of the bin.
   (a) Both in terms of moisture content and thermal energy
6. The drying and heating processes are reversible and there is no hysteresis between the sorption and desorption isotherms.

A.3 Variables and Additional Equations

$\rho_b = 0.948 \times MC + 4471.2$	(Khanali, 2012)[254]
$C_a = 1006$	(ASABE, 1979)[209]
$C_w = 4218.6 - 2.6 \times T_a + 4.8817 \times 10^{-2} \times T_a^2 - 2.5596 \times 10^{-4} \times T_a^3$	(ASABE, 1979)[209]
$C_v = 1858.7 + 0.2 \times T_o + 1.6 \times 10^{-3} \times T_o^2$	(ASABE, 1979)[209]
$C_g = 1110 + MC \times 44.8$	(ASABE, 2003)[255]
$h = 2502535.259 - 2385.76424 \times T$	(ASABE, 1979)[209]

Variable	Description	Unit
c_a	specific heat of dry air	J/(kg K)
c_g	specific heat of grain	J/(kg K)
c_v	specific heat of water vapor	J/(kg K)
c_w	specific heat of water	J/(kg K)
dmf	Dry matter fraction	no units
dx	Layer thickness	m
T_g	Initial grain temperature	°C
H_f	Absolute humidity of air leaving grain layer	(kg of water)/(kg of air)
H_o	Absolute humidity of air entering grain layer	(kg of water)/(kg of air)
h_v	Latent heat of vaporization	J/kg
M_f	Final moisture content of grain	% wet basis
M_o	Initial moisture content of grain	% wet basis
R	Grain dry matter to dry air mass ratio	(kg of grain)/(kg of dry air)
t	Time	seconds
T_f	Final air and grain temperature	°C
T_o	Initial air temperature	°C
ρ_a	Density of air	kg/m^3
ρ_g	Bulk density of grain	kg/m^3
v_a	Velocity of air	m/s

Table 1: List of variables and their descriptions

A.4 Drying Model Validation

In Figure A.1 there are differences between Jindal's data, model and this research's model. The two models shared fundamental assumptions and equations for heat and mass transfer, vapour pressure, latent heat from vapourization, and equilibrium moisture conditions. There are two main differences. This research used a different specific heat formula ($1110 + MC_o * 44.8$ from [255]) than the equation of the paper ($0.3153 + 0.0073Mw + 0.0009G_o$ from [256]). Furthermore, this work uses a different moisture equilibrium relationship through the Modified-Chung equation rather than the Sehgal (1980) formula reported in the paper. This work is a master's thesis and is specific to rice, whereas the Modified-Chung equation can accommodate many different commodities. This work is a more flexible representation of an updated or adapted model that maintains the same physical principles but incorporates more general empirical relationships. As a result, the results differ slightly from Jindal's data and model, but allow for many different commodities to be used, which this application requires. Furthermore, Jindal et al. noted the trouble with choosing proper values for free parameters in the eq 3.17. Jindal et al. found that when R was too low (below 0.27), the equilibrium model overestimates drying rates. When R is properly set at or above this threshold, their experiments showed that the model accurately predicts both drying and rewetting behaviour in rice beds. With this being said, let us recall the words of John von Neumann: "With four parameters I can fit an elephant, and with five I can make him wiggle his trunk."

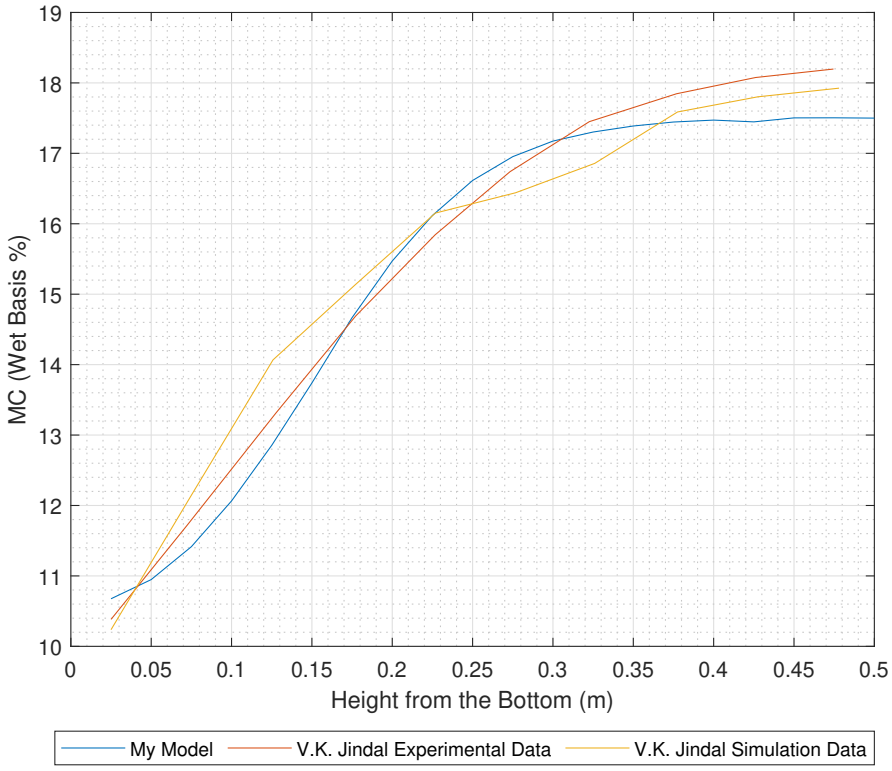

Figure 1: DRYING code vs data vs other simulation

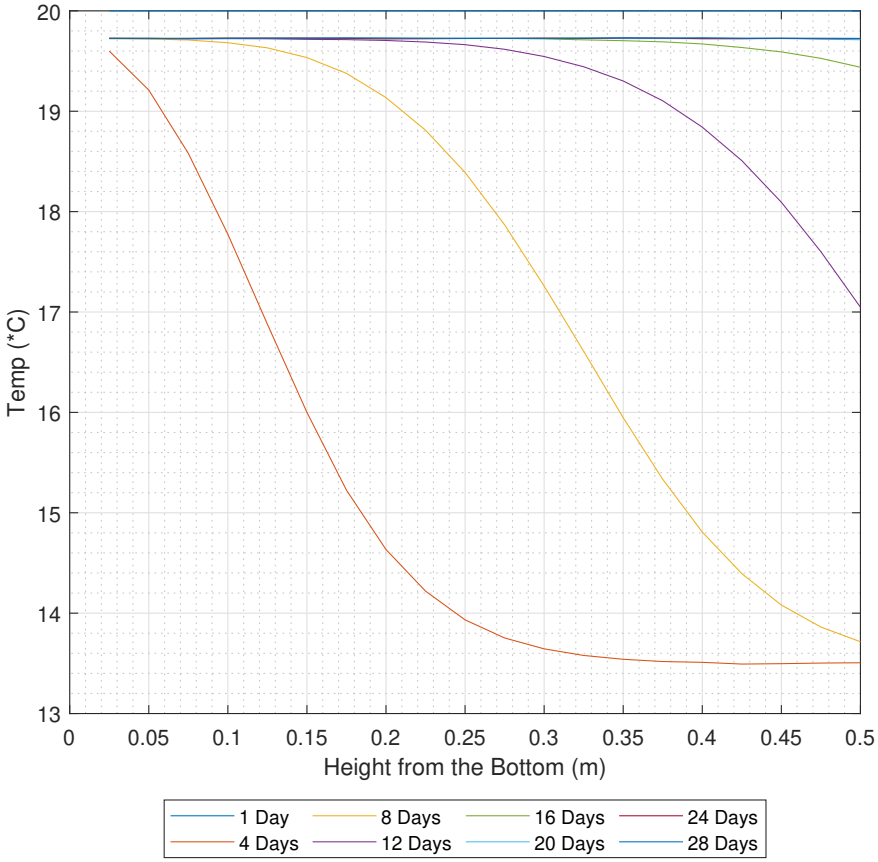

Figure 2: Temperature by Depth

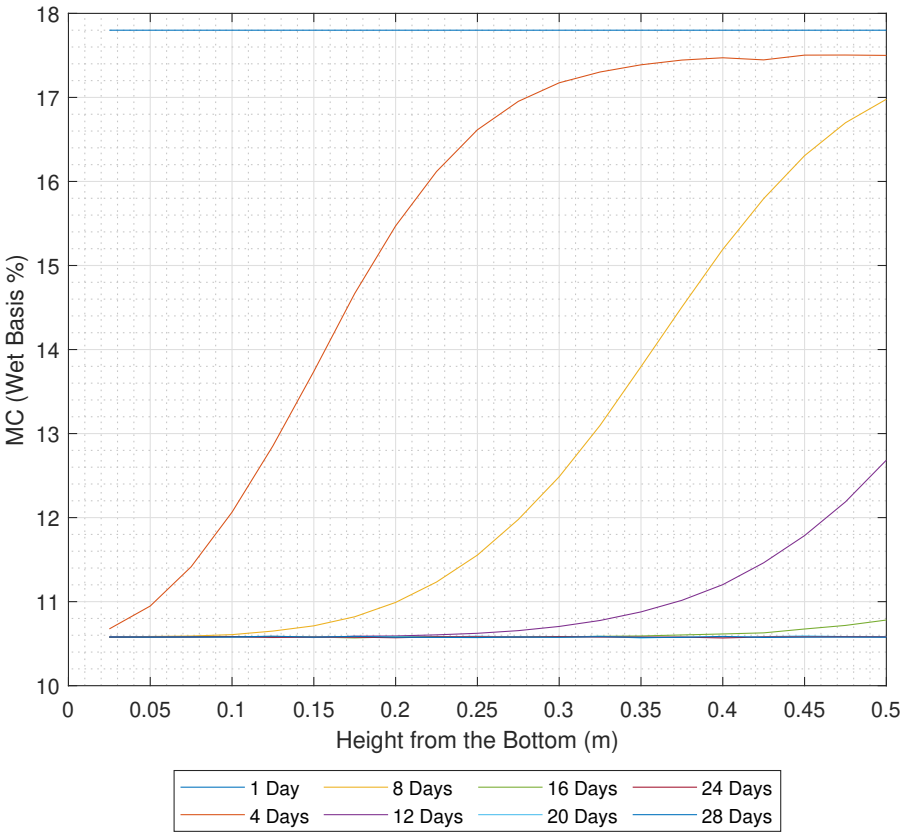

Figure 3: Temperature by Depth